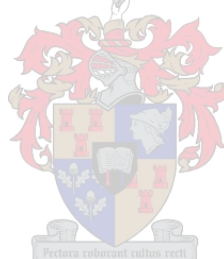


# Panaceas and Pitfalls in Electrodriven Chromatographic Techniques

*Astrid Sorina Buica*

Dissertation presented for the degree of Doctor of Philosophy at the  
University of Stellenbosch



Promoter: Prof Pat Sandra

Co-promoter: Prof Andrew Crouch

December 2007

## DECLARATION

I, the undersigned, hereby declare that the work contained in this dissertation is my own original work and that I have not previously in its entirety or in part submitted it at any university for a degree.

Signature: ..... Date: .....

## ***ABSTRACT***

---

In this thesis the main capillary electrodriven chromatographic techniques (*i.e.* Capillary Electrochromatography *CEC*, Micellar Electrokinetic Chromatography *MEKC* and Microemulsion Electrokinetic Chromatography *MEEKC*) were compared in terms of column manufacturing, fundamental chromatographic performance, and some applications were developed. The first stage of this thesis aimed at developing improved packed and open tubular *CEC* columns. For the manufacturing of packed *CEC* columns, the frit-burning step proved of critical importance, together with the slow build-up of the packed bed. The making of open tubular columns is a relatively simple, "one pot" sol-gel reaction taking place in mild conditions. The nature of the gel and the resulting selectivity of the column could easily be changed by changing the precursors.

In a second stage of this thesis the packed and open tubular *CEC* columns were evaluated chromatographically and compared with the results obtained by *MEKC* and *MEEKC*. All electrodriven separation techniques showed high efficiencies. The selectivity proved easier to tune with sol-gel chemistry for the making of open tubular columns. Resolution is acceptable for packed *CEC*, *MEKC* and *MEEKC*. For peak capacity, *CEC* has the advantage of a practically non-limited elution time, while *MEKC* and *MEEKC* suffer of the drawback of the existence of an elution window which is limited in time by the elution of the micelles.

Some applications were developed in this study on open tubular *CEC* columns and for the packed *CEC* columns. Various sugars derivatized with 9-aminopyrene-1,4,6-trisulfonic acid (*APTS*) could be separated with open tubular *CEC*, using an octyl, amino or cyano stationary phase. Open tubular columns containing  $\alpha$ ,  $\beta$  and  $\gamma$  cyclodextrins attached to the stationary phase were developed. This approach proved promising for the separation of positional isomers. A method was developed for the analyses of a mixture of carbamates and for several steroids with packed column *CEC* directly coupled with *MS*.

## ***OPSOMMING***

---

In hierdie studie word die vernaamste kapillêre elektro-gedrewe chromatografiese tegnieke (*i.e.* Kapillêre Elektrochromatografie *CEC*, Misellêre Elektrokinetiese Chromatografie *MEKC* en Mikro-emulsie Elektrokinetiese Chromatografie *MEEKC*) vergelyk in terme van kolomvervaardiging, fundamentele chromatografiese gedrag en sommige toepassings is ontwikkel. Die eerste fase van die studie was toegespits op die ontwikkeling van verbeterde gepakte en ongepakte intern bedekte *CEC* kolomme. Vir die vervaardiging van gepakte *CEC* kolomme blyk die brandproses van die frit krities te wees, asook die stadige opbou van die gepakte bed. Die vervaardiging van ongepakte kolomme is 'n relatief eenvoudige "een pot" sol-gel reaksie onder matige kondisies. Die aard van die gel en die meegaande selektiwiteit kon maklik verander word deur die reaksie voorlopers te verander.

In 'n tweede fase van die studie is die gepakte en ongepakte *CEC* kolomme chromatografies geëvalueer en vergelyk met resultate wat verkry is met *MEKC* en *MEEKC*. Al die elektrogedrewe skeidingstegnieke het hoë effektiwiteit getoon. Die selektiwiteit was makliker om aan te pas deur gebruik te maak van sol-gel chemie vir die vervaardiging van ongepakte kolomme. Resolusie is aanvaarbaar vir gepakte *CEC*, *MEKC* en *MEEKC*. Wat piek kapasiteit betref het *CEC* die voordeel van 'n bykans onbeperkte elueringstyd, terwyl *MEKC* en *MEEKC* die nadeel het van die teenwoordigheid van 'n elueringsvenster wat tydigewys beperk word deur die eluering van die miselle.

Sommige van die toepassings in die studie is vir beide gepakte en ongepakte *CEC* kolomme *CEC* ontwikkel. Verskeie suikers, gederivatiseer met 9-aminopireen-1,4,6-trisulfoonsuur (*APTS*), kon geskei word met ongepakte kolomme deur gebruik te maak van 'n oktiel, amino of siano stasionêre fase. Ongepakte kolomme bevattende  $\alpha$ ,  $\beta$  en  $\gamma$  siklodekstriene gebind aan die stasionêre fase is ontwikkel. Hierdie benadering blyk belowend te wees vir die skeiding van posisionele isomere. 'n Metode is ontwikkel vir die analiese van 'n mengsel van karbamate en vir verskeie steroïede met 'n gepakte kolom *CEC* direk gekoppel aan Massa Spektrometrie (*MS*).

## ***ACKNOWLEDGEMENTS***

---

I would like to thank Prof Pat Sandra for providing me the opportunity to work in his group, for his guidance and support.

My heartfelt thanks go to Prof Andrew Crouch for his support, encouragements and guidance.

My thanks go to Henk Lauer for offering me a home away from home, for his witty comments and his unique way of delivering them.

I want to thank Andrei Medvedovici for introducing me to the world of separations, his support and advice.

Thanks to my co-workers, especially Frédéric Lynen.

For all my friends, especially Andreas, Jessica, Priscilla and Elena for their patience, for sharing ideas, joys and frustrations and for accepting me just the way I am – thank you.

And to my family... For allowing me to be far from them.

*Gent, August 20, 2007*

v

## TABLE OF CONTENTS

Title page	page i
Declaration	page ii
Abstract	page iii
Abstract (Afrikaans)	page iv
Acknowledgements	page v
Table of Contents	page vi
List of Tables	page xi
List of Figures	page xiii
List of Abbreviations and Symbols	page xxi
List of Products	page xxv

### ***General Introduction and Scope..... 1***

## ***PART A: FUNDAMENTALS OF ELECTRODRIVEN SEPARATION METHODS***

<b><i>Chapter I – Theoretical Considerations..... 5</i></b>	<b>5</b>
I.1 Introduction .....	5
I.2 Fundamental aspects .....	6
I.2.1 Electrophoresis .....	6
I.2.2 Electroosmosis.....	7
I.2.3 Practical parameters influencing EOF .....	10
I.2.3.1 pH.....	10
I.2.3.2 Ionic strength .....	11
I.2.3.3 Temperature.....	11
I.2.3.4 Field strength .....	12
I.2.3.5 Mobile phase composition.....	12
I.2.3.6 Influence of the packed bed.....	13
I.2.4 Retention and selectivity in CEC .....	13

I.2.5 Band broadening in CEC.....	15
I.2.6 Modes of operation in CEC.....	17
I.3 Support materials and stationary phases for CEC.....	17
I.4 Limitations of CEC.....	18
Conclusions.....	19
<b>Chapter II – Instrumental Aspects .....</b>	<b>23</b>
II.1 Introduction .....	23
II.2 Sample injection .....	24
II.2.1 Hydrodynamic injection .....	24
II.2.2 Electrokinetic injection .....	25
II.3 Separation .....	26
II.3.1 Temperature control .....	26
II.3.2 High voltage power supply .....	26
II.4 Detection.....	26
II.4.1 UV-Vis.....	27
II.4.2 Laser-induced fluorescence (LIF) .....	28
II.4.3 MS.....	29
Conclusions .....	32
<b>Chapter III – Sol-gel Technology .....</b>	<b>34</b>
III.1 Introduction.....	34
III.2 Definitions.....	34
III.3 General reactions .....	35
III.4 Strategies and procedures.....	38
III.5 Applications .....	40
Conclusions.....	41
<b>Chapter IV – Column Manufacturing Techniques in CEC.....</b>	<b>43</b>
IV.1 Introduction .....	43
IV.2 Packed columns.....	43
IV.2.1 Frit formation in packed columns .....	44
IV.2.2 Column packing techniques .....	45
IV.2.3 Packing materials.....	46

IV.3 Open tubular columns .....	47
IV.3.1 Column manufacturing procedure.....	48
IV.4 Monolithic columns.....	49
Conclusions.....	50

**PART B: EXPERIMENTAL ELECTROCHROMATOGRAPHY**

**Chapter V – Peak and Sample Capacity in CEC, MEKC and MEEKC ..... 54**

V.1 Introduction .....	54
V.2 Experimental .....	57
V.2.1 Materials .....	57
V.2.2 Analytical conditions .....	57
V.3 Results and discussion .....	58
V.3.1 Peak capacity in CEC, MEKC and MEEKC.....	58
V.3.2 Sample capacity in CEC, MEKC and MEEKC.....	63
V.3.2.1 Influence of the injection time on the efficiency.....	63
V.3.2.2 Influence of the sample concentration on the efficiency ...	67
V.3.2.3 Evaluation of a 0.05% impurity level.....	70
Conclusions.....	71

**Chapter VI – Packed column CEC..... 73**

VI.1 Introduction .....	73
VI.2 Experimental.....	76
VI.2.1 Materials .....	76
VI.2.2 Packing procedure.....	77
VI.2.3 Analytical conditions .....	80
VI.3 Results and discussion.....	80
VI.3.1 Development of the packing procedure .....	80
VI.3.2 Evaluation of the columns .....	85
VI.3.3 Coupling to electrospray ionisation mass spectrometry .....	87
Conclusions.....	90

**Chapter VII – Open Tubular CEC..... 93**

VII.1 Sol-gel procedures.....	93
-------------------------------	----



VII.6.1.2 Sample preparation .....	121
VII.6.1.3 Analytical conditions .....	122
VII.6.2 Results and discussion .....	122
VII.6.2.1 Analysis on C8 columns.....	122
VII.6.2.2 Analysis on C18 columns.....	123
VII.6.2.3 Real sample analysis .....	125
VII.6.3 Conclusions .....	126
VII.7 Application: Separation of positional isomers by Open Tubular CEC.....	126
VII.7.1 Experimental .....	127
VII.7.1.1 Columns.....	127
VII.7.1.2 Test mixtures .....	128
VII.7.1.3 Analytical conditions .....	128
VII.7.2 Results and discussion .....	128
VII.7.2.1 Dihydroxybenzene positional isomers .....	128
VII.7.2.2 Nitrophenol positional isomers .....	130
VII.7.2.3 Mandelic acid enantiomers.....	131
VII.7.3 Conclusions .....	131
<b>General Conclusions .....</b>	<b>134</b>
<b>Summary .....</b>	<b>137</b>

# *L i s t o f T a b l e s*

---

## ***Chapter I – Capillary Electrochromatography***

<b>Table I.1</b>	Common modes of operation in electrodriven separation techniques	5
<b>Table I.2</b>	Mobile phases commonly used in CEC	12

## ***Chapter II – Instrumental Aspects***

<b>Table II.1</b>	Detection methods used in capillary electrodriven separation techniques	27
-------------------	---	----

## ***Chapter III – Sol-gel Technology***

<b>Table III.1</b>	Sol-gel applications in CEC	40
--------------------	-----------------------------	----

## ***Chapter IV – Column Manufacturing Techniques in CEC***

<b>Table IV.1</b>	Column formats used in CEC	43
-------------------	----------------------------	----

## ***Chapter V – Peak and sample capacity in CEC, MEKC and MEEKC***

<b>Table V.1</b>	Linear regression parameters for a plot of peak width at half height ( $w_{1/2}$ ) vs migration time for a phenone homologous series (acetophenone to hexanophenone)	58
<b>Table V.2</b>	Figures of merit for peak capacity in MEKC, MEEKC and CEC.	61

**Chapter VI – Packed column CEC**

<b>Table VI.1</b>	Influence of the length of empty capillary before the inlet frit on the obtained retention time of fluorene, plate number and current. Experiments performed on a capillary packed with 35 cm of 3 $\mu$ m ODS1.	84
<b>Table VI.2</b>	Run-to-run repeatability in terms of retention time and peak efficiency. n=5, column: 35 cm packed bed, total length: 44 cm. MP: 25 mM TRIS.HCl pH 8.0/CH <sub>3</sub> CN 30/70. Injection: 10kV*1s. Voltage: 30 kV. Detection: 200 nm.	86

**Chapter VII – Open Tubular CEC**

<b>Table VII.1</b>	Repeatability for one column run-to-run (A) and column-to-column reproducibility (B). (A) MP: 50/50 50mM TRIS pH 8/CH <sub>3</sub> CN; injection: electrokinetic, 5kV 3s; voltage 25kV. Average of 6 determinations, RT in min. (B) MP: 55/45 50mM TRIS pH 8/CH <sub>3</sub> CN; injection: electrokinetic, 5kV 3s; voltage 25kV. Average of 5 determinations, RT in min.	112
--------------------	---	-----

# L i s t o f F i g u r e s

## **Chapter I – Capillary Electrochromatography**

<b>Figure I.1</b>	Representation of the double layer at the capillary wall	9
<b>Figure I.2</b>	Flow profile and corresponding solute zone	10
<b>Figure I.3</b>	Schematic representation of a packed capillary column	10
<b>Figure I.4</b>	Effect of the pH on EOF mobility in silica [7]	11
<b>Figure I.5</b>	CEC of neutral (A) and charged (B-D) species	14
<b>Figure I.6</b>	HETP-v plots in pressure-driven (dotted lines) and electro-driven (full lines) systems using equation (I.14). Constants for HPLC: A=1.5; B=2 and C=0.1 and for CEC: A=0.7; B=0.2 and C=0.1. Legend: 5 $\mu\text{m}$ , 3 $\mu\text{m}$ and 1 $\mu\text{m}$ particles	16

## **Chapter II – Instrumental Aspects**

<b>Figure II.1</b>	Schematics of a CEC system, also applicable for MEKC and MEEKC	23
<b>Figure II.2</b>	Schematic drawing of a DAD set-up	28
<b>Figure II.3</b>	Schematic drawing of a fluorescence detector set-up	29
<b>Figure II.4</b>	Scheme of an electrospray ionization source and transfer units from atmospheric pressure to the high vacuum in a quadrupole mass spectrometer	30
<b>Figure II.5</b>	Schematic close-up of the electrospray ionization source	30
<b>Figure II.6</b>	Schematic representation of a quadrupole mass analyzer	31
<b>Figure II.7</b>	Basic elements of an ion trap mass spectrometer	32

### **Chapter III – Sol-gel Technology**

<b>Figure III.1</b>	Reactions involved in a sol-gel process	36
<b>Figure III.2</b>	Schematic representation of a sol-gel procedure	36
<b>Figure III.3</b>	General sol-gel reaction mechanism	37
<b>Figure III.4</b>	Non-hydrolytic sol-gel route to inorganic oxides, X=halide	37

### **Chapter IV – Column Manufacturing Techniques in CEC**

<b>Figure IV.1</b>	Schematic drawing of a packed capillary	44
--------------------	---	----

### **Chapter V – Peak and sample capacity in CEC, MEKC and MEEKC**

<b>Figure V.1</b>	Separation of phenones in CEC (top), MEKC (middle) and MEEKC (bottom). CEC: 25 mM TRIS pH 8/ CH <sub>3</sub> CN 85/15; MEKC: 60 mM SDS in 50 mM borate pH 9; MEEKC: 60 mM SDS in 50mM borate pH 9, containing 2% 1-butanol (w/v) and 0.41% n-heptane (w/v)	58
<b>Figure V.2</b>	Influence of SDS concentration on peak capacity in MEKC (left) and MEEKC (right). The numbers represent the SDS concentration in 50 mM borate pH 9. Other conditions as in figure V.1	60
<b>Figure V.3</b>	Calculated peak capacities ( $n_p$ ) for different elution windows for CEC (◆,◇), MEKC (■,□) and MEEKC (▲,△), according to equation V.1 (top) and V.4 (bottom). Separation conditions as in figure V.1, except for MEKC: 60 mM SDS in 50 mM borate pH 9 containing 10% CH <sub>3</sub> CN.	62
<b>Figure V.4</b>	Molecular structures of caffeine, theobromine and theophylline	63
<b>Figure V.5</b>	Efficiency vs injection time plots for MEKC, MEEKC and CEC. The dashed lines represent the 10% loss in	64

	efficiency for theobromine (◆), caffeine (■) and theophylline (▲).	
<b>Figure V.6</b>	Influence of injection time in MEKC. Running buffer: 60 mM SDS in 50 mM borate pH 9	65
<b>Figure V.7</b>	Influence of injection time in MEEKC. Running buffer: 60 mM SDS in 50 mM borate pH 9, containing 2% 1-butanol (w/v) and 0.41% n-heptane (w/v)	66
<b>Figure V.8</b>	Influence of injection time in CEC. Mobile phase: 25 mM NH <sub>4</sub> OAc with unadjusted pH / CH <sub>3</sub> CN 25/75	66
<b>Figure V.9</b>	Efficiency vs sample concentration plots for MEKC, MEEKC and CEC. The dashed lines represent the 10% loss in efficiency for theobromine (◆), caffeine (■) and theophylline (▲)	67
<b>Figure V.10</b>	Influence of sample concentration in MEKC. Running buffer: 60 mM SDS in 50 mM borate pH 9	68
<b>Figure V.11</b>	Influence of sample concentration in MEEKC. Running buffer: 60 mM SDS in 50 mM borate pH 9, containing 2% 1-butanol (w/v) and 0.41% n-heptane (w/v). *: impurity	69
<b>Figure V.12</b>	Influence of sample concentration in CEC. Mobile phase: 25 mM NH <sub>4</sub> OAc with unadjusted pH / CH <sub>3</sub> CN 25/75	69
<b>Figure V.13</b>	Illustration of 0.05% impurities separation in MEKC. Signal to noise ratio 5 for 1 s injection; signal to noise ratio 10 for 2 s injection	70
<b>Figure V.14</b>	Illustration of 0.05% impurities separation in MEEKC. Signal to noise ratio 5 for 2 s injection; signal to noise ratio 10 for 5 s injection	71

#### ***Chapter VI – Packed column CEC***

<b>Figure VI.1</b>	Schematic representation of the column manufacturing process	77
<b>Figure VI.2</b>	Schematic drawing of the tools used in the column manufacturing. A: packing set-up, B: close-up of	79

connection between capillary and packing reservoir (1: fused silica capillary, 2: 1/16" Swagelock nut, 3: 1/16" Swagelock back ferrule, 4: vespel ferrule (0.4mm ID), 5: 1/16"x1/16" Swagelock union, 6: 1/16" Waters ferrule, 7: 1/16" stainless steel HPLC tubing, 8: 1/16" Waters nut, 9: packing reservoir inlet, C: schematic drawing of the frit burning device

- Figure VI.3** Influence of the overheated frits on the peak shape of parabens. Column: 40 cm packed length. MP: 20 mM TRIS.HCl pH 8.9/CH<sub>3</sub>CN 30/70. Injection: 10 kV \* 1 s. Voltage: 30 kV. Peaks: 1: thiourea, 2: methylparaben, 3: ethylparaben, 4: acetophenone, 5: propylparaben, 6: benzene, 7: butylparaben, 8: naphthalene, 9: fluorene, 10: anthracene (800 µg/mL each). Insert: general structure of a paraben 83
- Figure VI.4** Influence of the void volume between column outlet and inlet frit. Packed bed 35 cm. A: 4mm void space before inlet frit, B: 2 mm void space before inlet frit, C: 0.5 mm void space before inlet frit. MP: 20 mM TRIS.HCl pH 8.9/CH<sub>3</sub>CN 30/70. Injection: 10 kV \* 1 s. Voltage: 30 kV. Peaks: 1: thiourea, 2: methylparaben, 3: phenol, 4: ethylparaben, 5: propylparaben, 6: butylparaben, 7: acetphenone, 8: benzene, 9: naphthalene, 10: fluorene, 11: anthracene (800 ppm each in CH<sub>3</sub>CN) 84
- Figure VI.5** Column repeatability. MP: 25 mM TRIS.HCl pH 8.0/CH<sub>3</sub>CN 30/70. Voltage: 30 kV. Injection: 10 kV \* 1 s. Detection: 200 nm. Peaks: 1: thiourea, 2: methylparaben, 3: phenol, 4: ethylparaben, 5: propylparaben, 6: butylparaben, 7: acetphenone, 8: benzene, 9: naphthalene, 10: fluorene, 11: anthracene 86
- Figure VI.6.A** Ohm's plot for the columns evaluated with 20 mM TRIS.HCl buffer, pH 8.9, 70% CH<sub>3</sub>CN 87
- Figure VI.6.B** Corresponding H-u plot for three increasingly retained compounds 87

<b>Figure VI.7</b>	CEC-MS base peak chromatogram of a mixture of 1: triamcinolone acetonide, 2: hydrocortisone acetate and 3: prednisolone	88
<b>Figure VI.8</b>	Base peak chromatogram of an analysis of a mixture of 10 carbamates by CEC-MS. Signal identity (100 ppm each), 1: aldicarb sulfone, 2: 3-hydroxycarbofuran, 3: oxamyl, 4: methomyl, 5: aldicarbsulfoxide, 6: aldicarb, 7: propoxur, 8: carbofuran, 9: sevin (carbaryl), 10: methiocarb	89

### **Chapter VII – Open Tubular CEC**

<b>Figure VII.1</b>	Reaction scheme for the derivatization of cyclodextrins with isocyanatopropyltriethoxysilane	95
<b>Figure VII.2</b>	TGA and DSC of a C8 gel	96
<b>Figure VII.3</b>	TGA and DSC for a C18 gel	97
<b>Figure VII.4</b>	TGA and DSC for amino gel	98
<b>Figure VII.5</b>	TGA and DSC for the cyanopropyl/tetraethoxysilane	98
<b>Figure VII.6</b>	TGA and DSC for $\beta$ CD gel	99
<b>Figure VII.7</b>	SEM images of 50 $\mu$ m capillaries coated with an inhomogeneous C18 gel (A), with a homogeneous C18 gel (B) and with C8 gel (C)	100
<b>Figure VII.8</b>	Parabens separation on C8 column. Mobile phase: 50 mM MES pH 6/CH <sub>3</sub> CN 75/25. Injection: 30 mbar 3 s. Voltage: 25 kV. Peaks: 1. thiourea, 2. methyl-; 3. ethyl-; 4. propyl-; 5. butyl-paraben. The graph indicates the efficiencies for the corresponding peaks	103
<b>Figure VII.9A</b>	PAHs separation on C8 column. Mobile phase: 50 mM MES pH 6/CH <sub>3</sub> CN 55/45. Injection: 50 mbar 3 s. Voltage: 25 kV. Peaks: 1. thiourea, 2. naphthalene; 3. bi-phenyl; 4. fluorene; 5. anthracene; 6. fluoranthene. The graph indicates the efficiencies for the corresponding peaks	103
<b>Figure VII.9B</b>	PAHs separation on C18 column. Mobile phase: 50 mM	104

MES pH 6/CH<sub>3</sub>CN 40/60. Injection: 3 kV 3 s. Voltage: 25 kV. Peaks: 1. thiourea, 2. naphthalene; 3. fluorene; 4. anthracene; 5. fluoranthene. The graph indicates the efficiencies for the corresponding peaks

- Figure VII.10A** Phenones separation on C8 column. Mobile phase: 50 mM MES pH 6/CH<sub>3</sub>CN 50/50. Injection: 40 mbar 2 s. Voltage: 25 kV. Peaks: 1. thiourea, 2. C3-phenone; 3. C4-phenone; 4. C6-phenone; 5. C7-phenone; 6. C8-phenone. The graph indicates the efficiencies for the corresponding peaks 104
- Figure VII.10B** Phenones separation on C18 column. Mobile phase: 50 mM MES pH 6/CH<sub>3</sub>CN 40/60. Injection: 3 kV 3 s. Voltage: 25 kV. Peaks: 1. C3-phenone; 2. C4-phenone; 3. C6-phenone; 4. C7-phenone; 5. C8-phenone. The graph indicates the efficiencies for the corresponding peaks 105
- Figure VII.11** Effect of acetonitrile percentage variation on the current (◇C8 column, △C18 column) and on the EOF velocity (◆C8 column, ▲C18 column). Average of 3 determinations 106
- Figure VII.12** In *k* vs percentage of acetonitrile for parabens (◆ methyl-, ■ ethyl-, ▲ propyl-, \* butyl-paraben) on a C8 column. Average of 3 determinations 106
- Figure VII.13** Influence of pH on the EOF velocity for ■ C8 and ▲C18 stationary phase. Mobile phase: 20 mM phosphate/CH<sub>3</sub>CN 50/50. Voltage: 25 kV. Average of 3 determinations 107
- Figure VII.14** EOF velocity vs pH for amino columns. Buffer: 20 mM phosphate. Voltage: ± 25kV. Average of 3 determinations 108
- Figure VII.15** Efficiency versus buffer concentration for the methyl- (◇), ethyl- (△), propyl- (□) and butyl- (x) paraben on a C8 column. Average of 3 determinations. Mobile phase: MES pH 6/ CH<sub>3</sub>CN 45/55. Voltage: 25kV 109

<b>Figure VII.16</b>	EOF velocity vs applied voltage for C8 (■) and C18 (▲) columns. Mobile phase: 50 mM MES/ CH <sub>3</sub> CN 50/50. Average of 3 determinations	110
<b>Figure VII.17</b>	<i>h-u</i> plot for thiourea (A) and anthracene (B) at 15°C (■), 20°C (◆) and 25°C (▲). Average of 3 determinations. Mobile phase: 50 mM TRIS pH 8/ CH <sub>3</sub> CN 50/50	111
<b>Figure VII.18</b>	Reductive amination reaction	113
<b>Figure VII.19</b>	Derivatization reagent (fluorescent label) 9-aminopyrene-1,4,6-trisulfonic acid (APTS) and oligosaccharides used for the test mixture (M=mannose, M <sub>x</sub> *= x mannose units in a molecule, * indicates the presence of isomers)	113
<b>Figure VII.20</b>	Separation of G5-G7-APTS derivatives on C8 column. Mobile phase: 25 mM NH <sub>4</sub> AcO/CH <sub>3</sub> CN 80/20. Voltage: -25 kV	115
<b>Figure VII.21</b>	Separation of APTS-derivatized RNaseB sugars on C8 column. Buffer: 25 mM NH <sub>4</sub> AcO/CH <sub>3</sub> CN A. 70/30, B. 80/20. Voltage: -25 kV	116
<b>Figure VII.22</b>	Maltooligosaccharide ladder. APTS-derivatives separated on amino column. Buffer: 25 mM NH <sub>4</sub> AcO. Voltage: -25 kV	117
<b>Figure VII.23</b>	Separation of APTS-derivatized RNaseB sugars on amino column. Buffer: 25 mM NH <sub>4</sub> AcO. Voltage: -25 kV	118
<b>Figure VII.24</b>	Separation of A. APTS-derivatized G5-G7 test mix and B. APTS-derivatized RNaseB sugars on cyano column. Buffer: 25 mM NH <sub>4</sub> AcO. Voltage: -25 kV	119
<b>Figure VII.25</b>	Influence of organic modifier content on the separation of APTS-derivatized RNaseB sugars on cyano column. Buffer: 25 mM NH <sub>4</sub> AcO containing 0, 5 and 10% CH <sub>3</sub> CN. Voltage: -25 kV	120
<b>Figure VII.26</b>	Molecular structures of caffeine, theobromine and theophylline	121
<b>Figure VII.27</b>	Influence of SDS concentration on the separation of	123

	theobromine (1), caffeine (2) and theophylline (3) on C8 stationary phase. Buffer: 10 mM borate pH 8.6 containing A. 10 mM SDS, B. 0 mM SDS. Voltage: 20 kV	
<b>Figure VII.28</b>	Influence of buffer concentration on the separation of theobromine (1), caffeine (2) and theophylline (3) on C18 stationary phase. Buffer: A. 10 mM borate pH 8.5 containing 10 mM SDS, B. 25 mM borate pH 8.5 containing 10 mM SDS. Voltage: 10 kV	124
<b>Figure VII.29</b>	Influence of buffer concentration on the separation of theobromine (1), caffeine (2) and theophylline (3) on C18 stationary phase. Buffer: A. 10 mM borate pH 9.0 containing 10 mM SDS, B. 25 mM borate pH 9.0 containing 10 mM SDS. Voltage: 10 kV	125
<b>Figure VII.30</b>	Analysis of instant cocoa beverage. Separation conditions 25 mM borate containing 10 mM SDS, voltage: +10 kV, injection: 50 mbar * 6 s, temperature: 20°C	125
<b>Figure VII.31</b>	Analysis of instant cocoa and malt beverage. Separation conditions 25 mM borate containing 10 mM SDS, voltage: +10 kV, injection: 50 mbar * 6 s, temperature: 20°C	126
<b>Figure VII.32</b>	Inclusion complexation scheme	127
<b>Figure VII.33</b>	Influence of organic modifier content on the separation of dihydroxybenzenes on $\beta$ cyclodextrin stationary phase. Mobile phase: 50 mM phosphate pH 7.3/ CH <sub>3</sub> CN A. 100/0, B. 95/5, C. 90/10. Voltage: 25 kV. Peaks: 1. EOF marker, 2. m-, 3. o-, 4. p- dihydroxybenzene	129
<b>Figure VII.34</b>	Inclusion complexes for positional isomers	130
<b>Figure VII.35</b>	Influence of the nature of the organic modifier on the separation of nitrophenols on $\beta$ cyclodextrin stationary phase. Mobile phase: 50 mM MES pH 6.1/organic modifier 95/5. Organic modifier: A. CH <sub>3</sub> CN, B: methanol. Peaks: 1. EOF marker, 2. m-, 3. o-, 4. p- nitrophenol	131

## List of Abbreviations and Symbols

<b>Abbreviation</b>	<b>Description</b>
<i>%RSD</i>	Relative Standard Deviation
<i>μLC</i>	micro Liquid Chromatography
<i>AFM</i>	Atomic Force Microscopy
<i>APCI</i>	Atmospheric Pressure Chemical Ionization
<i>API</i>	Atmospheric Pressure Ionization
<i>API</i>	Active Pharmaceutical Ingredient
<i>APTS</i>	aminopropyl triethoxysilane
<i>APTS</i>	9-aminopyrene-1,4,6 trisulfonic acid
<i>ATR</i>	Attenuated Total Reflectance
<i>C18TMOS</i>	octadecyl trimethoxysilane
<i>C8TEOS</i>	octyl triethoxysilane
<i>CD</i>	cyclodextrin
<i>CE</i>	Capillary Electrophoresis
<i>CEC</i>	Capillary Electrochromatography
<i>CF-FAB</i>	Continuous Flow-Fast Atom Bombardment
<i>cGC</i>	Capillary Gas Chromatography
<i>CGE</i>	Capillary Gel Electrophoresis
<i>cLC</i>	capillary LC
<i>CZE</i>	Capillary Zone Electrophoresis
<i>DAD</i>	Diode Array Detection
<i>DMS</i>	dynamically adsorbed stationary phases
<i>DSC</i>	differential scanning calorimetry
<i>EKC</i>	Electrokinetic Chromatography
<i>EOF</i>	Electroosmotic Flow
<i>ESI</i>	Electrospray Ionization
<i>FT-IR</i>	Fourier transform infrared microscopy
<i>GPTMS</i>	glycidoxypropyl trimethoxysilane
<i>HPLC</i>	High Pressure Liquid Chromatography

<i>HR-TEM</i>	High Resolution Transmission Electron Microscopy
<i>HVPS</i>	High Power Voltage Supply
<i>ICPTS</i>	isocyanatopropyl triethoxysilane
<i>IEF</i>	Isoelectric Focusing
<i>ITP</i>	Isotachophoresis
<i>LC</i>	Liquid Chromatography
<i>LIF</i>	Laser Induced Fluorescence
<i>MEEKC</i>	Microemulsion Electrokinetic Chromatography
<i>MEKC</i>	Micellar Electrokinetic Chromatography
<i>MES</i>	2-[N-morpholino]ethanesulfonic acid]
<i>MIP</i>	Molecularly Imprinted Polymers
<i>MP</i>	Mobile Phase
<i>MS</i>	Mass Spectrometry
<i>NMR</i>	Nuclear Magnetic Resonance
<i>NP</i>	Normal Phase
<i>ODS</i>	octadecyl silica
<i>OTCEC</i>	Open Tubular CEC
<i>PAS</i>	Physically Adsorbed Stationary Phases
<i>pCEC</i>	packed CEC
<i>PEC</i>	Pressure-assisted Chromatography
<i>RP</i>	Reversed Phase
<i>SAX</i>	Strong Anion Exchanger
<i>SCX</i>	Strong Cation Exchanger
<i>SEM</i>	Scanning Electron Microscopy
<i>SP</i>	stationary phase
<i>SSQO</i>	silsesquioxanes
<i>TEOS</i>	tetraethoxysilane
<i>TGA</i>	Thermogravimetric Analysis
<i>TMOS</i>	Tetramethoxysilane
<i>TRIS</i>	tris[hydroxymethyl]aminomethane
<i>UV-Vis</i>	Ultra Violet-Visible

## List of symbols

$\mu_e$	electrophoretic mobility
$\mu_{EO}$	EOF mobility
$1/k$	double layer thickness
$A$	eddy diffusion term (van Deemter)
$B$	longitudinal diffusion term (van Deemter)
$c$	Concentration
$C$	mass resistance term (van Deemter)
$d_c$	open tube internal diameter
$d_f$	film thickness
$d_p$	particle diameter
$E$	applied electric field
$F_E$	electric force
$F_F$	friction force
$ID$	internal diameter
$k$	retention factor
$k_C$	CEC retention factor
$k_E$	velocity factor (CE)
$L$	column length
$pK_a$	acidity constant
$q$	ion charge
$Q$	quantity
$r$	ion radius (spherical)
$Rs$	resolution
$r$	capillary radius
$RT$	retention time
$T$	temperature (K)
$t_0$	retention time (unretained analyte)
$t_E$	elution time
$t_M$	migration time (EOF marker)
$t_R$	retention time (retained analyte)

$v$	ion velocity
$V$	applied voltage
$v_p$	EOF velocity generated by the packing surface
$a$	selectivity
$\delta$	double layer thickness
$\epsilon$	electric permittivity
$\epsilon_0$	permittivity of vacuum
$\epsilon_C$	total column porosity
$\zeta$	zeta potential
$\zeta_p$	zeta potential generated at the particle surface
$\zeta_w$	zeta potential generated at the wall surface
$\eta$	solution viscosity
$\sigma$	charge density
$\sigma^*$	packed segment conductivity
$\sigma^*/\sigma_b$	conductivity ratio
$\sigma_b$	open segment conductivity

## *L i s t o f p r o d u c t s*

---

Fused silica capillaries 50  $\mu\text{m}$  ID were purchased from Polymicro Technologies (Phoenix, AZ, USA). TRIS, MES, triethylamine, formic acid, were provided by Sigma-Aldrich (Atlasville, South Africa). Packed capillaries (48.5 cm  $L_{\text{tot}}$ , 100  $\mu\text{m}$  ID packed with 3  $\mu\text{m}$  octadecylsilica particles) were purchased from Agilent (Waldbronn, Germany). Hydrochloric acid was from Merck (Darmstadt, Germany). All solvents ( $\text{CH}_3\text{CN}$ , MeOH, benzyl alcohol and toluene) were HPLC grade and were provided by Riedel-de Haën (Midrand, South Africa). Milli-Q water was obtained by purification and deionisation of tap water in a Milli-Q plus water system (Millipore, Bedford, MA, USA).

3  $\mu\text{m}$  Spherisorb ODS-1 was kindly donated by Dr. P. Meyers (X-Tec, Leeds, UK). Nucleosil 300-5 pure silica particles used for the temporary frit production were purchased from Macherey-Nagel (Düren, Germany). The sodium silicate solution was made by dissolving 180 mg native Nucleosil silica in 500  $\mu\text{L}$  of a 19% (w/w) NaOH solution. After one hour in an ultrasonic bath heated at 50°C, a transparent solution is obtained.

Maltopentaose, -hexaose and -heptaose, dextrin 15 and bovine ribonuclease B (RNaseB) were obtained from Sigma-Aldrich (St. Louis, MO). Peptide-N-glycosidase F (Roche Diagnostics GmbH, Mannheim, Germany). Carbograph column (Alltech, Lokeren, Belgium). 8-aminopyrene-1,4,6-trisulfonic acid (APTS) (Beckman-Coulter, Fullerton, CA)

### **Instruments**

LC-307 pump, Gilson Medical, Villiers le Bel, France (packing, **Chapter VI**)

Ultrasonic bath used for packing (**Chapter VI**) was an Ultrasonic LC20H from BJ Oberholzer & Co, Cape Town, South Africa.

GC 8340 system from Fisons Instruments, Milano, Italy (thermal treatment, sol-gel capillaries, **Chapter VII**)

SEM images have been provided by a fully analytical scanning electron microscope, model LEO S440 (**Chapter VII**).

TDS and DSC analysis were performed on TGA Q500 V6.3, TA Instruments and DSC Q100 V9.0, TA Instruments (**Chapter VII**).

CEC-UV chromatograms were obtained with the Agilent <sup>3D</sup>CE (Hewlett-Packard GmbH, Waldbronn, Germany) instrument equipped with a DAD detector. Pressurization was not necessary in the case of OTCEC. The <sup>3D</sup>CE system comprises the <sup>3D</sup>CE instrument and the <sup>3D</sup>CE ChemStation software.

CEC-LIFD analyses (**Chapter VII**) were performed on a Beckman P/ACE 2100 capillary electrophoresis system equipped with a laser-induced fluorescence detector (3 mW, 488-nm Ar ion laser).

CEC-MS analyses (**Chapter VI**) were performed on an HP<sup>3D</sup>CE system equipped with a diode array detector (Agilent Technologies, Waldbronn, Germany).

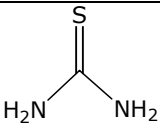
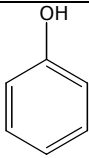
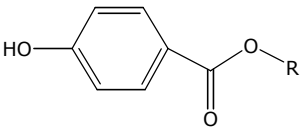
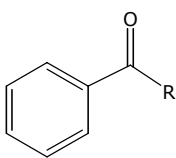
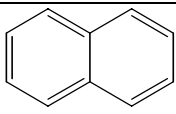
A commercially available sheath flow interface was used for ESI/MS detection on an Agilent MSD Ion Trap XCT system (Agilent Technologies, Waldbronn, Germany).

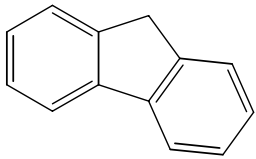
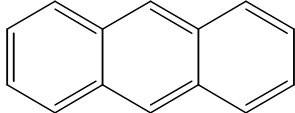
**Table A.1** Sol-gel precursors (**Chapter VII**)

3-aminopropyl triethoxysilane (APTS)	$\text{NH}_2(\text{CH}_2)_3\text{Si}(\text{OEt})_3$	Fluka, Buchs, Switzerland
3-cyanopropyl triethoxysilane (CPTS)	$\text{NC}(\text{CH}_2)_3\text{Si}(\text{OEt})_3$	Aldrich, Milwaukee, WI, USA
Octadecyl trimethoxysilane (C18TMOS)	$\text{CH}_3(\text{CH}_2)_{16}\text{CH}_2\text{Si}(\text{OMe})_3$	Fluka, Buchs, Switzerland
Octyl triethoxysilane (C8TEOS)	$\text{CH}_3(\text{CH}_2)_6\text{CH}_2\text{Si}(\text{OEt})_3$	Aldrich, Milwaukee, WI, USA
Tetraethoxyorthosilane (TEOS)	$\text{Si}(\text{OEt})_4$	Fluka, Buchs, Switzerland

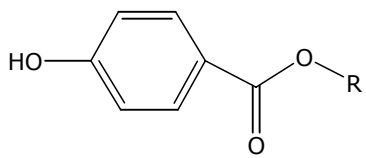
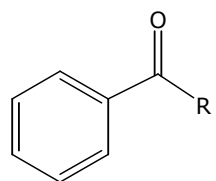
## Sample mixtures

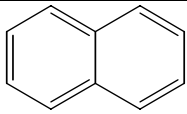
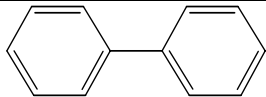
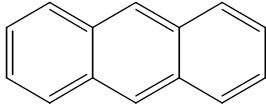
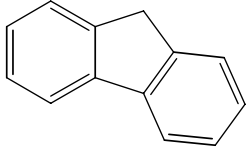
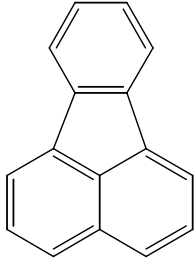
**Table A.2** Packed CEC test mixture for column evaluation (*Chapter VI*)

Compound	Structure	Supplier
Thiourea		Fluka Chemie AG, Buchs, Switzerland
Phenol		Merck, Darmstadt, Germany
Methylparaben	R=CH <sub>3</sub> 	Fluka Chemie AG, Buchs, Switzerland
Ethylparaben	R=CH <sub>2</sub> CH <sub>3</sub>	Fluka Chemie AG, Buchs, Switzerland
Propylparaben	R=(CH <sub>2</sub> ) <sub>2</sub> CH <sub>3</sub>	Fluka Chemie AG, Buchs, Switzerland
Butylparaben	R=(CH <sub>2</sub> ) <sub>3</sub> CH <sub>3</sub>	Fluka Chemie AG, Buchs, Switzerland
Acetophenone	R=CH <sub>3</sub> 	Sigma-Aldrich, Atlasville, South Africa
Benzene		Sigma-Aldrich, Atlasville, South Africa
Naphthalene		Merck, Darmstadt, Germany

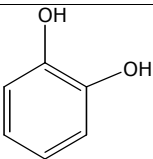
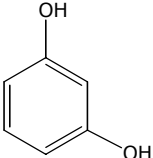
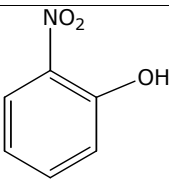
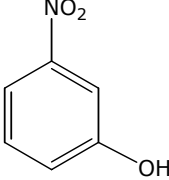
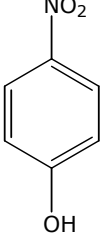
Compound	Structure	Supplier
Fluorene		Sigma-Aldrich, Atlasville, South Africa
Anthracene		Sigma-Aldrich, Atlasville, South Africa

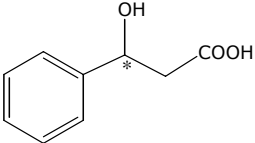
**Table A.3** Open tubular CEC test mixtures for column and system evaluation (*Chapter VII*)

Test mixtures	Compound	Structure	Supplier
Parabens	Methylparaben	R=CH <sub>3</sub> 	Fluka Chemie AG, Buchs, Switzerland
	Ethylparaben	R=CH <sub>2</sub> CH <sub>3</sub>	Fluka Chemie AG, Buchs, Switzerland
	Propylparaben	R=(CH <sub>2</sub> ) <sub>2</sub> CH <sub>3</sub>	Fluka Chemie AG, Buchs, Switzerland
	Butylparaben	R=(CH <sub>2</sub> ) <sub>3</sub> CH <sub>3</sub>	Fluka Chemie AG, Buchs, Switzerland
	Thiourea	See table A.2	Fluka Chemie AG, Buchs, Switzerland
Phenones	Propiophenone	R=CH <sub>2</sub> CH <sub>3</sub> 	Sigma-Aldrich, Atlasville, South Africa
	Butyrophenone	R=(CH <sub>2</sub> ) <sub>2</sub> CH <sub>3</sub>	Sigma-Aldrich, Atlasville, South Africa
	Hexanophenone	R=(CH <sub>2</sub> ) <sub>4</sub> CH <sub>3</sub>	Sigma-Aldrich,

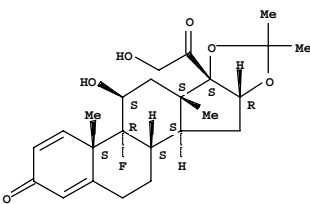
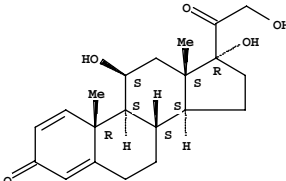
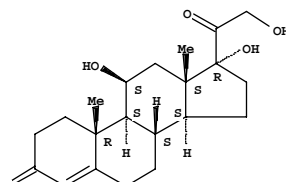
Test mixtures	Compound	Structure	Supplier
			Atlasville, South Africa
	Heptanophenone	$R=(CH_2)_5CH_3$	Sigma-Aldrich, Atlasville, South Africa
	Octanophenone	$R=(CH_2)_6CH_3$	Sigma-Aldrich, Atlasville, South Africa
	Thiourea	See table A.2	Fluka Chemie AG, Buchs, Switzerland
<b>PAHs</b>	Naphthalene		Merck, Darmstadt, Germany
	Bi-phenyl		Fluka Chemie AG, Buchs, Switzerland
	Anthracene		Fluka Chemie AG, Buchs, Switzerland
	Fluorene		Fluka Chemie AG, Buchs, Switzerland
	Fluoranthene		Fluka Chemie AG, Buchs, Switzerland
	Thiourea	See table A.2	Fluka Chemie AG, Buchs, Switzerland

**Table A.3** Positional isomers test mixtures (*Chapter VII*)

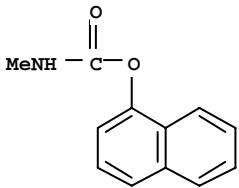
Test mixtures	Compound	Structure	Supplier
<b>Cresols</b>	o-dihydroxybenzene		Merck, Darmstadt, Germany
	m-dihydroxybenzene		Merck, Darmstadt, Germany
	p-dihydroxybenzene		Merck, Darmstadt, Germany
	Thiourea	See table A.2	Fluka Chemie AG, Buchs, Switzerland
<b>Nitrophenols</b>	o-nitrophenol		Judex Chemicals, Sudbury, UK
	m-nitrophenol		Hopkin&Williams Ltd, Chadwell Heath, UK
	p-nitrophenol		BDH Chemicals Ltd, Poole, UK
	Thiourea	See table A.2	Fluka Chemie AG, Buchs,

			Switzerland
<b>Racemate</b>	±mandelic acid		

**Table A.4** Packed CEC-MS test mixtures (*Chapter VI*)

Test mixtures	Compound	Structure	Supplier
<b>Steroids</b>	triamcinolone acetone		Merck, Darmstadt, Germany
	prednisolone		Merck, Darmstadt, Germany
	hydrocortisone		Merck, Darmstadt, Germany
<b>Carbamates</b>	oxamyl	$\text{Me}_2\text{N}-\overset{\text{O}}{\parallel}{\text{C}}-\overset{\text{SMe}}{\text{C}}=\text{N}-\text{O}-\overset{\text{O}}{\parallel}{\text{C}}-\text{NHMe}$	Supelco, Bornem, Belgium
	methomyl	$\text{MeNH}-\overset{\text{O}}{\parallel}{\text{C}}-\text{O}-\text{N}=\overset{\text{SMe}}{\text{C}}-\text{Me}$	Supelco, Bornem, Belgium

	aldicarb sulfone		Supelco, Bornem, Belgium
	aldicarb		Supelco, Bornem, Belgium
	aldicarb sulfoxide		Supelco, Bornem, Belgium
	3-hydroxycarbofuran		Supelco, Bornem, Belgium
	methiocarb		Supelco, Bornem, Belgium
	carbofuran		Supelco, Bornem, Belgium
	propoxur		Supelco, Bornem, Belgium

	carbaryl	 <chem>CNC(=O)c1ccc2ccccc12</chem>	Supelco, Bornem, Belgium
--	----------	--	-----------------------------

## *General Introduction and Scope*

---

In the past two decades many variants of capillary electrophoresis (CE) have emerged. Of particular interest thereby are the techniques combining an electrophoretic separation with a chromatographic partitioning process. The latter can take place on an immobilized stationary phase or in a two phase solution, one of which being the pseudostationary phase.

In the case of Micellar Electrokinetic Chromatography (MEKC), micelles that are formed in the running buffer when the surfactant concentration is above its critical micelle concentration (CMC) form the pseudostationary phase. In the case of Microemulsion Electrokinetic Chromatography (MEEKC), stable, surfactant-coated nanometre-sized oil droplets dispersed in a microemulsion form the pseudostationary phase. Capillary electrochromatography (CEC) can be considered a variant of high performance liquid chromatography (HPLC), in which the mobile phase flow is electro-driven instead of pressure-driven. Packed column CEC was the first approach to this electrodriven separation mode, based on the intuitive translation from pressure-driven LC towards electro-driven CEC and on the direct availability of the stationary phases from HPLC. Open tubular CEC came into consideration due to ease of column manufacture, the low back-pressure and the expected ease of coupling to electrospray ionization mass spectrometry (ESI-MS).

All techniques show the potential of achieving high efficiencies as the flow boundary is flat as opposed to the parabolic flow in pressure driven systems. In addition, the selectivity can be easily manipulated by changing the nature of the stationary phase and of the micelle's composition.

Currently, the main drawbacks in the case of MEKC and MEEKC arise from difficulties of coupling with MS, due to the presence of non-volatile compounds in

the running buffer. For packed column CEC, also problems with MS coupling have been extensively reported. This problem is related to bubble formation at the frits immobilizing the packed bed. Open tubular CEC columns cannot suffer from this drawback and should be easily coupled with MS detection. However, these columns suffer from low phase ratio and slow loss of the stationary phase by bleeding.

Even though the techniques are based on the combination of the same two phenomena (electrophoretic and chromatographic), a direct comparison is difficult to achieve because of the different experimental conditions required and because different types of samples are often used. This leads to a lack of understanding of the strengths and drawbacks of these techniques.

In this thesis the advantages and disadvantages of the various capillary electrodriven chromatographic techniques – namely CEC in its packed and open tubular column format, MEKC and MEEKC are investigated. The techniques are evaluated from column manufacturing (in the case of CEC columns) to the testing of their basic chromatographic characteristics and on their applicability compared to HPLC. Special attention is also given to the robustness of all electrodriven separation methods.

In *Chapter I* fundamental notions in electrodriven separations, such as electrophoresis, electroosmosis and factors influencing these phenomena, are discussed.

*Chapter II* outlines the instrumentation currently used for CEC, MEKC and MEEKC analysis.

In *Chapter III* the current status of sol-gel technology to be used for the making of capillary columns is discussed.

In *Chapter IV* the present state of column technology for CEC, for both packed and open tubular formats is examined. Issues related to packing materials, column designs, packing techniques and reproducibility of the manufacturing

process are presented for the packed column format. For open tubular columns, stationary phase requirements and column formats are discussed.

In *Chapter V*, three techniques are compared in terms of separation power and sample capacity. Packed CEC, MEKC and MEEKC are tested in similar conditions and the peak capacity is calculated in order to determine the separation power of each technique. The sample capacity is determined through a number of different approaches. To the best of our knowledge, this is the first precise comparison of these aspects for the three techniques.

In *Chapter VI*, the manufacturing and evaluation of packed CEC columns is described, and ways of suppressing bubble formation are investigated for coupling to MS.

In *Chapter VII*, the manufacturing and evaluation of open tubular CEC columns is discussed. Physical means of characterisation, such as SEM, TGA and DSC, are used to describe the types of gels further used as stationary phases. These columns are evaluated in CEC for various applications.

Finally, the thesis advances some guidelines related to the practical use of electrodriven chromatographic methods and to robustness issues.

**PART A:**  
**Fundamentals of Electrodriven Separation Methods**

## Chapter I

# Theoretical Considerations

### I.1 Introduction

Electrodriven separation methods comprise a family of techniques in which the separation of analytes is achieved by differences in their migration rates in an electric field and/or by a partitioning mechanism between a (pseudo) stationary phase and a liquid phase, which is driven by the electric field.

The versatility of these techniques derives from the numerous modes of operation, the most important of which are overviewed in Table I.1.

**Table I.1** Common modes of operation in electrodriven separation techniques

Mode	Separation mechanism
Capillary Zone Electrophoresis (CZE)	▪ Free solution mobility
Micellar Electrokinetic Chromatography (MEKC)	▪ Hydrophobic/ionic interactions with micelles
Microemulsion Electrokinetic Chromatography (MEEKC)	▪ Hydrophobic/ionic interactions with stabilized micelles
Capillary Gel Electrophoresis (CGE)	▪ Size and charge
Isoelectric Focusing (IEF)	▪ Isoelectric point
Isotachopheresis (ITP)	▪ Moving boundaries
Capillary Electrochromatography (CEC)	▪ Partitioning between immobilized bed and mobile phase ▪ Free solution mobility

CZE is the most widely used mode due to its simplicity of operation and versatility.

The first five modes (see Table I.1) differ from capillary electrochromatography (CEC) in the way that the former are free solution techniques, while CEC involves a stationary phase. Ample literature is already available about MEKC and MEEKC.

These techniques will not be discussed in this chapter and therefore the emphasis will be on CEC.

*Capillary electrochromatography (CEC)* can be considered a variant of HPLC, in which the mobile phase flow is electro-driven instead of pressure-driven. This flow is a result of the formation of an electrical double layer through the deprotonation of silanol groups on the capillary wall and the silica particles. When along this double layer an electric field is applied, the bulk of the liquid in the capillary will be put in motion. This phenomenon is called the *electroosmotic flow (EOF)*.

The use of an electro-driven flow in CEC as compared to a pressure-driven flow in HPLC leads to much higher efficiencies in CEC as compared to HPLC. Efficiencies can easily reach 300,000 plates/m. A more detailed discussion will follow in this chapter.

## **I.2 Fundamental aspects**

The presence of an electric field causes the movement of sample ions by *electrophoresis* and bulk flow of the electrolyte solution by *electroosmosis*.

### **I.2.1 Electrophoresis**

**Electrophoresis** is defined as the differential movement of charged solutes (ions) in an electrolyte solution under the influence of an electric field. Therefore, separation by electrophoresis is based on the differences in solute velocity in an electric field. The velocity of an isolated ion in solution is given by

$$v = \mu_e E \quad (I.1)$$

where  $v$  is the ion velocity,  $\mu_e$  its electrophoretic mobility and  $E$  the applied electric field.  $E$  is a function of the applied voltage ( $V$ ) over the capillary length ( $L$ ).

$$E = \frac{V}{L} \quad (I.2)$$

The mobility, for a given ion and medium in which the separation takes place, is a characteristic constant for each ion at infinite dilution. It can be derived from two forces acting on the ion.

An electric force that can be expressed as

$$F_E = qE \quad (I.3)$$

and a friction force counter-balancing it is given by

$$F_F = -6\pi\eta rv \quad (I.4)$$

where  $q$  is the ion charge,  $\eta$  the solution viscosity and  $r$  the ion radius (spherical).

During electrophoresis the ion obtains a constant velocity and the balance between the electric and friction force is in equilibrium, which leads to

$$qE = -6\pi\eta rv \quad (I.5)$$

By substituting  $v$  (I.1) in (I.5), the ion mobility can be expressed as

$$\mu_e = \frac{q}{6\pi\eta r} \quad (I.6)$$

From equation I.6 it can be seen that small, highly charged ions have high mobilities and large ions with low charges have low mobilities.

Mobility values can be found in tables as physical constants, calculated at the point of full ion charge and at infinite dilution. These theoretical values differ substantially from the ones determined experimentally. The latter are called *effective mobilities* and are dependent on pH and composition of the running buffer.

### 1.2.2 Electroosmosis

Under the influence of an applied electric field, a liquid containing an electrolyte will move relative to a stationary charged surface, a process known as *electroosmosis* [1]. The *electroosmotic flow (EOF)* is the bulk flow of liquid in a fused silica capillary and it is a consequence of the surface charge on the interior

capillary wall when an electric field is applied (Figure I.1). The surface charge is usually acquired as a result of ionisation. Under aqueous conditions, most solid surfaces have an excess of negative charge. This results from ionisation of the surface and/or from adsorption of ionic species at the surface. In the case of a silica surface, the EOF is mainly controlled by the number of silanol groups (SiOH) that can exist in ionized form (SiO<sup>-</sup>). Experimentally, for silica, the EOF becomes significant above pH 4. Counterions are drawn to the negatively charged surface (wall) (with potential  $\psi_0$ ) to maintain a charge balance in the solution, and a double layer is formed. The potential associated with this layer at the plane of shear is known as the *zeta potential*,  $\zeta$ . The wall potential ( $\psi_0$ ) will fall exponentially through the diffuse layer and eventually reaches zero. The distance from the wall where this potential has dropped by a factor  $e^{-1}$  is known as the *double layer thickness* ( $\delta$ ). The thickness of the electrical double layer is related to the concentration (c) and the valence (z) of the electrolyte by means of the ionic strength (I)

$$\delta = \sqrt{\frac{\varepsilon RT}{2000F^2 I}} \quad (I.7)$$

where R is the gas constant, T the absolute temperature, F the Faraday constant and  $\varepsilon = \varepsilon_0 \varepsilon_r$  in which  $\varepsilon_0$  is the permittivity of a vacuum and  $\varepsilon_r$  the relative permittivity, or dielectric constant, of the medium. When voltage is applied across the capillary, the cations forming the diffuse double layer are attracted towards the cathode. Because they are solvated, their movement drags the bulk solution in the capillary towards the cathode as well (Figure I.1).

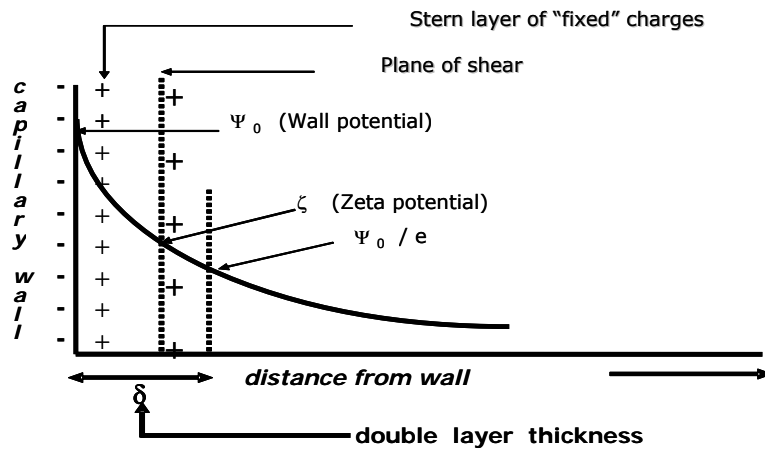


Figure I.1 Representation of the double layer at the capillary wall

The magnitude of the EOF can be expressed in terms of velocity ( $v_{EO}$ ) or mobility ( $\mu_{EO}$ ) to make it independent of the capillary length and the applied voltage (with  $\epsilon$  being the dielectric constant).

$$v_{EO} = \frac{\epsilon \zeta}{\eta} E \quad (I.8)$$

or

$$\mu_{EO} = \frac{\epsilon \zeta}{\eta} \quad (I.9)$$

A unique feature of the EOF is its flat flow profile. Since the driving force is uniformly distributed across and along the capillary, the flow is nearly uniform throughout. This is in contrast to the laminar or parabolic flow generated by a pump (Figure I.2). In the latter case the flow rate drops rapidly near the capillary wall. This is due to the boundary condition that there is no slip at the wall surface.

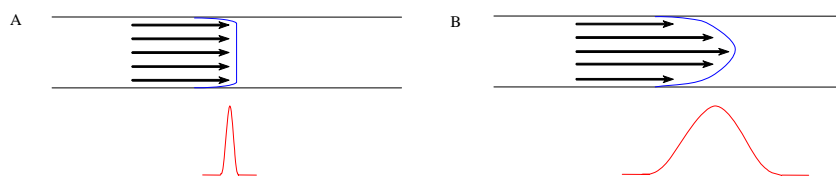


**Figure I.2** Flow profile and corresponding solute zone

The majority of columns used in CEC are packed columns. Commonly, a packed column includes a packed and an open segment (Figure I.3). The electroosmotic phenomenon in porous media is complex and at the same time of great importance. The EOF is responsible for the bulk transport of the mobile phase and analytes. In the absence of EOF, only species with an appropriate charge will be able to migrate. The principles and mechanism of this parameter are not yet fully understood in CEC. Theoretical and practical considerations affecting the EOF have been extensively treated in the literature [2-6].

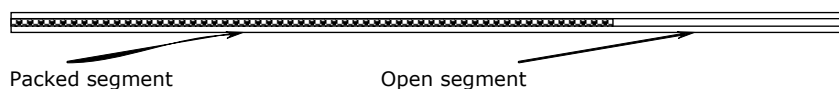


**Figure I.3** Schematic representation of a packed capillary column

### I.2.3 Practical parameters influencing EOF

#### I.2.3.1 pH

The most important parameter influencing the EOF is the pH of the mobile phase. The zeta potential is essentially determined by the surface charge on the capillary walls, which is in itself dependent on the pH. The silanol groups on fused silica have a  $pK_a$  value of 5-6, hence an EOF can be observed from a pH of 3 and a plateau is observed around pH 8 (Figure I.4) [7].

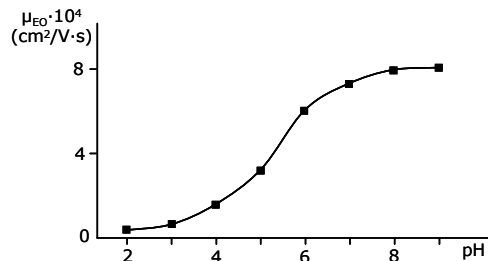


Figure I.4 Effect of the pH on EOF mobility in silica [7]

The addition of organic modifiers usually results in a shift of the  $pK_a$  values of the silanol groups to higher values [7].

### I. 2.3.2 Ionic strength

The zeta potential (and, hence, the EOF) is dependent on the ionic strength ( $I = \frac{1}{2} \sum_i z_i^2 c_i$ ) of the buffer (see double layer theory). An increased ionic strength results in double-layer compression, a decreased zeta-potential and therefore a reduced EOF. This phenomenon is further amplified by an increase of the viscosity of the mobile phase with increasing ionic strength leading to another reduction of the EOF [7-10]. In practice, ionic strengths originating from electrolyte concentrations between 1 and 20 mM are generally used [5]. Low ionic strengths combined with higher temperatures (to reduce viscosity) have been used by some authors [14].

### I.2.3.3 Temperature

Temperature changes the EOF velocity because of its effects on the viscosity of the medium, its dielectric constant and the zeta potential. In general, an increase in the temperature of the mobile phase will increase its velocity.

#### I.2.3.4 Field strength

From the theoretical relationship (I. 8) between the EOF velocity and the applied electric field,  $v_{EO}$  should be directly proportional to  $E$ , or to the applied voltage  $V$ , if the column length  $L$  is kept constant.

Deviations from linearity have been noticed at high field strengths because of Joule heating which reduces the viscosity and hence increases the EOF (I.2.3.3) [8, 9].

#### I.2.3.5 Mobile phase composition

Typically, mobile phases in CEC consist of a mixture of an aqueous buffer with one or more organic modifiers such as acetonitrile. Even though some authors have used, non-buffered mobile phases [10], there is severe concern about the stability of the EOF and thus about the reproducibility of the data obtained.

The use of zwitterionic buffers is often favoured as the current generated by these buffers is much lower compared to their inorganic analogues. An overview of the most commonly used mobile phase compositions is given in Table I.2.

**Table I.2** Mobile phases commonly used in CEC

Type of mobile phase	Organic modifier
<ul style="list-style-type: none"> <li>• aqueous</li> </ul>	acetonitrile, methanol, ethanol, tetrahydrofuran
<ul style="list-style-type: none"> <li>• non-aqueous</li> </ul>	n-hexane, dimethylformamide, acetonitrile, methanol
<b>Buffers</b>	
<ul style="list-style-type: none"> <li>• inorganic</li> </ul>	phosphate, tetraborate, chloride
<ul style="list-style-type: none"> <li>• organic</li> </ul>	2-[N-morpholino]ethanesulfonic acid] (MES), cetyl trimethylammonium bromide (CTAB) tris[hydroxymethyl]aminomethane (TRIS),

The *organic modifier* in the mobile phase plays a role, which is difficult to predict since many variables are affected by changes of the organic modifier: viscosity, dielectric constant and zeta potential.

The majority of papers published on CEC have dealt with the use of C18 particles as packing material and to a lesser extent C8, using organic/aqueous mobile phases. Acetonitrile is the most commonly used organic modifier, although methanol is also employed. It has been generally observed that as the

percentage of acetonitrile is increased, the EOF increases. Unexpectedly, high EOF velocities have been noticed at high acetonitrile concentrations [10, 12, 15, 16]. Plots of EOF velocity vs. methanol concentration have shown a maximum at around 60% methanol [17].

Though CEC with non-aqueous mobile phases is not commonly used, a number of applications have been developed [18-20].

#### **1.2.3.6 Influence of the packed bed**

In packed CEC (*pCEC*), both the capillary wall and the column packing carry surface charges that are capable of generating EOF. To date, most of the work carried out suggests that the packing has the higher contribution to the EOF due to the high surface area of the porous particles. However, the EOF velocity in a packed bed is usually lower than in an open tube. This is due to the tortuosity (external channels in the packed bed) and the internal porosity of the packing material [17, 21-23]. The EOF is, however, independent of the particle diameter. This is in marked contrast with its pressure-driven analogues.

#### **1.2.4 Retention and selectivity in CEC**

The separation mechanism in CEC is a hybrid differential migration process, which involves the features of both HPLC and CZE, *i.e.* chromatographic retention and electrophoretic migration.

The *retention factor*  $k$  in HPLC is a dimensionless parameter that specifies the location of a peak in a chromatogram and provides thermodynamic insights into the interaction between the sample components and the stationary/mobile phases. So far, this definition of the retention factor has been extended to CEC. Due to the dual separation mechanisms that occur in CEC, the system is significantly more complicated by comparison to HPLC and it is therefore difficult to develop an expression for  $k$  which would have all the attributes it has in "regular" chromatography [24].

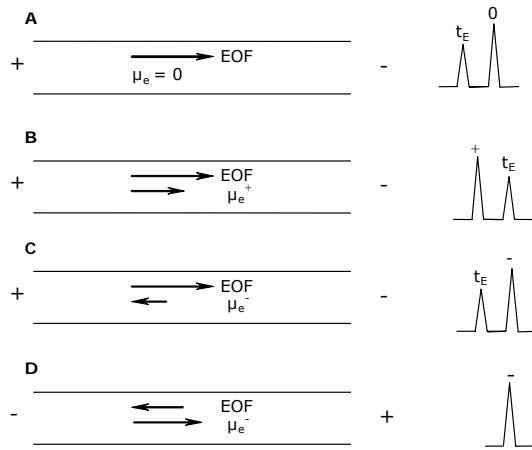


**Figure 1.5** CEC of neutral (A) and charged (B-D) species

The concept of "virtual migration lengths" [25] allows a CEC retention factor ( $k_C$ ) to be defined. In HPLC the retention factor ( $k$ ) is given by:

$$k = \frac{t_R - t_0}{t_0} \quad (\text{I.10})$$

where  $t_R$  is the retention time of a retained solute and  $t_0$  the elution time of a non-retained component.

In CZE, the velocity factor ( $k_E$ ) is correspondingly defined as

$$k_E = \frac{t_E - t_M}{t_M} \quad (\text{I.11})$$

where  $t_E$  corresponds to the dwell time of the EOF, represented by the migration of a small, neutral and also non-retained compound, and  $t_M$  corresponds to the migration time of a charged or neutral solute.

Combining equations I.10 and I.11 leads to

$$k_M = k + k k_E + k_E \quad (\text{I.12})$$

The term  $k k_E$  is the consequence of simultaneous chromatography and electrophoresis. If  $k_E = 0$ , then  $k_C = k$ , and only HPLC phenomena occur. If  $k = 0$ , then  $k_C = k_E$ , and the only process is CE.

Selectivity ( $\alpha$ ) is a thermodynamic factor that is a measure of the relative retention of two substances, fixed by a certain stationary phase and mobile phase composition.

$$\alpha = \frac{k_2}{k_1} \quad (\text{I.13})$$

where  $k_1$  and  $k_2$  are the respective capacity factors.

### I.2.5 Band broadening in CEC

As mentioned above, instead of applying pressure to pump the mobile phase through the column, the application of an electric field to the capillary induces an EOF, which is responsible for the bulk transport. The favourable flow dynamics of EOF translate into high chromatographic efficiencies in CEC separations. Moreover, since the EOF velocity is independent of the particle size in the packed bed, in contrast with HPLC, smaller particles and longer columns can be employed with favourable consequences in efficiency,  $N$  and resolving power.

In packed CEC and HPLC columns all terms of the simplified van Deemter equation (I.14) should be used.

$$H = Ad_p + B \frac{D_M}{u} + C \frac{d_p^2}{D_M} u \quad (\text{I.14})$$

where  $H$  is the height equivalent of a theoretical plate,  $A$ ,  $B$  and  $C$  are constants,  $d_p$  represents the particle size,  $D_M$  the diffusion coefficient of the mobile phase, and  $u$  the mobile phase velocity.  $H$  is related to the column length  $L$  by the following expression:

$$H = \frac{L}{N} \quad (\text{I.15})$$

$N$  representing the efficiency (number of theoretical plates/column).

In the absence of extra-column effects, the first term in the equation I.14 represents the plate height contribution from the tortuous flow path in the packed column. The second term stands for band spreading resulting from longitudinal diffusion of the sample and contributes significantly to the plate height only at low flow velocities. As in traditional HPLC, this term is negligibly small for common CEC operation conditions. The third term arises from mass

transfer resistances encountered by the sample components in the retention process based on their distribution between the mobile and stationary phases [26].

Equation I.14 clearly indicates that for both HPLC and CEC the particle size ( $d_p$ ) is the most important parameter whereas the diffusion coefficients ( $D_M$ ) of solutes in the mobile phase only play a significant role when large molecules are eluted.

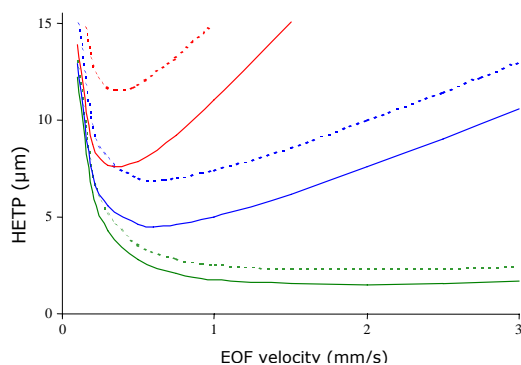


**Figure I.6** HETP-u plots in pressure-driven (dotted lines) and electro-driven (full line) systems using equation (I.14). Constants for HPLC:  $A=1.5$ ;  $B=2$  and  $C=0.1$  and for CEC:  $A=0.7$ ;  $B=0.2$  and  $C=0.1$ . Legend:  $5 \mu\text{m}$ ,  $3 \mu\text{m}$  and  $1 \mu\text{m}$  particles

A display of the calculated H-u curves for  $\mu\text{LC}$  and CEC [44] is shown in Figure I.6. It clearly depicts that higher efficiencies in CEC are related to the much reduced  $Ad_p$ -term. This is attributed to the EOF plug-like profile reducing multi-path band dispersion by a factor of 2. The  $C$ -term has been shown to be higher in HPLC than in CEC for packing materials with a pore size larger than  $300 \text{ \AA}$ . This can be related to the fact that there is no substantial EOF transport through the pores of standard particles ( $80 \text{ \AA}$ ) because of possible double layer overlapping.

On the other hand perfusive EOF in silica material with channel diameters of  $2000 \text{ \AA}$  has been described [27, 28]. The perfusive EOF minimizes the plate height by eliminating the stagnant pools of mobile phase, where mass transfer is by diffusion only.

From Figure I.6 and equation (I.14) it can be concluded that superior efficiencies should be achievable in CEC as compared to its pressure-driven analogue. In

HPLC reduced plate heights ( $h=H/d_p$ ) of 2 are the lowest achievable for a packed column. It is clear that in CEC this value is substantially lower, mainly as a result of a much reduced  $A$ -term.

CEC results with charged solutes under isocratic conditions are often comparable to those obtained by gradient LC [29]. It is believed that this phenomenon is due to the formation of an internal gradient in the CEC system that gives rise to concomitant peak compression.

It is unlikely that further improvements can be expected with gradient-CEC.

### **1.2.6 Modes of operation in CEC**

Although, in principle, all HPLC modes are conceivable in CEC as long as an electric double layer is present to generate the EOF, CEC has almost exclusively been performed in the reversed phase mode. In this mode, the interaction with the stationary phase is dependent on the relative hydrophobicity of the analytes. Separation is based on a combination of partitioning with electrophoretic mobility if the analytes are charged.

Normal phase CEC has also been described [30-32]. This technique requires a polar stationary phase, such as silica or silica derivatized with polar functions (*e.g.* amino, diol or cyano).

Ion-exchange CEC has been demonstrated with both silica and polymeric columns, monolithic and packed, providing selectivities based on electrostatic interactions and electrophoretic mobilities [33-35].

A mixed mode CEC separation has been described for a single column whereby selective retention is probably obtained by two or more mechanisms [29].

### **1.3 Support materials and stationary phases for CEC**

The manufacturing of highly efficient, stable and reproducible columns remains the main bottleneck in CEC. Several approaches were reported, including packed columns, open tubular columns, monoliths and microfabricated structures. These are briefly outlined below.

Presently, CEC is most commonly performed in the *packed column format*, using spherical, silica-based reversed phase particles. The materials used for pCEC are often commercially available supports developed for HPLC. The wide variety of stationary phases used in HPLC, with well-characterized retention and selectivity mechanisms, are transferable to CEC.

The *monolithic columns* are considered alternatives to packed columns. They eliminate the difficulties encountered with packed columns, particularly with the fabrication of retaining frits. The monoliths are porous in nature and can be either rigid structures or soft gels. Organic and inorganic polymeric rods can be fabricated by introducing the monomeric precursors into the capillary and allowing the polymerization reaction to take place *in situ*.

In *open tubular CEC*, a stationary phase capable to support an EOF, is attached to the walls of the fused silica capillary. The main benefit of an open tube is its 20-30 times higher permeability as compared to packed columns. The open tubular format of a separation column has one main drawback, however, namely the very low phase ratio, defined as the ratio of the volume of stationary phase and volume of mobile phase. This will limit the sample loadability of open tubular columns. In combination with the small detection volume and short linear detection range, this can compromise the limit of detection.

In addition to capillary columns, *microchip based* CEC devices have also been fabricated [36, 37]. Open tubular electrochromatography using isocratic and gradient elution on microchips modified with a C18 stationary phase for separation of fluorescent dyes has been demonstrated [38, 39]. With optimized channel geometry, plate heights of less than 2  $\mu\text{m}$  have been measured [40].

#### **I.4 Limitations of CEC**

CEC has developed in the recent years into an efficient separation technique. The present lack of robustness of this technique particularly in terms of column preparation, column and EOF stability, however, gave CEC a position of complementarity rather than making it a competing technique comparable to

HPLC [41]. The industry – especially the pharmaceutical industry – is still reluctant to accept it. This is mostly because of the poor performance in the field of applications. Even if acid and neutral compounds are well resolved, the performance for the separation of basic compounds needs quite a lot of work still. Since the majority of pharmaceutical compounds contain basic amine functions, this is a big hindrance to the progression of this technique.

The vast majority of CEC columns are made from silica and once a detection window is burnt and the protective polyimide layer is removed, they become extremely fragile. Since these capillaries are so easily broken, this puts a serious constraint on the use of the technique, especially with regard to the ease of column handling. There is also concern over the fragility and behaviour of the retaining frits in pCEC.

CEC instrumentation is also very limited. Even though companies like Agilent Technologies and Beckmann offer instruments for CEC, they are in fact modifications of existing CE systems.

Further developments in stabilizing the flow in CEC together with a more sensitive detection should help to overcome the current drawbacks associated with electrodriven chromatographic techniques. In general, the reproducibility of reliable data depends on various factors, including the stationary phase and the packing procedure, the frit formation process, the injection method and the specific separation conditions. But as long as the majority of columns are produced in-house, there remains an urgent need to overcome the technical difficulties related to their fabrication in order to produce robust and reproducible columns [42-44].

### **Conclusions**

CEC is still an emerging technique, which is theoretically more powerful than CE or HPLC. The main limitations of CEC are of a practical nature and should be overcome in a near future.

The nature of CEC readily lends the technique to miniaturization. The use of ultra-short columns and high electric fields, combined with optimized stationary

phases and operating conditions, may facilitate future applications in CEC and shape the technique into a powerful tool for several industrial challenges.

---

## References

1. KD Bartle, P Myers – *J Chromatogr A* 916 (2001) 3-23
2. G Choudhary, Cs Horvath – *J Chromatogr A* 781 (1997) 161-183
3. Q-L Luo, JD Andrade – *J Microcol Sep* 11 (1999) 682-687
4. Q-H Wan – *J Phys Chem B* 101 (1997) 8449-8453
5. AS Rathore, Cs Horvath – *Anal Chem* 71 (1999) 2633-2641
6. MG Cikalo, KD Bartle, P Myers – *J Chromatogr A* 836 (1999) 25-34
7. *High Performance Capillary Electrophoresis – An Introduction*, Hewlett-Packard Company, publication no 12-5091-6199E, 1997
8. E Grushka, RM Mc Cormick, JJ Kirkland – *Anal Chem* 61 (1989) 241-246,
9. G Chen, U Tallarek, A Seidel-Morgenstern, Y Zhang – *J Chromatogr A* 1044 (2004) 287-294
10. PB Wright, AS Lister, JG Dorsey – *Anal Chem* 69 (1997) 3251-3259
11. T Adam, S Ludtke, KK Unger – *Chromatographia* 49 (1999) S49-S55
12. X Cahours, P Morin, M Dreux – *J Chromatogr A* 845 (1999) 203-216
13. F Moffat, PA Cooper, KM Jessop – *Anal Chem* 71 (1999) 1119-1124
14. LA Colon, G Burgos, TD Maloney, JM Cintron, RL Rodriguez – *Electrophoresis* 21 (2000) 3965
15. A Banholczer, U Pyell – *J Chromatogr A* 869 (2000) 329-337
16. MG Cikalo, KD Bartle, P Myers – *J Chromatogr A* 836 (1999) 35-51
17. MM Dittmann, G Rozing – *J Microcol Sep* 9 (1997) 399-408
18. M Girod, B Chankvetadze, G Blaschke – *J Chromatogr A* 887(1-2) (2000) 439-55
19. C Karlsson, H Wikstrom, DW Armstrong, PK Owens – *J Chromatogr A* 897(1+2) (2000) 349-363
20. D Wistuba, K Cabrera, V Schurig – *Electrophoresis* 22(12) (2001) 2600-2605
21. AS Rathore, Cs Horvath – *Anal Chem* 70 (1998) 3271-3274
22. M Zhang, Z El Rassi – *Electrophoresis* 19 (1998) 2068-2072
23. C Yang, Z El Rassi – *Electrophoresis* 21 (2000) 1977-1984

24. AS Rathore, AP McKeown, MR Euerby – *J Chromatogr A* 1010 (2003) 105-111
25. Cs Horvath, WR Melander in "*Chromatography, part A*", ed. E Heftmann (Journal of Chromatography Library, vol 22A), Elsevier, Amsterdam, 1983, p A27
26. AS Rathore – *Electrophoresis* 23 (2002) 3827-3846
27. D Li, VT Remcho – *J Microcol Sep* 9 (1997) 389-397
28. PT Vallano, VT Remcho – *Anal Chem* 72 (2000) 4255-4265
29. K Mistry, I Krull, N Grinberg – *J Sep Sci* 25 (2002) 935-958
30. W Wei, GA Luo, GY Hua, C Yan – *J Chromatogr A* 817(1 + 2) (1998) 65-74
31. EPC Lai, E Dabek-Zlotorzynska – *Electrophoresis* 20(12) (1999) 2366-2372
32. H Zhong, Z El Rassi – *J Sep Sci* 29(13) (2006) 2023-2030
33. S Zhang, M Macka, PR Haddad – *Electrophoresis* 27(5-6) (2006) 1069-1077
34. JP Hutchinson, EF Hilder, M Macka, N Avdalovic, PR Haddad – *J Chromatogr A* 1109(1) (2006) 10-18
35. AP McKeown, MR Euerby, H Lomax, Helen – *J Sep Sci* 25(15-17) (2002) 1257-1268
36. JP Kutter, SC Jacobson, N Matsubara, JM Ramsey – *Anal Chem* 70 (1998) 3291-3297
37. SC Jacobson, R Hergenroder, LB Koutny, JM Ramsey – *Anal Chem* 66 (1994) 2369-2373
38. J Jiskra, HA Claessens, CS Cramers – *J Sep Sci* 26 (2003) 1305-1330
39. S Shrinivasan, MC Breadmore, B Hosticka, JT Landers, PM Norris – *J Noncryst Solids* 350 (2004) 391-396,
40. RD Oleschuk, LL Schultz-Lockyear, Y Ning, DJ Harrison – *Anal Chem* 72 (2000) 585-590
41. BC Giordano, A Terray, GE Collins – *Electrophoresis* 27 (2006) 4295-4302  
MT Dulay, C Yan, DJ Rakestraw, RN Zare – *J Chromatogr A* 725 (1996) 361-366
42. P Coufal, HA Claessens, CA Cramers – *J Liq Chromatogr* 16 (1993) 3623-3652

43. J Wang, DE Schaufelberger, NA Guzman – *J Chromatogr Sci* 36 (1998) 155-160
44. A Dermaux – *PhD Dissertation*, University of Gent, Belgium, 1999

## Chapter II

# I n s t r u m e n t a l   A s p e c t s

### II.1 Introduction

Electrochromatography (*i.e.* CEC, MEKC and MEEKC) can be performed using modified standard CE equipment or in-house assembled equipment.

The basic elements are the same as for capillary electrophoresis with the inclusion of pressurization ( $\sim 10$  bar) at both inlet and outlet to suppress air bubble formation, which is common in CEC (Figure II.1).

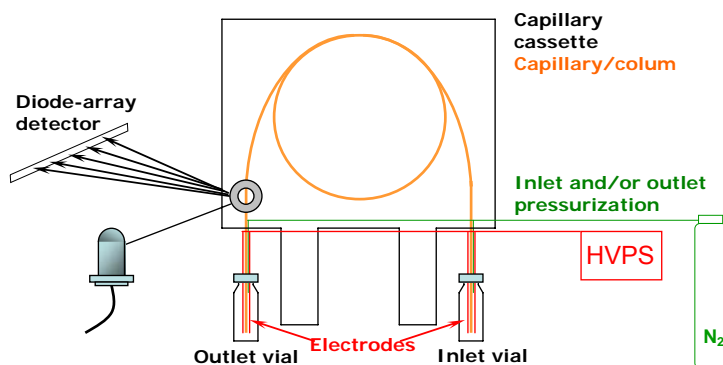


**Figure II.1** Schematics of a CEC system, also applicable for MEKC and MEEKC

Today's systems are highly automated and allow sequential analysis as required for high throughput analysis. The systems have one or two trays containing the vials with the different solutions; the vials can be placed around the capillary by a robotic arm. The samples are introduced by pressure or electrokinetically (*i.e.* by the application of an electrical field). Because the viscosity of a solution in the capillary and hence the migration time of the analyte is highly dependent on the temperature of the environment, the capillary is thermostated with a liquid or an air cooling device.

Many detection methods have been developed for CE and derivatives, such as UV-DAD (diode array detection), (laser induced) fluorescence, electrochemical detection and mass spectrometry.

The individual components for injection, separation and detection are described in the following sections. Discussions include different types of sample injection, capillary thermostating, high voltage power supply (HVPS) considerations and types of detection used in CEC.

## II.2 Sample injection

In order to maintain high efficiency, only very small sample sizes should be loaded into the column. As a rule of thumb, the sample plug length should be less than 1 to 2% of the total capillary length [1]. In the case of a 50 cm capillary 50  $\mu\text{m}$  ID, this corresponds to an injection plug length of less than 10 mm, or to approximately 20 nL. The small sample size required in capillary techniques is advantageous when a limited amount of the sample is available, but is often detrimental as it further reduces the sensitivity of the technique. If larger and/or more concentrated sample plugs are introduced this can lead to overloading which results in peak broadening and distorted peak shapes. The overloading thereby leads to a mismatched conductivity between the mobile phase and the sample zone.

### II.2.1 Hydrodynamic injection

This is the most widely used method. It can be accomplished by (1) application of pressure at the injection end of the column, (2) vacuum at the exit end or (3) siphoning action obtained by elevating the injection vial relative to the exit vial. In commercial CEC systems the first approach is commonly used.

The volume of loaded sample ( $V_L$ ) on a capillary or open tubular CEC column can be calculated using the Hagen-Poiseuille equation:

$$V_L = \frac{\Delta P d^4 \pi t}{128 \eta L} \quad (\text{II.1})$$

where  $\Delta P$  is the pressure applied during the injection time  $t$ ,  $d$  the capillary ID,  $L$  the total capillary length and  $\eta$  the viscosity of the bulk fluid.

Note that siphoning can constitute an unwanted phenomenon that leads to reproducibility problems. Therefore, the liquid levels of the sample and buffer reservoirs should be equal.

In general, repeatability of sample injection in terms of peak area is better than 1-2% RSD.

### II.2.2 Electrokinetic injection

In electrokinetic injection, analytes enter the capillary by both migration and pumping action of the EOF. Practically, injection is performed by replacing the electrolyte vial with the sample vial and applying voltage. A unique property of electrokinetic injection is that the quantity loaded is also dependent on the electrophoretic mobility ( $\mu_e$ ) of the individual solutes. Hence, discrimination will occur for different ionic species. The quantity injected,  $Q$ , can be calculated by

$$Q = \frac{(\mu_e + \mu_{EOF})V\pi r^2 Ct}{L} \quad (\text{II.2})$$

where  $V$  is the voltage applied during the injection time  $t$ ,  $r$  the capillary radius,  $C$  the analyte concentration and  $L$  the capillary length.

Variations in conductivity, which can occur *e.g.* due to matrix effects, result in differences in voltage drop and quantity loaded. Therefore, electrokinetic injection is generally not as repeatable as hydrodynamic injection. Despite its shortcomings, electrokinetic injection is preferred when viscous media or gels are employed in the capillary.

In the case of packed column CEC, hydrodynamic injection would take an exceedingly long time due to the commonly encountered high backpressure in conjunction with a low injection pressure ( $\leq 10$  bar). Therefore electrokinetic injection is preferred [2].

## **II.3 Separation**

### **II.3.1 Temperature control**

Effective control of capillary temperature is important for separation reproducibility. In a non-thermostated capillary a decrease in the viscosity of the buffer leads to faster migration and to higher currents, which will heat the solution eventually leading to the formation of gas bubbles in the capillary and to a breakdown of the analysis.

Liquid and/or air cooling are used for thermostating the capillary. While liquid thermostating is theoretically more effective, forced air at  $\approx 10$  m/s is usually sufficient to remove the quantity of heat generated in CEC [1].

### **II.3.2 High voltage power supply**

Typically, a DC power supply is used to apply up to 30 kV with maximum current levels of 200 to 300 mA. Proper regulation of the voltage is required to maintain high repeatability of migration.

The power supply should have the capability to switch polarity. As the detector positioning predetermines the inlet and the outlet ends of a column, polarity switching must be performed by the power supply. With a dual polarity power supply the high voltage electrode and the ground remain fixed. That is, the high voltage electrode is either positive or negative with respect to the ground electrode [1].

Constant current or constant power mode can be used during a run in order to minimize Joule heating and hence, to obtain a higher repeatability of analysis. In the constant current mode, for example, viscosity changes are compensated by proportional changes in the applied voltage, maintaining constant elution time.

The constant voltage mode is the most widely used. In order to avoid column stress, it is recommended that a short ramp be used in the beginning of the run, to bring the voltage from 0 to the value required during the run.

## **II.4 Detection**

Detection is a challenge in CE and CEC as a result of the small capillary dimensions. A number of detection methods have been used in CEC, many

similar to those employed in HPLC. Table II.1 contains an overview of the detection methods used in capillary electrodriven techniques, along with some of their figures of merit.

**Table II.1** Detection methods used in capillary electrodriven separation techniques [3]

Method	Mass detection limit (moles)	Concentration detection limit (molar) *	Advantages/ disadvantages
<b>UV-Vis absorption</b>	$10^{-13} - 10^{-16}$	$10^{-5} - 10^{-8}$	<ul style="list-style-type: none"> <li>• universal</li> <li>• diode-array offers spectral information</li> </ul>
<b>Fluorescence</b>	$10^{-15} - 10^{-17}$	$10^{-7} - 10^{-9}$	<ul style="list-style-type: none"> <li>• sensitive</li> <li>• usually requires sample derivatization</li> </ul>
<b>Laser Induced Fluorescence (LIF)</b>	$10^{-18} - 10^{-20}$	$10^{-14} - 10^{-16}$	<ul style="list-style-type: none"> <li>• extremely sensitive</li> <li>• usually requires sample derivatization</li> <li>• expensive</li> </ul>
<b>MS</b>	$10^{-16} - 10^{-17}$	$10^{-8} - 10^{-9}$	<ul style="list-style-type: none"> <li>• sensitive and offers structural information</li> <li>• interface between CEC/MS can be a problem</li> </ul>
<b>Indirect UV, fluorescence, amperometry</b>	10-100 times less than direct method	--	<ul style="list-style-type: none"> <li>• universal</li> <li>• lower sensitivity than direct methods</li> </ul>

\*Injection volume: 10 nL (for a 50  $\mu$ m I.D. capillary)

The detectors used in the framework of this study are described below.

#### II.4.1 UV-Vis detection

UV-Vis absorption spectroscopy is the most widely used detection method in CEC. Often single or multiple wavelengths are used for detection, but since the introduction of diode array detection (DAD) it became possible to collect entire

UV spectra facilitating compound identification. Multiple wavelength or DAD detection has the additional advantage of peak purity assessments.

A schematic drawing of a DAD detection system is shown in Figure II.2.

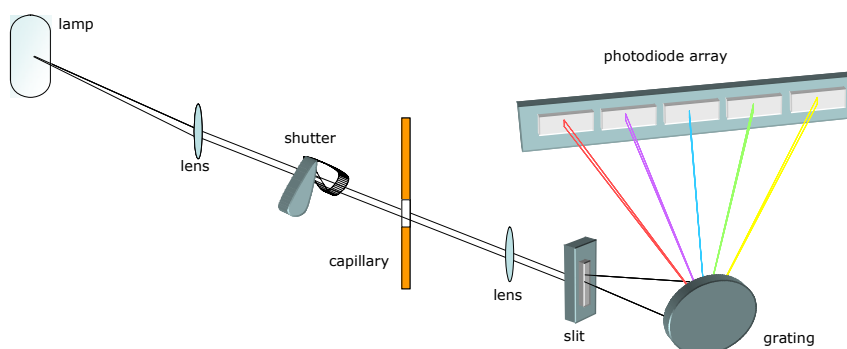


**Figure II.2** Schematic drawing of a DAD set-up

In practice, the detection window is made by removing the polyimide coating from a small area of the capillary. Direct or on-column detection is done by positioning the window into a detection cell. In the case of on-column detection, the signal is collected from the unpacked section after the column outlet frit. With in-column detection, detection is performed through the packed bed. This inevitably leads to sensitivity loss due to severe light scattering [4,5].

One of the drawbacks of UV-Vis detection in CE techniques is the limited sensitivity due to the reduced optical path length. This can be improved by increasing the inner diameter of the capillary. Two approaches have been used to achieve this, *i.e.* capillaries with an enlarged diameter where the detection takes place (bubble cells) and the use of a high sensitivity cell. The latter increases detection sensitivity by a factor of ten compared to standard detection [6]. This new type of cell is expected to increase substantially the utility of CE/CEC for impurity analysis of chiral drugs and trace analysis in biological and environmental samples [7].

#### II.4.2 Laser Induced Fluorescence (LIF) detection

(Laser induced) fluorescence is several orders of magnitude more sensitive than UV-absorption spectroscopy [8, 9]. The principle is based on the relaxation of photo-excited molecules through the emission of radiation. The emitted radiation

has always a longer wavelength compared to the excitation light. The isotropicity of the emitted radiation allows a smart detection, orthogonal to the excitation beam, resulting in the collection of an almost background free, highly selective and sensitive signal.

A schematic drawing of a LIF set-up used for CE and CEC is shown in Figure II.3.

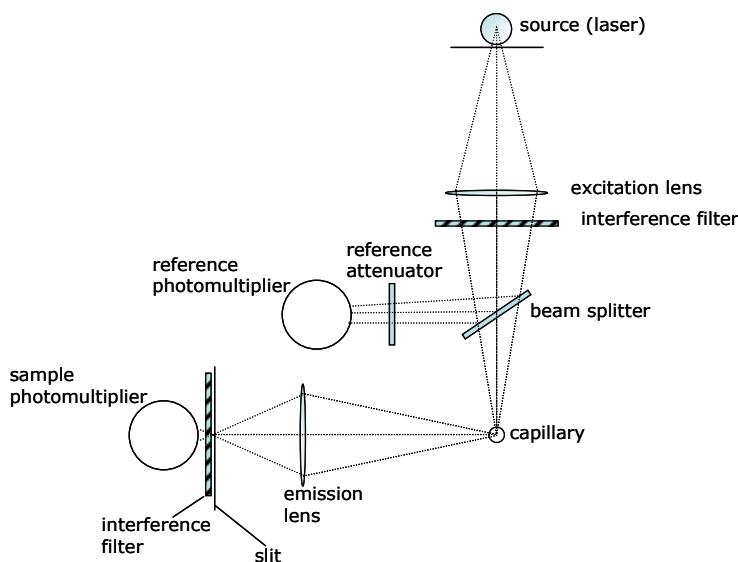


Figure II.3 Schematic drawing of a fluorescence detector set-up

A drawback of LIF is that relatively few molecules possess natural fluorescence. Therefore derivatization or label tagging schemes have been developed. This approach is often used in CE for the analysis of DNA and carbohydrates (see Chapter VII).

### II.4.3 MS

Mass spectrometry is one of the most powerful detection techniques because of its high sensitivity and the amount of extra information it can provide about the detected molecules through their mass spectra.

CEC is a separation technique in the condensed phase. This requires a fast transition of the analytes from this environment (at atmospheric pressure) to the high vacuum in the MS. Simultaneously the analyte has to be ionized, and this process has to be done without sacrificing the separation efficiency. The

atmospheric pressure electrospray ionization (APESI) method is considered to be the most suitable choice for ionization of the compounds separated by CE. Electrospray ionization (ESI) is a very soft ionization technique and is able to transfer molecules directly from the liquid to the gas phase. The term "electrospray" is appointed to a small flow of liquid (10  $\mu\text{L}/\text{min}$ ) from a capillary needle when a potential difference of 3-6 kV is applied between the end of the capillary and a cylindrical electrode located 0.3-2 cm away (Figure II.4). Under these circumstances, the liquid leaving the capillary does not leave as a jet, but rather as a spray, or fine mist. The spray consists of highly charged liquid droplets, and these droplets may be positively or negatively charged depending on the sign of the applied voltage. Molecular ions of the sample molecules are obtained in this process by evaporation of the solvent reducing the size of the droplets until the desolvation is supported by repulsive coulombic forces, overcoming the cohesive forces in the droplet, by which they break down into smaller ones.

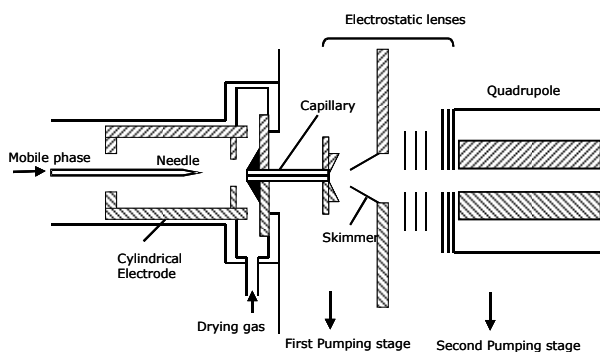


**Figure II.4** Scheme of an electrospray ionization source and transfer units from atmospheric pressure to the high vacuum in a quadrupole mass spectrometer

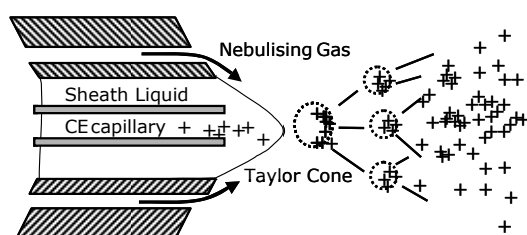


**Figure II.5** Schematic close-up of the electrospray ionization source

Because the flow rate in a CEC capillary is in the range of only nanoliters per minute, it is difficult to obtain a stable spray for such low flow rates. Therefore, the CEC-MS interface uses a make-up or sheath liquid flow of several  $\mu\text{L}/\text{min}$  through a tube concentric with the capillary as shown in Figure II.5. The sheath liquid is added at a much higher flow rate than the CE flow and is therefore dominating the ESI process. The sheath liquid is often composed of combinations of methanol or isopropanol and water with small amounts of volatile buffers like ammonium acetate, triethylamine or formic acid depending on the polarity of the ionization.

Once ions of the analyte have been produced, they are separated according to their mass-to-charge ( $m/z$ ) ratios. Although there are many different types of mass analysers, this discussion is limited to the (single) quadrupole and the ion-trap (or quistor) mass spectrometers, which are relevant to this work.

Quadrupole analysers are made of four equidistant rods as is shown in Figure II.6. A positive ion entering the space between the rods will be drawn towards a negative rod. If the potential changes sign before it discharges itself on this rod, the ion will change direction.

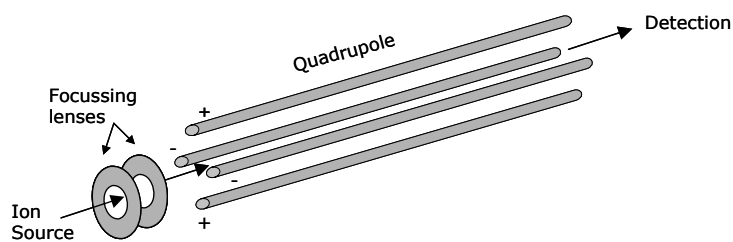


**Figure II.6** Schematic representation of a quadrupole mass analyzer

By applying an adequate combination of constant and alternating voltages on the rods, a situation is created whereby in a short period of time only an ion with a specific  $m/z$  ratio can reach the detector. By covering the range of applicable constant and alternating voltages, a full scan of the ions can be obtained in approximately 100 ms. Quadrupole analysers have the advantage of low cost and ease of operation for analyses of ions of masses up to 2000-3000 Da.

The ion-trap mass spectrometer can conceptually be imagined as a quadrupole bent on itself in order to form a closed loop. The inner rod is then reduced to a point; the outer rod is the ring electrode, and the top and bottom rod make the caps (Figure II.7). The overlapping of a direct potential with an alternating one gives a kind of “three dimensional quadrupole” in which the ions of all masses are trapped in a three dimensional 8-shaped trajectory. A mass scan is obtained by the stepwise application of a resonant frequency along the z-axis by which in each time lapse ions with a specific mass are expelled from the trap towards the detector. A major feature of this MS analyser is the ease by which MS-MS and MS<sup>(n)</sup> can be performed.

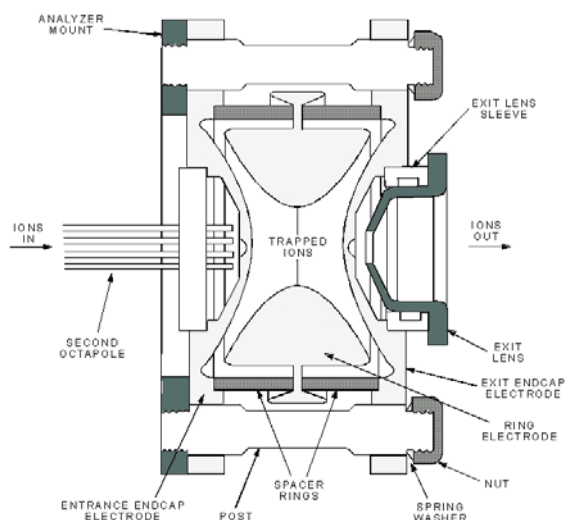


Figure II.7 Basic elements of an ion trap mass spectrometer

The possibility of MS<sup>n</sup> analysis (multiple MS for analysis of fragments of fragments etc.) is a unique feature of the ion trap MS which cannot be obtained with quadrupole instruments for which the practical limit is MS/MS (MS<sup>2</sup>) [10].

**Conclusions**

A brief overview of the instrumental aspects of relevance to CEC in its current form has been described in this chapter. Because CEC is a constantly evolving technique, completely new approaches might appear in the future.

---

**References**

1. *High Performance Capillary Electrophoresis – An Introduction*, Hewlett-Packard Company, publication no 12-5091-6199E, 1997
2. NW Smith in "*Capillary Electrochromatography*" – ed KD Bartle and P Myers, The Royal Society of Chemistry, Cambridge, 2001, 23-31
4. AG Ewing, RA Wallingford, TM Olefirowicz – *Anal Chem* 61 (1989) 292A-303A
5. H Rebscher, U Pyell – *Chromatographia* 38 (1994) 737
6. A Banholczer, U Pyell – *J Microcol Sep* 10 (1998) 28
7. [http://chem.external.hp.com/cag/peak/peak1-97/ce\\_cell.html](http://chem.external.hp.com/cag/peak/peak1-97/ce_cell.html)
8. C Desiderio, S Rudaz, J-L Veuthey, MA Raggi, S Fanali – *J Sep Sci* 25(15-17) (2002) 1291-1296
9. KD Altria – *J Chromatogr A* 856 (1999) 443-463
10. CE Mactaylor, AG Ewing – *Electrophoresis* 19 (1998) 3022
11. E Hoffman, J Charette, V Stroobant – *Mass Spectrometry Principles and Applications*, ed. John Wiley & Sons, New York, 1994

## Chapter III

# S o l - G e l   T e c h n o l o g y

### III.1 Introduction

The sol-gel reaction is a two-step mechanism including a hydrolysis and a polycondensation. It was initially used for the preparation of inorganic materials like glasses and ceramics [1-3]. Because the methodology is also suitable to make organic/inorganic hybrid materials, it provides a way to prepare stationary phases for chromatography. The products from a sol-gel reaction are known as "ceramers", "ormosils" or "ormocers". Sol-gel chemistry offers the potential to provide unique combinations that cannot be obtained by other processes [4].

The preparation, characterization and applications of these hybrid materials have become a fast expanding area of research in material science. Through the combination of different inorganic and organic components, various types of primary and secondary bonding can be developed leading to materials with properties that are particularly interesting for chromatographic applications.

An overview of the general sol-gel chemistry, practical synthetic aspects, polymer characterization and applications, is given in this chapter.

### III.2 Definitions

- A *sol* is a dispersion of colloidal particles in a liquid.
- A *colloid* is a suspension of solid particles with diameters of 1-100 nm in a liquid.
- A *gel* is an interconnected, rigid molecular network with pores of sub-micrometer dimensions and polymeric chains whose average length is greater than a micrometer.
- *Ageing* of a gel (also called *syneresis*) involves maintaining the gel for a period of time immersed in liquid.

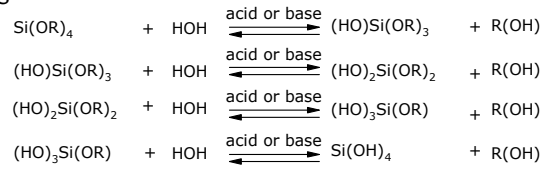
- When the liquid is removed at or near ambient pressure by thermal evaporation and when shrinkage occurs, the product is called a *xerogel*.
- An *aerogel* is the product obtained when the liquid is removed under supercritical conditions and the network does not collapse [5].

### III.3 General reactions

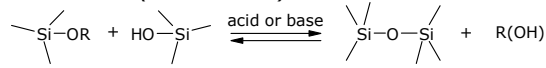
The sol-gel reaction consists of two steps: hydrolysis of metal alkoxides to produce free hydroxyl groups, followed by polycondensation of the hydroxyl groups and residual alkoxy groups to form a 3D network. The reaction scheme is represented in Figure III.1, with a general silicone alkoxide as an example.

The sol-gel process is generally performed in a solution of monomeric, metal or semimetal alkoxide precursors  $M(OR)_n$  in an alcohol or other organic solvent and water. M represents a network-forming element such as Si, Ti, Zr, Al, B, etc. and R is an organic group. Generally, both the hydrolysis and condensation reactions occur simultaneously once the hydrolysis reaction has been initiated. Low molecular weight by-products (water and alcohol) are generated in the process. These molecules are removed from the system and this would lead, in the extreme, to a tetrahedral  $SiO_2$  network. The removal of by-products from the hydrolysis and condensation reactions also contributes to high *shrinkage* that occurs during the classical sol-gel process [4].

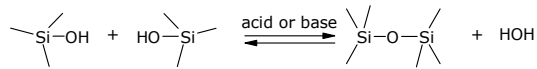
1) Hydrolysis



2A) Alcohol condensation (alcoxolation)



2B) Water condensation (oxolation)



C) Overall reaction

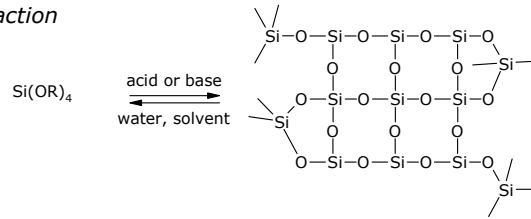


Figure III.1 Reactions involved in a sol-gel process

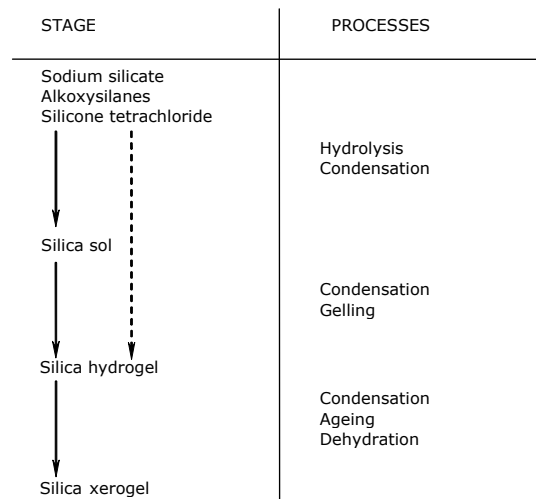
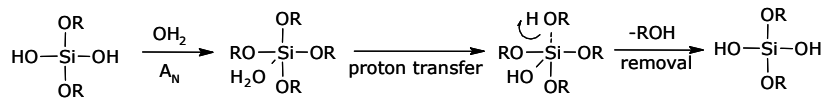


Figure III.2 Schematic representation of a sol-gel procedure

Both hydrolysis and condensation occur by nucleophilic substitution ( $S_N$ ) mechanisms which involve three steps: nucleophilic addition ( $A_N$ ), proton transfer

within the transition states and removal of the protonated species such as water and alcohol (Figure III.3).



**Figure III.3** General sol-gel reaction mechanism

For non-silicate metal alkoxides, generally no catalyst is needed for the reactions as they are very reactive. In the case of silicone-based alkoxides, the hydrolysis and condensation reaction typically proceeds with either an acid or a base as catalyst.

In the case of the common silicon alkoxides, since the hydrolysis rate is high under an acidic environment relative to that of condensation, acid catalysis promotes the development of more linear or polymer-like molecules in the initial stages. On the other hand, base catalysis results in a higher condensation rate. Therefore, this environment tends to produce more of a dense-cluster growth, leading to colloidal particulate structures [4, 6-8]. Hence the structure and morphology of the resulting network strongly depend on the nature of the catalyst and in particular on the pH of the reaction.

Alternatively, a non-hydrolytic sol-gel (NHS) route has been described, involving the reaction of a metal halide with an oxygen donor such as an alkoxide, an ether, an alcohol and so forth, under non-aqueous conditions to form an inorganic oxide [9]. The by-product of this reaction is commonly an alkyl halide whose structure depends on the nature of the oxygen donor molecule (Figure III.4).

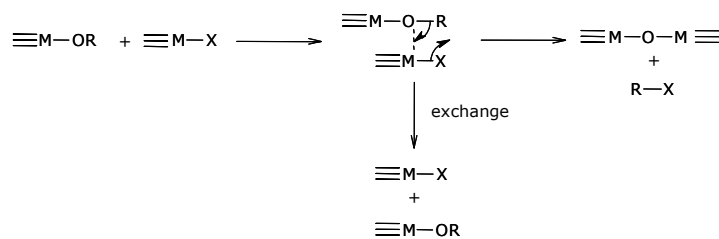


**Figure III.4** Non-hydrolytic sol-gel route to inorganic oxides, X=halide

Many organic species have been successfully incorporated within inorganic networks by different synthetic approaches. The chemical bond between inorganic and organic phases can be introduced mainly by three approaches: (1) functionalize organic molecules with silane, silanol, or other functional groups that can undergo hydrolysis and condensation with metal alkoxides; (2) utilize already existing functional groups within the organic molecules; (3) use alkoxysilanes ( $R'Si(OR)_3$ ) as the sole or one of the precursors [4, 10].

A direct way to introduce smaller organic moieties into a hybrid network through chemical bonding is to use bifunctional and/or trifunctional alkoxysilanes ( $R'_nSi(OR)_{4-n}$ ,  $n=1-3$ ,  $R$ =alkyl,  $R'$ =organic group) as one or more of the precursors for the sol-gel reaction. Trifunctional alkoxysilanes  $R'Si(OR)_3$  are the most common precursors because a variety of such compounds is commercially available.

The hybrid materials obtained using this approach can be viewed more as a molecular type of hybrid network, as the organic groups have been chemically bonded with the inorganic component *before the reaction*. While these types of hybrid network suffer the same drawbacks as classical sol-gel materials – generation of large quantities of by-products and shrinkage during the drying process –, they have attracted considerable interest. By *tailoring* the structure of the organic group  $R'$ , the properties of the resulting composite materials can be controlled [4].

#### III.4 Strategies and procedures

Although the sol-gel reactions can be considered as a complete synthesis, various practical steps are involved to ensure that a polymer with good properties is produced [5].

1. *Mixing*. A solution of (a) precursor(s) is hydrolyzed in water. The hydrolysis and polycondensation reactions initiate as mixing starts.
2. *Casting*. Since the sol is a low-viscosity liquid, it can be cast into a mould.
3. *Gelation*. With time, the colloidal particles and condensed silica species link together to become a 3D network. The physical characteristics of the gel

network depend greatly upon the size of the particles and the extent of the cross-linking prior to gelation.

4. *Ageing*. Ageing of a gel involves maintaining the gel for a period of time immersed in liquid. During this time, polycondensation continues in localized solution pockets and reprecipitation of the gel network occurs.
5. *Drying*. During drying, the liquid is removed from the interconnected pore network by heating or by applying vacuum. Gels can crack at this stage, unless the process is properly controlled.
6. *Dehydration or chemical stabilization*. The removal of surface silanol bonds from the porous network results in a chemically stable ultra-porous solid.
7. *Densification*. Heating the porous gel at high temperatures causes densification to occur. The pores are eliminated and the density ultimately becomes equivalent to that of fused silica.

Polymer characterization is a discipline in itself, including many techniques. The most important are briefly discussed in this section.

The porosity of a material can be measured with N<sub>2</sub> or Ar sorption techniques or mercury intrusion measurements. The surface chemistry can be studied by solid state NMR, X-ray scattering, Fourier-transform infrared spectroscopy (FT-IR), fluorescence and attenuated total reflectance spectroscopy.

Scanning electron microscopy (SEM) is a powerful tool to study the surface characteristics and fine structural details of a wide range of micro-objects. It is the most widely used technique to evaluate the morphology of a sol-gel stationary phase. Usually, SEM images of a cross sectional view of the prepared capillary column are used to illustrate the structural characteristics of the sol-gel stationary phase, its adherence to the capillary wall, integrity of the structure, the porosity of the sol-gel material and the distribution of the pores in the stationary phase [11-13]. In the case of open tubular columns, SEM can reveal the uniformity, the thickness and the structural defects of the applied coating.

Thermogravimetric analysis (TGA) provides a quantitative measurement of any weight changes associated with thermally induced transitions that involve dehydration or decomposition. In differential scanning calorimetry (DSC)

technique, the sample is subjected to a precisely programmed temperature change. Thermal transitions due to physical or chemical changes with release or absorption of heat are registered in this process. Because DSC measures both temperature and enthalpy of a transition or the heat of a reaction, it has become one of the most widely used thermal analysis techniques [12].

### III.5 Applications

Many applications have been described in the literature covering a range of fields. Of interest for this study are the chromatographic applications of the sol-gel technology, reviewed already in a number of articles [11, 14-17]. A brief overview is given in Table III.3.

**Table III.1** Sol-gel applications in CEC

stationary phase	precursor	application	ref
• alkyl			
C18	GPTMS, esterification with stearic acid	OTCEC	30
			18
C18	TEOS, reaction with dimethyloctadecylchlorosilane	OTCEC	31
			19
C18	N-octadecyldimethyl[3-(trimethoxysilyl)propyl]ammonium	OTCEC	13, 20, 21
C8, C18	C8TEOS, C18TEOS, TEOS	OTCEC	22, 23, 24
C8-C18	C8-C18TEOS, TEOS	OTCEC	25, 26
• functionalized alkyl			
cyano	GPTMS, followed by 3-hydroxypropionitrile	monolith	16
cyano	3CPTS	monolith	27
amino	APTS	monolith	27
aminopropyl	APTS, TEOS and APTS, meTEOS	monolith	28
amino	APTS	OTCEC	29
isocyanate	ICPTS	monolith	27

Abbreviations: C18 octadecyl, C8 octyl, GPTMS glycidoxypropyl trimethoxysilane, TEOS tetraethoxy orthosilane, C8TEOS octyl triethoxysilane, C18TEOS octadecyl triethoxysilane, 3CPTS 3cyanopropyl trimethoxysilane, APTS aminopropyl

trimethoxysilane, ICPTS isocyanatopropyl trimethoxysilane, OTCEC open tubular capillary electrochromatography

### Conclusions

Organic/inorganic hybrid materials prepared by the sol-gel approach are an important field of research in materials science. The explosion of activity in this area in the past decade has made great progress in both the fundamental understanding of the sol-gel process and the development and applications of new organic/inorganic hybrid materials [4]. Although the number of commercial hybrid sol-gel products is still relatively small, the promise of their use in new technological applications remains high.

---

### References

1. LC Klein, GJ Garvey – *ACS Symposium Series* 194 (1982) 293-304
2. DR Ulrich – *CHEMTECH* 18 (1988) 242-249
3. LL Hench, SH Wang – *Phase Transitions* 24-26 (1990) 785-834
4. J Wen, GL Wilkes – *Chem Mater* 8 (1996) 1667-1681
5. A Fidalgo, ME Rosa, LM Ilharco – *Chem Mater* 15 (2003) 2186-2192
6. L Matejka, O Dukh, D Hlavata, B Meissner, J Brus, Jiri – *Macromolecules* 34 (2001) 6904-6914
7. DJS Birch, CD Geddes – *Chem Phys Lett* 320 (2000) 229-236
8. IC Tilgner, P Fischer, FM Bohnen, H Rehage, WF Maier – *Microporous Materials* 5 (1995) 77-90
9. JN Hay, HM Raval – *Chem Mater* 13 (2001) 3396-3403
10. U Schubert, N Huesing, A Lorenz – *Chem Mater* 7 (1995) 2010-2027
11. W Li, DP Fries, A Malik – *J Chromatogr A* 1044 (2004) 23-52
12. HH Willard, LL Merritt Jr, JA Dean, FA Settle Jr – *Instrumental Methods of Analysis* – Wadsworth Publishing Company, Belmont, California, USA, 1988
13. Y Zhao, R Zhao, D Shangguan, G Liu – *Electrophoresis* 23 (2002) 2990-2995
14. E Guihen, JD Glennon – *J Chromatogr A* 1044 (2004) 67-81
15. B Riegel, S Bitterdorf, W Kiefer, S Hofacker, M Muller, G Schottner – *J Non-Cryst Solids* 315 (2003) 197-205

16. C Legido-Quigley, ND Marlin, V Melin, A Manz, NW Smith – *Electrophoresis* 24 (2003) 917-944
17. D Allen, Z El Rassi – *Electrophoresis* 24 (2003) 408-420
18. AL Crego, JC Diez-Masa, MV Dabrio - *Anal Chem* 65 (1993) 1615-1621
19. JD Hayes, A Malik – *Anal Chem* 73 (2001) 987-996
20. W Li , D Fries, A Alli, A Malik – *Anal Chem* 76 (2004) 218-27
21. SA Rodriguez, LA Colon – *Chem Mater* 11 (1999) 754-762
22. Y Guo, LA Colon – *Anal Chem* 67 (1995) 2511
23. Y Guo, LA Colon – *J Microcol Sep* 7 (1995) 481-491
24. S Rodriguez, LA Colon – *Analitica Chimica Acta* 397 (1997) 207-215
25. S Constantin, R Freitag – *J Chromatogr A* 887 (2000) 253-263
26. S Constantin, R Freitag – *J Sep Sci* 25 (2002) 1245-1251
27. D Allen, Z El Rassi – *J Chromatogr A* 1029 (2004) 239-247
28. S Huh, JW Wiench, J-C Yoo, M Pruski, V S-Y Lin – *Chem Mater* 15 (2003) 4247-4256
29. BV Zhmud, J Sonnefeld – *J Non-Cryst Solids* 195 (1996) 16-27

## Chapter IV

### Column Manufacturing Techniques in CEC

#### IV.1 Introduction

In all chromatographic separation techniques, the column is "the heart" of the system. In CEC the stationary phase plays a dual role as it provides the source for electroosmotic flow in addition to solute-stationary phase interactions as in conventional HPLC [1]. The retention of solutes in CEC is therefore determined by these interactions and by the electrophoretic mobility of the solutes being analyzed. The retention of uncharged compounds is solely determined by their interaction with the stationary phase.

In this chapter, the different types of column formats are presented. Each type is then described together with the stationary phases used (Table IV.1).

**Table IV.1** Column formats used in CEC

column format	type of stationary phase
open tubular	<ul style="list-style-type: none"><li>• physically adsorbed</li><li>• covalently bonded</li><li>• porous layers</li><li>• sol-gel</li></ul>
packed	<ul style="list-style-type: none"><li>• silica based</li><li>• polymer based</li></ul>
monolithic (rod)	<ul style="list-style-type: none"><li>• silica based</li><li>• polymer based</li></ul>

#### IV.2 Packed columns

The emergence of packed columns as the first approach for CEC is mainly based on the intuitive translation from pressure-driven LC towards electro-driven CEC, on the relative ease of column manufacturing and on the direct availability of the

stationary phases from HPLC. A packed column presents the advantages of a reasonable porosity, a high carbon load and the experimental evidence of high efficiencies predicted by theory.

The packed column consists of the following sections (Figure IV.1): inlet frit (1), packed bed (2), outlet frit (3), detection window (4) and extending capillary towards the outlet electrode (5).



Figure IV.1 Schematic drawing of a packed capillary

The critical aspects for the successful manufacturing of a packed CEC capillary are the frit formation and the actual packing technique.

#### IV.2.1 Frit formation in packed columns

A frit is a piece of the capillary where the silica particles are coagulated due to the application of intense heat and pressure (sintering). This leads to the formation of a Si—O—Si bond from two Si—OH (silanol) groups with the expulsion of water. The frits should be sufficiently tight to retain the particles, but porous enough to allow an unobstructed flow of the mobile phase [2].

There are four procedures for sintering [3, 4]: (a) using a mixture of potassium silicate and formamide; (b) dipping the capillary end into a slurry of silica gel and potassium silicate and sintering; (c) sintering pure silica particles packed in the column after the packing process; and (d) sintering a portion of the chromatographic packing itself after having flushed the column with water. This last sintering method produces frits most suitable for CEC, but sometimes the *in situ* process removes the polyimide coating of the capillary, making it fragile.

The sodium content in silica was found to be of importance for obtaining stable frits; on heating above 550°C, sodium silicate is formed. If purer silicas are used (*i.e.* with a low sodium content), frit manufacture was usually unsuccessful. Also, sintered frits may lead to a variation in EOF due to the different flows originating in the frit and the column packing. This phenomenon might be one of the causes of bubble formation. Pressurization at both ends of the column (8-12 bars) is

normally employed in order to avoid this bubble formation. However, this approach makes the pCEC coupling to MS impossible.

*Tapered columns* offer a viable alternative to frits in pCEC. A taper of ca. 10  $\mu\text{m}$  ID (internal or external taper) at the outlet of the column obviates the need for an outlet frit to retain 3  $\mu\text{m}$  particles of the packing. This phenomenon is called the "particulate keystone effect" [5]. The flow of liquid through the taper is at least as good as through a sintered silica frit.

"*Glueing*" of individual particles can lead to another type of fritless column. The packing particles can be sintered inside the column [6]. This results in the virtual formation of a monolith where the particles are joined by grain boundaries. After sintering, the ODS layer has to be renewed with a solution containing dimethyloctadecyl chlorosilane.

Another way is to embed the packing in a rigid sol-gel matrix. The particles are thereby trapped in a one-step procedure. Tetraethyl orthosilane [7] or a mixture of tetramethyl orthosilane and ethyltrimethyl orthosilane [8] are used as sol-gel precursors.

#### **IV.2.2 Column packing techniques**

Several packing strategies, roughly comparable in terms of column performance, have been described [9-12]. Gravity, centripetal and electrokinetic forces have been used for column packing. However, slurry packing with conventional HPLC pumps has been favoured in most studies. Next to common HPLC solvents, supercritical fluids have also been used for packing [11]. A retaining frit is sintered at the capillary outlet. The slurry of packing material is prepared in a solvent (or in supercritical  $\text{CO}_2$ ) and is forced into the capillary by means of an external pump.

Knox and Grant were the first to report high column efficiencies in CEC on quartz columns of 200  $\mu\text{m}$  ID [13, 14]. No outlet (retaining) frit was used. The inlet frit was made by sintering a paste of native silica gel "wetted" with sodium silicate. By using a combination of packing against gravity and ultrasonic agitation, to maximize the time the slurry is kept in suspension, it is possible to slow down

the packing process, leading to homogeneously packed beds [15]. With this procedure, good results can be obtained by preparing frits from the packed bed with sintering in water.

### IV.2.3 Packing materials

Conventional (LC) bonded phases are mostly prepared by surface modification with monofunctional C18 silanes. This type of bonded phase is relatively easy to prepare and is often *end-capped* in order to reduce or even eliminate residual silanol activity. Because residual silanols are probably essential for generating EOF, end-capped phases are not very suitable for CEC [1, 16].

An increased number of surface silanols is, however, present in *non-end-capped* phases and/or materials with a lower surface coverage of alkyl ligands [17].

A possible way of ensuring sufficient EOF is a segmented capillary, where one segment is packed with octadecyl silica (ODS) and serves as the separation segment while the other segment is packed with bare silica and functions as the EOF accelerator segment [18]. Another approach is mixing a reversed phase material with a strong cation exchange material. By using a stationary phase provided with sulfonic acid groups, a constant EOF can be obtained across a wide pH interval from 2.5 to 10. A common feature of these mixed mode phases is that they have a lower carbon loading than that of their HPLC equivalents [19]. Peak tailing for basic analytes is also worse due to the huge amount of free anions on the phase.

Initially, 5  $\mu\text{m}$  particle size silica was used for CEC. As smaller particles (3  $\mu\text{m}$  or even 1.5  $\mu\text{m}$ ) became available, columns were packed with these types of sorbents in order to increase efficiency. Using 3  $\mu\text{m}$  particles, column efficiencies approached 400,000 plates/m [20, 21]. Very fast separations have been achieved with 1.5  $\mu\text{m}$  C18 non-porous silica particles [22].

An EOF can be created by using particles as small as 20 nm in diameter. However, to take advantage of the flat flow profile, particles of 80 nm or larger should be used. A high perfusive flow can be generated with pore sizes as small as 5 nm, although 30 nm is deemed optimal [23].

Other *particle formats* have also been suggested in order to increase efficiency. Porous layer beads have a solid core with a porous shell (layer) and provide short diffusion distances. The time for mass transfer in the stagnant mobile phase is hereby reduced. This type of particles can be useful for fast separations, but suffer from the drawback of a low phase ratio ( $\beta$ ), which results in small retention factors ( $k$ ) and low sample loading capacities [2].

Another approach to reducing the mass transfer time in the stagnant mobile phase without sacrificing sample loading capacity is to utilize a porous particle through which the eluent flows. This type of packing has through-pores of several hundred nanometers and a network of smaller pores that branch out of the through-pores. The perfusive character of these packings provides the possibility of increased efficiency (due to the reduced effective mass transfer distances) and enhanced loading capacity (due to an increase in the effective accessible surface area) [2].

Similarly, in the case of monolithic columns (which are going to be discussed in more detail below), specific conditions for the polymerization process can produce wide channels that allow a less obstructed flow of the mobile phase through the bed.

### **IV.3 Open tubular columns**

The interest in open tubular capillary electrochromatography ensues from the experiments on open tubular LC (OTLC), which was evaluated as an alternative to (classical) packed LC [24-30]. The attractiveness of OTLC is related to the high column permeability and the smaller influence of convective dispersion when an electric field is applied. Therefore, longer columns can be used and larger plate numbers are obtainable compared to packed columns [31]. As described for packed column CEC, in open tubular CEC (OT-CEC) the stationary phase has to provide for an environment for molecular interaction and a driving source for EOF.

The general features of OT-CEC column manufacturing are described below.

It should be noted that OT columns have one main disadvantage compared with packed bed columns, namely the very low phase ratio ( $\beta$ ). A low phase ratio will limit the sample loadability in open tubular columns and therefore the limits of detection achievable.

The phase ratio,  $\beta$ , of an OT capillary column can be estimated from:

$$\beta = \frac{r_c^2}{(r_c - d_f)^2} \quad (\text{IV.1})$$

in which  $d_f$  is the film thickness and  $r_c$  the inner radius of the column. For a packed column, a value of 0.1 for  $\beta$  is typical. For a 10  $\mu\text{m}$  ID capillary coated with a monolayer of an alkylsilane (2.5 nm) a value of 0.001 is calculated. If a thick stationary phase is deposited (e.g. 0.1  $\mu\text{m}$ ), the phase ratio increases to 0.04. However, this will contribute significantly to band broadening [32].

This problem can be alleviated by etching the silica wall, using a sol-gel procedure to obtain the stationary phase, and as mentioned below, depositing thin layers of stationary phase onto the capillary walls.

### IV.3.1 Column manufacturing procedure

Several methods of preparing open tubular columns for CEC have been developed.

Depending on the type of bonding between the stationary phase and the inner wall of the fused silica capillary, the following types of coatings can be distinguished [27]:

- a. Physically attached/adsorbed
- b. Chemically bonded ligand phases
- c. Etched capillaries, chemically bonded
- d. Molecularly imprinted polymers
- e. Porous layers
- f. Sol-gel derived stationary phases

Sol-gel chemistry is the approach used in this study. With a sol-gel phase a truly retentive layer is formed. The layer thickness can be adjusted by variation of the precursor ratio and sol-gel reaction conditions. Moreover, the retentive layer is

not bonded to the surface via siloxane bonds as in the conventional binding procedures, but is incorporated into the bulk of the layer. This leads to increased longevity and stability for a wide pH range over extended periods. Control of EOF in magnitude and direction can be achieved by the use of appropriate precursors.

The manufacturing of a sol-gel column generally includes the following steps:

- 1. Capillary pre-treatment.* In order to increase silanol concentration, the bare capillary is first washed with various solvents, followed by drying of the cleaned surface by purging with a gas. Chemical treatment is performed, either by washing with an alkali solution (typically 0.1 M NaOH), followed by water (at room temperature), or by hydrothermal treatment. In the latter case, the reaction proceeds with water at elevated temperature (about 250°C). The activated capillary is sometimes dried at high temperature (180°C) under gas purge [33].
- 2. Preparation of the sol.* As described in Chapter III, the sol-gel reaction generally takes place at ambient temperature. The homogeneous product obtained in this step has to be coated onto the capillary wall.
- 3. Coating procedure.* The capillary is filled with the sol, using either a syringe or another type of pressurizing device. After a determined period of time, the gel is forced out of the column, leaving a thin coating on the column wall. During this step and the following, surface silanol groups on the wall will undergo condensation reactions with the sol-gel active species present in the coating.
- 4. Thermal treatment of the coated capillary.* In this step, solvent and water are eliminated from the wet gel matrix and a xerogel is obtained. An inert gas flows through the column to help remove solvent vapours.
- 5. Conditioning for CEC.* The coated capillary is flushed with an organic solvent (e.g. methanol, ethanol, acetone), water and then the mobile phase, followed by voltage conditioning.

#### **IV.4 Monolithic columns**

Monolithic columns offer the advantage of a high permeability (when pressure driven) and that no frits are required to retain the stationary phase [34]. Zone broadening is minimized by a combination of reduced eddy diffusion and mass

transfer contributions as a result of the flat flow profile of the EOF, in contrast to the parabolic flow profiles encountered with a pressure-drive. [36-41].

The organic polymer columns are prepared by *in-situ* polymerization, using free radical, thermal or UV initialization. The photopolymerization allows for a reduced curing time in comparison to over 12 h for the thermal methods. Long columns can be fabricated, as there are no limitations associated with column packing. The column porosity can be controlled by appropriate selection of a porogen and the ratio of monomer to porogen [42-46].

The silica-based monoliths can be produced by three different approaches, namely (1) fusion of silica particles by thermal sintering, (2) cross-linking/entrapping silica particles in a packed bed using the sol-gel process, and (3) polymerization of silicon alkoxide precursors using the sol-gel process. Thus far, the last approach is the most widely used for fabricating silica monoliths [46].

In a typical procedure, the sol-gel process is used to produce a silica network. The starting solution contains tetraethyl or tetramethyl orthosilane as the sole precursor and a porogen (polyethyleneoxyde, PEO or polyethyleneglycol, PEG). The wet gel is introduced in the capillary and thermal treatment follows. The three dimensional silica network is then rinsed to remove the porogen. In order to tailor the mesopores, an extensive wash with ammonia is performed. The result is a porous silica network in which functional groups are introduced by derivatization reactions [9, 41, 45, 47].

### **Conclusions**

At this stage it is difficult to predict which type of column format will dominate the future of CEC. The straightforward transfer from LC to packed column CEC is certainly an advantage for this type of column although the pernicious effects of the frits remain a serious drawback.

The increasing quality of monolithic columns used in pressure-driven techniques could lead to a renewed interest in CEC as well. The advantages of monolithic

columns are clear but most concerns currently lay in the reproducibility of this type of columns.

Open tubular CEC columns could be more promising if long columns with a sufficient phase ratio can be produced.

---

### References

1. M Pursch, LC Sander – *J Chromatogr A* 887 (2000) 313-326
2. C Fujimoto – *TrAC* 18 (1999) 291-301
3. H Rebscher, U Pyell – *Chromatographia* 38 (1994) 737
4. B Behnke, E Grom, E Bayer – *J Chromatogr A* 716 (1995) 207
5. GA Lord, DB Gordon, P Myers, BW King – *J Chromatogr A* 768 (1997) 9
6. R Asiaie, X Huang, D Farnan, Cs Horvath – *J Chromatogr A* 806 (1998) 251
7. MT Dulay, RP Kulkarny, RN Zare – *Anal Chem* 70 (1998) 5103
8. Q Tang, B Xin, ML Lee – *J Chromatogr A* 837 (1999) 35
9. Q Tang, ML Lee – *TrAC* 19 (2000) 648-663
10. TD Maloney, LA Colon – *J Sep Sci* 25 (2002) 1215-1225
11. S Roulin, R Dmoch, R Carney, KD Bartle, P Meyers, MR Euerby, C Johnson – *J Chromatogr A* 887 (2000) 307-312
12. LA Colon, G Burgos, TD Maloney, JM Cintron, RL Rodriguez – *Electrophoresis* 21 (2000) 3965-3993
13. JH Knox, IH Grant – *Chromatographia* 32 (1991) 317-328
14. JH Knox, IH Grant – *Chromatographia* 24 (1987) 135-143
15. RJ Boughtflower, T Underwood, CJ Paterson – *Chromatographia* 40 (1995) 329-335
16. U Pyell – *J Chromatogr A* 892 (2000) 257-278
17. C Yang, Z El Rassi – *Electrophoresis* 19 (1999) 2061
18. C Yang, Z El Rassi – *Electrophoresis* 20 (1999) 18
19. MM Robson, MG Cikalo, P Myers, MR Euerby, KD Bartle – *J Microcol Sep* 9 (1997) 357-372  
24K Jinno, H Sawada – *TrAC* 19 (2000) 664-675
20. NW Smith, MB Evans – *Chromatographia* 38 (1994) 649
21. MM Robson, S Roulin, SM Schariff, MW Raynor, KD Bartle, AA Clifford, P Meyers, MR Euerby, CM Johnson – *Chromatographia* 43 (1996) 313

22. R Dadoo, RN Zare, C Yan, DS Anex – *Anal Chem* 70 (1998) 4787
23. R Stol, H Poppe, WT Kok – *Anal Chem* 75 (2003) 5246-5253
24. K Jinno, H Sawada – *TrAC* 19 (2000) 664-675
25. LA Colon, G Burgos, TD Maloney, JM Cintron, RL Rodriguez – *Electrophoresis* 21 (2000) 3965-3993
26. C-Y Liu – *Electrophoresis* 22 (2001) 612-628
27. E Guihen, JD Glennon – *J Chromatogr A* 1044 (2004) 67-81
28. H Zou, M Ye – *Electrophoresis* 21 (2000) 4073-4095
29. A Malik – *Electrophoresis* 23 (2003) 3973-3992
30. W Li, DP Fries, A Malik – *J Chromatogr A* 1044 (2004) 23-52
31. R Swart, JC Kraak, H Poppe – *TrAC* 16 (1997) 332-342
32. MM Dittmann and GP Rozing in "*Capillary Electrochromatography*", ed KD Bartle and P Myers, The Royal Society of Chemistry (2001) 64-86
33. S Constantin, R Freitag – *J Sep Sci* 25 (2002) 1245-1251
34. S Hjerten, A Vegvari, T Srichaiyo, H-X Zhang, C Ericson, D Eaker – *J Cap Electrophoresis* 1/2 (1998) 13-26
36. K Mistry, I Krull, N Grinberg – *J Sep Sci* 2002, 25, 935-958
37. AM Siouffi – *J Chromatogr A* 1000 (2003) 801-818
38. D Allen, Z El Rassi – *Electrophoresis* 24 (2003) 3962-3976
39. F Svec, EC Peters, D Sykora, C Yu, MJ Fréchet – *J High Resol Chromatogr* 23 (2000) 3-18
40. CK Ratnayake, CS Oh, MP Henry – *J High Resol Chromatogr* 23 (2000) 81-88
41. N Tanaka, H Nagayama, H Kobayashi, T Ikegami, K Hosoya, N Ishizuka, H Minakuchi, K Nakanishi, K Cabrera, D Lubda – *J High Resol Chromatogr* 23 (2000) 111-116
42. C Yu, F Svec, MJ Fréchet – *Electrophoresis* 21 (2000) 120-127
43. EC Peters, M Petro, F Svec, MJ Fréchet – *Anal Chem* 69 (1997) 3646-3649
44. T Jiang, J Jiskra, HA Claessens, CA Cramers – *J Chromatogr A* 923 (2001) 215-227
45. D Hoegger, R Freitag – *J Chromatogr A* 914 (2001) 211-222
46. D Allen, Z El Rassi – *Electrophoresis* 24 (2003) 3962 – 3976
47. H Zhong, Z El Rassi – *J Sep Sci* 29 (2006) 2031-2037

**PART B:**  
**Experimental Electrochromatography**

## Chapter V

### Peak and Sample Capacity in CEC, MEKC and MEEKC\*

#### V.1 Introduction

Capillary electrochromatography (CEC), micellar electrokinetic chromatography (MEKC) and microemulsion electrokinetic chromatography (MEEKC) are useful alternatives to (micro-) LC as they offer different selectivities and higher efficiencies compared to their pressure-driven analogues. Notwithstanding these features, the techniques are not often implemented yet in e.g. the pharmaceutical industry because of concerns about the robustness and the sensitivity of these techniques.

Electrodriven separation techniques are still young and have not benefited from the many years of instrumental improvements, as has been the case with HPLC and GC. It can be assumed that aspects such as more reproducible injection and EOF will further improve in future instrument designs. The lower sensitivity of capillary electrodriven separation techniques is a bigger concern. This issue has to be resolved to ensure the future of these techniques and can probably be improved by the application of dedicated detection using e.g. tunable lasers to increase the intensity of the light source. Another important part of the solution to the sensitivity issue in capillary separations is to enhance the sample capacity of the CE mode used. It may be expected that through the combination of both these aspects capillary electrodriven techniques should be able to meet the most stringent requirements in e.g. pharmaceutical validation. Another requirement in this context is the need for "generic" techniques.

The high efficiency and resulting peak capacity of electrodriven techniques can offer answers to this. However, thus far these issues have not been thoroughly

---

\* Results presented in the poster "*Study on the Peak and Sample Capacity in Electrodriven Chromatographic Techniques*", authors A Buica, F Lynen, A Crouch and P Sandra at *HPLC 2007*, Gent, Belgium

investigated or compared for the modern CE modes. In this chapter the peak and sample capacity of MEKC, MEEKC and CEC are investigated.

All three techniques are based on both electrokinetic and chromatographic separation mechanisms. Two effects therefore determine the separation in these systems: the chromatographic effect (the difference in partition coefficients of analytes between the (pseudo) stationary and mobile phases), and the electrophoretic effect (the difference in migration velocities of analytes in the electric field). [1]. Even though the separation mechanism of MEEKC is similar to that of MEKC, the pseudostationary phases employed in the two systems are quite different. In MEKC, micelles that are formed in the running buffer when the surfactant concentration is above its critical micelle concentration (CMC) form the pseudostationary phase. In MEEKC, stable, dispersed, and surfactant-coated nanometre-sized oil droplets in microemulsion form the, often charged, pseudostationary phase. [2].

Peak capacity ( $n_p$ ) is a better parameter to express the separation power of a chromatographic technique compared to efficiency ( $N$ ) and reduced plate height ( $h$ ). While  $N$  and  $h$  refer to a single peak in the chromatogram,  $n_p$  and resolution ( $R_s$ ) estimate the overall separation potential of a technique [3]. *Peak capacity* is defined as the maximum number of components that can be separated with a specified value of resolution, within a given separation window. In practice, a value of 1 for the resolution is considered sufficient. Grushka derived equation (V.1), which shows the effect of elution time ( $t$ ) and efficiency ( $N$ ) on peak capacity for an isocratic analysis:

$$n_p = 1 + \frac{\sqrt{N}}{4} \ln \frac{t_n}{t_1} = 1 + \frac{\sqrt{N}}{4} \ln(1 + k) \quad (\text{V.1})$$

where  $k$  is the capacity factor of the peak eluting at time  $t_n$  and  $t_1$  that of an unretained marker [4,5]. For a homologous series of compounds, a linear relationship exists between peak width at half-height,  $w_{1/2}$ , and the retention time,  $t$ , which can be described as

$$w_{1/2} = at + b \quad (\text{V.2})$$

where  $a$  and  $b$  are constants [6].

From equation (V.2) and the expression for column efficiency

$$N = 5.54 \left( \frac{t}{w_{1/2}} \right)^2 \quad (\text{V.3})$$

another expression for peak capacity can be deduced:

$$n_p = 1 + \frac{\sqrt{5.54}}{4a} \ln \frac{at_n - b}{at_1 - b} \quad (\text{V.4})$$

This equation is considered to be more representative if isocratic conditions are used and a sample containing a homologous series of compounds is analyzed. It is therefore important that good linearity is obtained and that the intercept ( $b$ ) is as close as possible to 0 (equation V.2). Hence, when applying equation (V.2), the regression coefficient ( $R^2$ ) should be close to 1 and  $b$  close to 0.

The advantage of equation (V.4) compared to (V.1) is that it is independent of the efficiency,  $N$ . By using equation (V.1), the differences in measured efficiencies are often complicating the estimation of  $n_p$ .

From equation (V.4) it can be seen that  $n_p$  is affected by the value of the constant  $b$ . When the influence of retention on column efficiency can be neglected ( $b \rightarrow 0$ ), equation (V.4) reduces to equation (V.1).

Both equations will be used to compare the techniques studied in this work.

As seen from equation (V.1), peak capacity has a logarithmic dependence on the capacity factor  $k$ , which means that it soon reaches a plateau. The only other way of increasing  $n_p$  is by considerably increasing efficiency, as the peak capacity has only a square root dependence on  $N$  [7]. In this matter, electrodriven separation methods have the advantage over pressure driven methods due to their inherent flat flow profile, which leads to higher plate numbers.

*Sample capacity* is defined as the amount of sample that can be introduced into a column before overloading occurs. This is defined as the amount of sample that causes the efficiency of that column to drop below 90 percent of its normal value.

In this work the peak capacity and sample capacity obtainable with MEKC, MEEKC and CEC are compared for various solute mixtures. The sample capacity is measured from plots representing the efficiency versus quantity of injected

analyte and by investigating the 0.05% impurity level relative to a main compound (as required in the pharmaceutical industry).

## **V.2 Experimental**

### **V.2.1 Materials**

Fused silica capillaries of 50  $\mu\text{m}$  I.D. were from Polymicro Technologies (Phoenix, AZ, USA). Packed capillaries (48.5 cm  $L_{\text{tot}}$ , 100  $\mu\text{m}$  I.D. packed with 3 $\mu\text{m}$  octadecylsilica particles) were purchased from Agilent (Waldbronn, Germany). Sodium dodecylsulfate (SDS), the phenone series and the xanthenes (caffeine, theobromine, theophylline) were from Sigma (Bornem, Belgium). All solvents used were of HPLC purity Aldrich (Bornem, Belgium). The phenones were dissolved in acetonitrile, 200 ppm each. Caffeine and theobromine were dissolved in water, theophylline in 0.1N NaOH at 5000ppm each. All dilutions were made to the desired concentration with running buffer.

### **V.2.2 Analytical conditions**

All electrodriven experiments were performed on an Agilent <sup>3D</sup>CE instrument, equipped with a diode array detector Agilent Technologies (Waldbronn, Germany). CEC columns were submitted to a voltage conditioning process by stepwise increase of the voltage up to 30 kV in 60 min. For MEKC and MEEKC experiments, the fused silica capillaries were equilibrated with new running buffers for 45 min.

For the peak capacity experiments, the buffer compositions are detailed in the results and discussion part. Injection was performed hydrodynamically for the MEKC and MEEKC experiments (3 s \* 40 mbar) and electrokinetically for CEC experiments (3 s \* 10 kV).

For the sample capacity experiments, the following optimized running buffers were used. For MEKC 60 mM SDS in 50 mM borate pH 9, for MEEKC: 60 mM SDS in 50 mM borate pH 9, containing 2% 1-butanol (w/v) and 0.41% n-heptane (w/v) and for CEC 25 mM  $\text{NH}_4\text{OAc}$  with unadjusted pH/acetoneitrile 25/75.

### V.3 Results and discussion

#### V.3.1 Peak capacity in CEC, MEKC and MEEKC

In order to use the general equation (V.4) for establishing the peak capacity of a technique, a homologous series of compounds has to be used and a linear relationship between peak width at half-height ( $w_{1/2}$ ) and elution time is required. The peak widths of a series of phenones (phenylketones) were therefore plotted vs time and the corresponding results are given in Table V.1. The values presented were calculated for the acetophenone to hexanophenone peaks. Representative separations are shown in Figure V.1.

**Table V.1** Linear regression parameters for a plot of peak width at half height ( $w_{1/2}$ ) vs migration time for a phenone homologous series (acetophenone to hexanophenone).

technique	a	b	R <sup>2</sup>	$t_2-t_1$	$n_p^{\text{eq V.1}}$	$n_p^{\text{eq V.4}}$
CEC	0.0105	-0.0116	0.9976	15.982	89	68
MEKC	0.016	-0.0044	0.8504	4.457	51	40
MEEKC	0.0339	-0.1022	0.9671	6.257	57	15

Separation conditions as described for figure V.1.  $n_p^{\text{eq V.1}}$  and  $n_p^{\text{eq V.4}}$  represent the peak capacity values calculated according to equations (V.1) and (V.4), respectively.

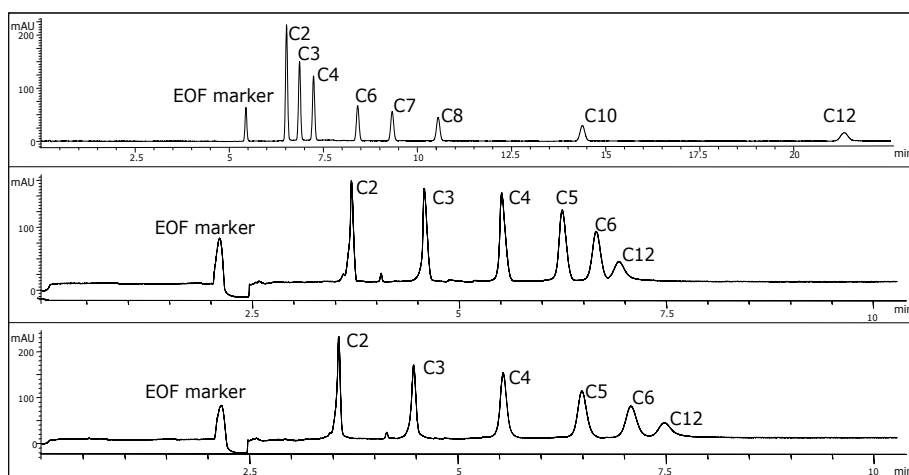


**Figure V.1** Separation of phenones in CEC (top), MEKC (middle) and MEEKC (bottom). CEC: 25 mM TRIS pH 8/ CH<sub>3</sub>CN 85/15; MEKC: 60 mM SDS in 50 mM borate pH 9; MEEKC: 60 mM SDS in 50 mM borate pH 9, containing 2% 1-butanol (w/v) and 0.41% n-heptane (w/v)

It can be noticed that the correlation coefficient R<sup>2</sup> for linear regression is best for CEC and worst for MEKC. For the latter technique, equation (V.1) could

therefore be more appropriate for calculating the peak capacity. Also, in MEEKC, the difference in the values for  $n_p$  as calculated with the two equations can be explained by the finding that the intercept ( $b$ ) is more different from 0 than in CEC and MEKC.

In both MEKC and MEEKC, increasing the SDS concentration from 60 mM to 120 mM leads to a better linear regression of the peak width at half height vs time for the same phenone series, but also to a large increase in current affecting the repeatability of the experiments.

For the calculation of the peak capacity, an elution time window, created by thiourea as unretained compound and dodecanophenone as micelle marker, in MEKC and MEEKC was used. CEC is not limited by the existence of an elution window, as is the case with the other two techniques. The results obtained for MEKC and MEEKC can be directly compared, while in order to make a comparison with CEC, a strongly retained compound (*i.e.* hexanophenone) had to be chosen to determine the elution interval. The values used for the calculations (such as average efficiency,  $N$ ) are based on the experimental data for the acetophenone to hexanophenone peaks.

For the same concentrations of borate and SDS in the running buffer (60 and 50 mM, respectively) and similar values of the average efficiency  $N$  (approximately 70,000 plates/m or 28,000 plates/column), MEEKC has the advantage of a larger elution window (6.26 min vs 4.46 min) and of a higher peak capacity (57 vs 51; Table V.1).

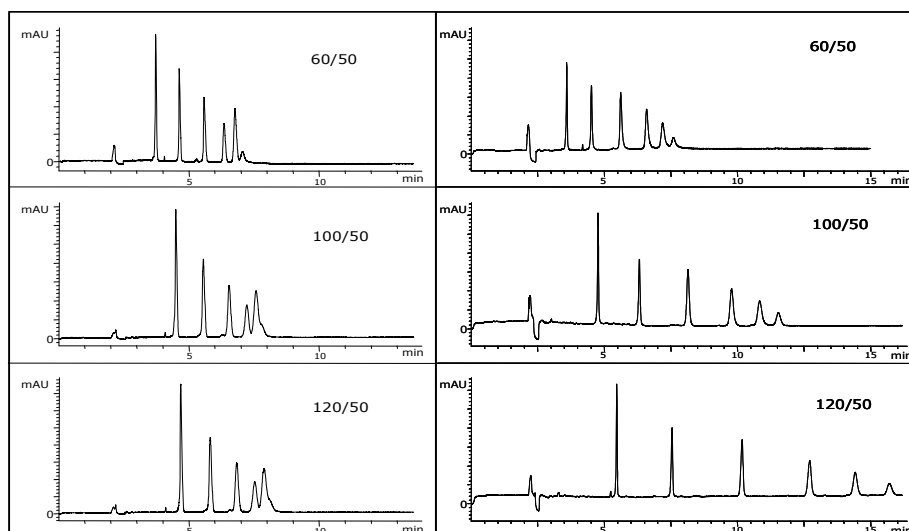


**Figure V.2** Influence of SDS concentration on peak capacity in MEKC (left) and MEEKC (right). The numbers represent the SDS concentration in 50 mM borate pH 9. Other conditions as in Figure V.1

Increasing the SDS concentration in the running buffer affected the separations in MEKC and MEEKC differently. In MEKC, when SDS concentration increased from 60 mM to 120 mM, even though the EOF did not vary and the elution window was similar, the efficiency decreased leading to a drop in peak capacity (53 vs 41). In MEEKC, for the same variation of SDS concentration, the elution window became almost three times as long. The efficiency remained similar and the peak capacity more than tripled (40 vs 129) (Figure V.2 and Table V.2).

By increasing the voltage at which the experiments are run, the analysis time decreases. This can affect MEKC and MEEKC by a reduction in the elution window and an increase in the efficiency. As the peak capacity depends on both  $N$  and  $t_2/t_1$  (equation V.1), it was considered interesting to evaluate these opposing factors and their combined influence on the peak capacity.

In MEKC, when the voltage was increased from 10 to 30 kV, the elution window decreased from 10.44 min to 3.86 min, while efficiency increased from 9,275 to 44,912 plates/column. The overall effect was an increase in peak capacity from 27 to 65 (as calculated with equation V.1). In MEEKC, for the same voltage interval, the elution window decreased from 10.1 min to 3.44 min, while efficiency increased from 8,974 to 22,629 plates/column. The overall effect was an increase in peak capacity from 25 to 44 (calculated with equation V.1).

Hence, it can be concluded that for both techniques an increase in voltage leads to an increase in peak capacity and a drastic reduction in separation time (Table V.2).

**Table V.2** Figures of merit for peak capacity in MEKC, MEEKC and CEC.

voltage, kV	running buffer* SDS conc, mM	MEKC		MEEKC		CEC	
		$n_p^{eq V.1}$	$n_p^{eq V.4}$	$n_p^{eq V.1}$	$n_p^{eq V.4}$	$n_p^{eq V.1}$	$n_p^{eq V.4}$
25	60	53	22	40	16	-	-
25	100	46	14	86	29	-	-
25	120	41	13	129	48	-	-
10	60	27	8	25	11	-	-
25	60	53	22	40	16	-	-
30	60	65	26	44	17	-	-
----- %acetonitrile							
25	80	-	-	-	-	152	115
25	85	-	-	-	-	89	68
25	90	-	-	-	-	85	68

\* SDS concentration in 50 mM borate pH 9; %acetonitrile in 25 mM TRIS pH 8. Other conditions as in Figure V.1.

In order to compare MEKC and MEEKC to CEC, the limitations of the elution window should be taken into consideration. In Figure V.3 the peak capacities (calculated with equations V.1 and V.4) are plotted for various time windows. The solid symbols represent measured data points for MEKC, MEEKC and CEC. The open ones represent the extrapolated points according to equations (V.1) and (V.4).

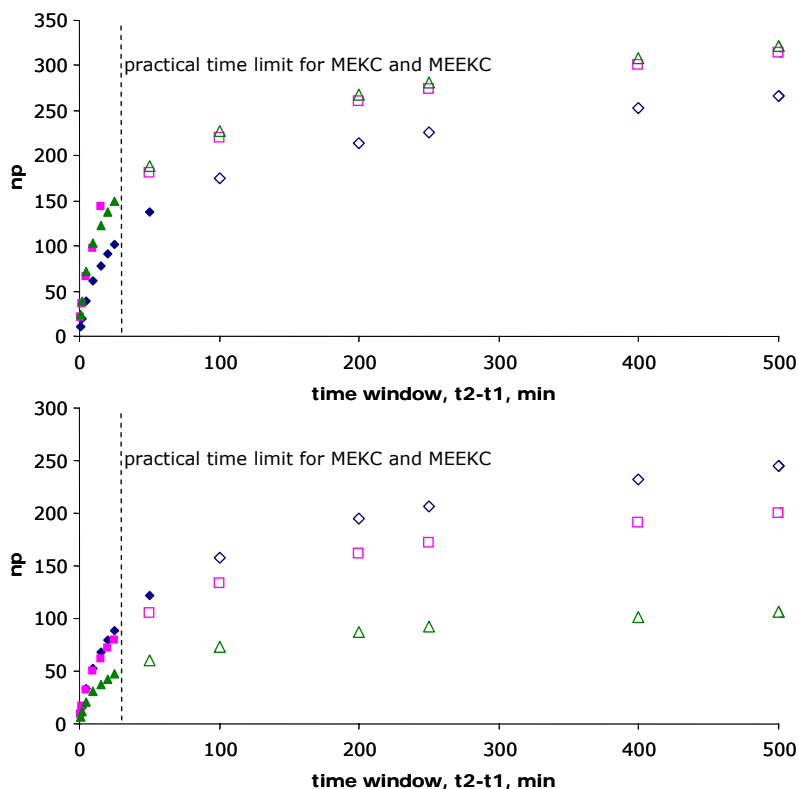


**Figure V.3** Calculated peak capacities ( $n_p$ ) for different elution windows for CEC ( $\blacklozenge$ ,  $\blacklozenge$ ), MEKC ( $\blacksquare$ ,  $\square$ ) and MEEKC ( $\blacktriangle$ ,  $\triangle$ ), according to equation V.1 (top) and V.4 (bottom). Separation conditions as in Figure V.1, except for MEKC: 60 mM SDS in 50 mM borate pH 9 containing 10%  $\text{CH}_3\text{CN}$ .

The extrapolation shows a flattening of the curves for all three techniques. Although values of  $n_p$  of 100 or more are predicted for all techniques, it should be realized that in practice this could only be obtained for CEC where there is no limit to the size of the elution window. The practical limits for MEKC and MEEKC are shown by the vertical lines. The maximum values achievable are calculated with equation V.4 because these are independent of the plate numbers of the individual peaks. From the results shown in Figure V.3 (bottom), it appears that CEC is outperforming MEKC and MEEKC.

### V.3.2 Sample capacity in CEC, MEKC and MEEKC

The sample capacity study was divided into three sets of experiments: the evaluation of the injection time on the efficiency, the evaluation of the sample concentration on the efficiency and the investigation of a 0.05% impurity level.

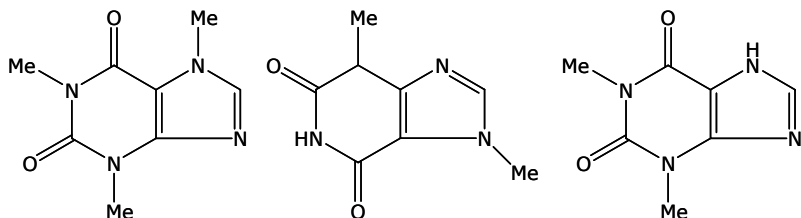


**Figure V.4** Molecular structures of caffeine, theobromine and theophylline

#### V.3.2.1 Influence of the injection time on the efficiency

A sample containing 100 ppm of three xanthines (*i.e.* caffeine, theobromine, theophylline, see Figure V.4) was used. The injection time was varied from 1 s to 25 s in the case of MEKC and MEEKC at 40 mbar injection pressure, and between 5 and 50 s for CEC at 10 kV by electrokinetic injection. The results are depicted in Figure V.5.

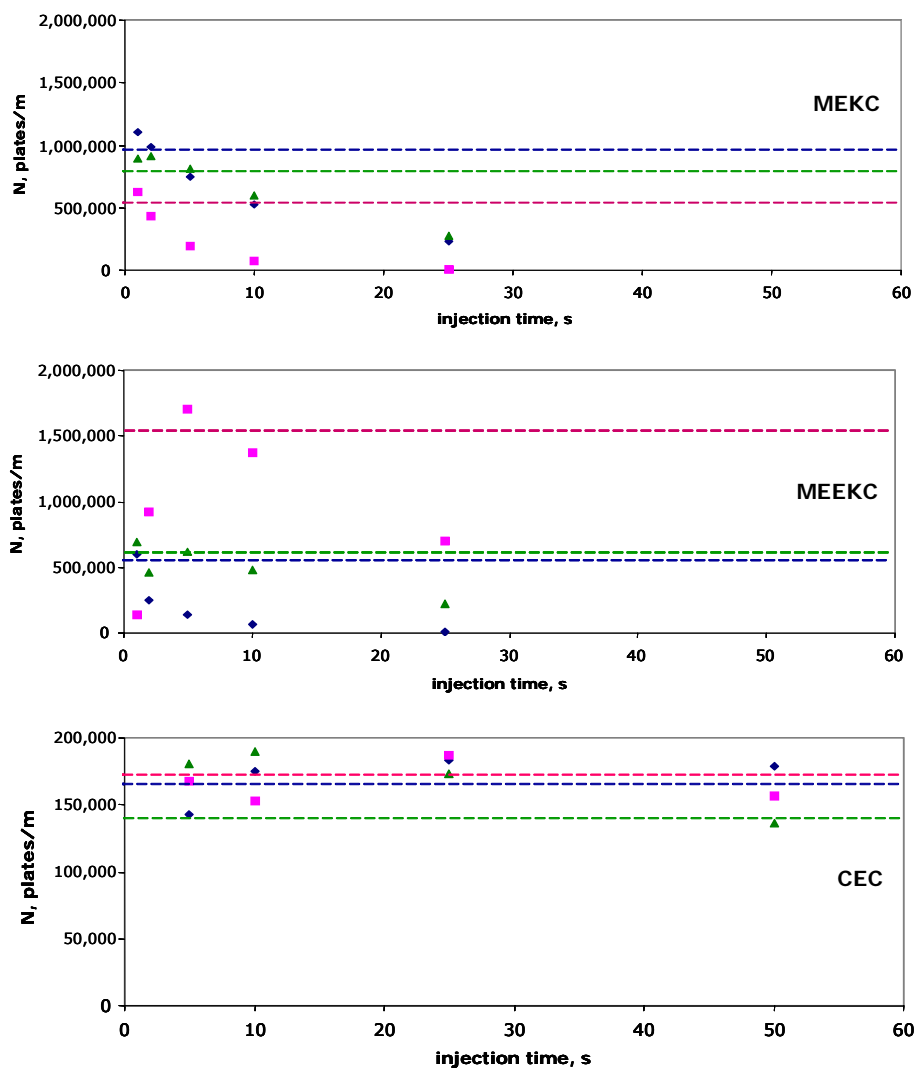


**Figure V.5** Efficiency vs injection time plots for MEKC, MEEKC and CEC. The dashed lines represent the 10% loss in efficiency for theobromine (◆), caffeine (■) and theophylline (▲).

For MEKC, the efficiency shows a steady decrease with increasing injection time. The most marked decreases in efficiency are registered for the caffeine and theobromine peaks, for which a 10% loss in efficiency (and hence sample capacity) is already reached between 1 and 2 s injection. For theophylline, the sample capacity is reached at 5 s injection.

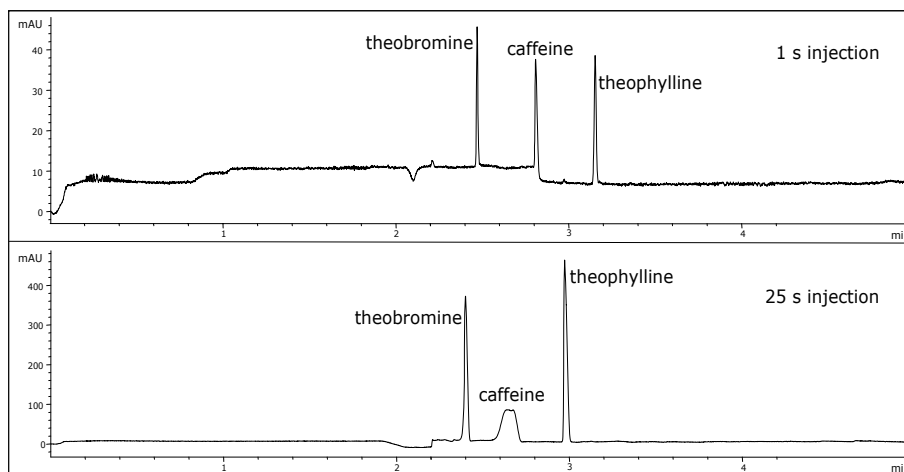


**Figure V.6** Influence of injection time in MEKC. Running buffer: 60 mM SDS in 50 mM borate pH 9

Representative separations displaying the influence of injection time are shown in Figure V.6. The severe broadening of the caffeine peak is probably related to a destacking effect in the caffeine plug.

In MEEKC, theobromine and theophylline follow the same trend, with a rapid decrease, reaching sample capacity at 2 and 5 s respectively. Caffeine shows a different behaviour, with a quick increase in plate number from 1 to 5 s injection time (phenomenon possibly due to a stacking effect). After 5 s injection time, the trend continues as expected, with a steady decrease in number of plates. Representative separations are shown in Figure V.7.

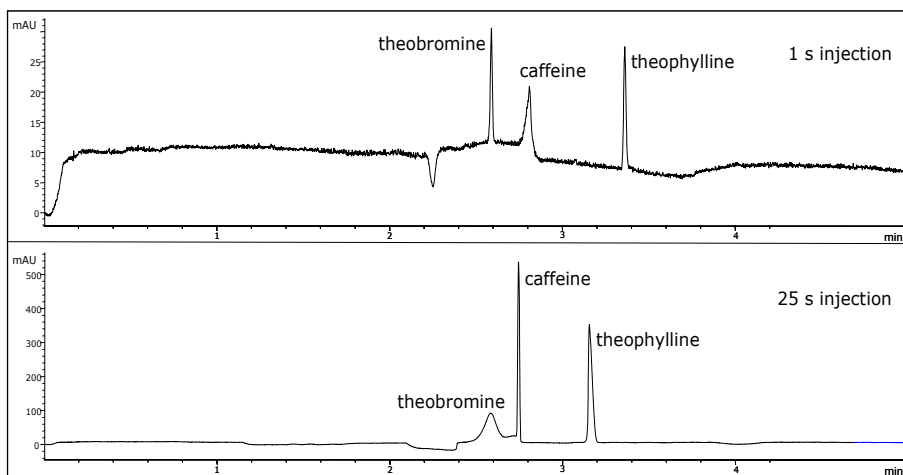


**Figure V.7** Influence of injection time in MEEKC. Running buffer: 60 mM SDS in 50 mM borate pH 9, containing 2% 1-butanol (w/v) and 0.41% n-heptane (w/v)

For CEC, the injection time has (for the investigated time range) hardly any effect on the efficiency of all three compounds of interest. Also it can be noticed that the efficiency is at least five times lower in the case of CEC than for MEKC or MEEKC. This is due to the polar nature of the compounds chosen for the sample; the interaction of these polar compounds with the active silanol sites present in the packing material negatively affects peak shape and efficiency.

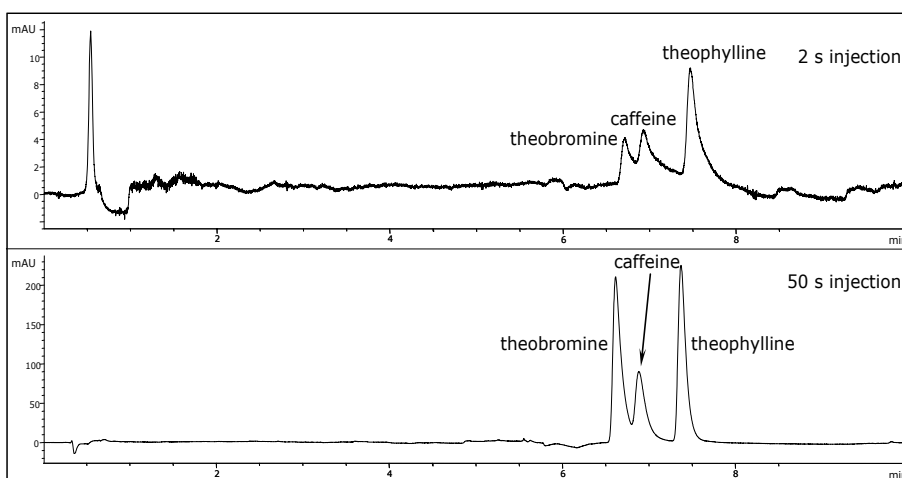


**Figure V.8** Influence of injection time in CEC. Mobile phase: 25 mM  $\text{NH}_4\text{OAc}$  with unadjusted pH /  $\text{CH}_3\text{CN}$  25/75

### V.3.2.2 Influence of the sample concentration on the efficiency

All compounds (concentration range 50-1000ppm each) were injected for 2 s at 50 mbar in the case of MEKC and MEEKC, and for 5 s at 10 kV for CEC. The results are shown in Figure V.9.

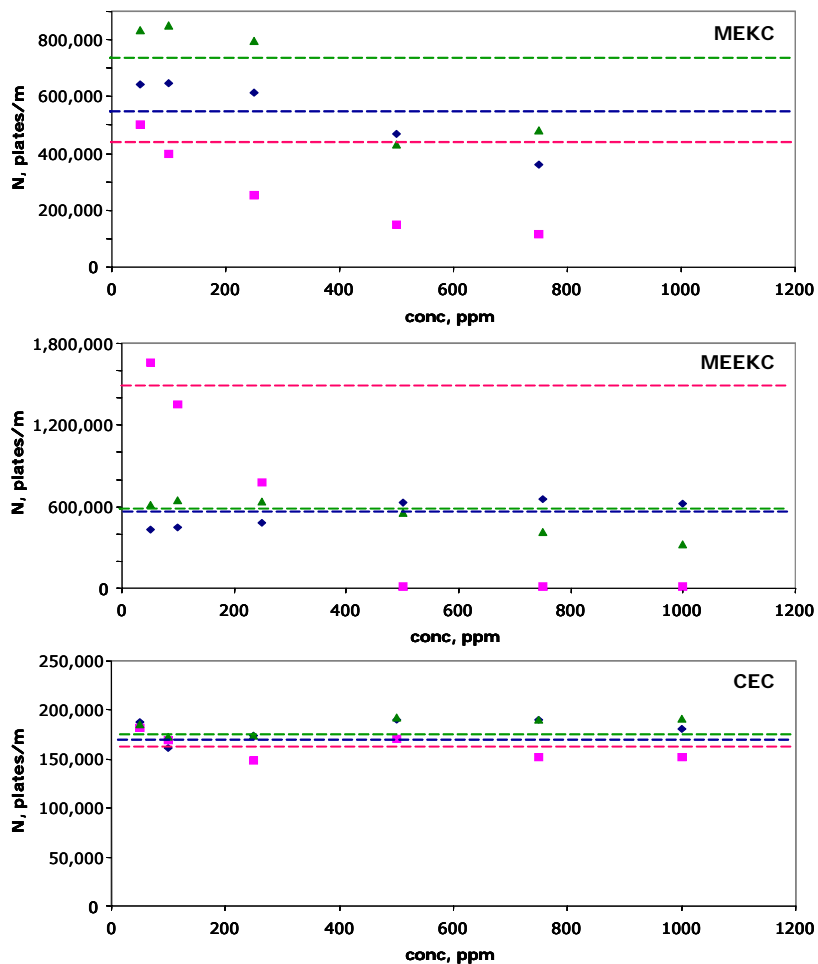


**Figure V.9** Efficiency vs sample concentration plots for MEKC, MEEKC and CEC. The dashed lines represent the 10% loss in efficiency for theobromine (◆), caffeine (■) and theophylline (▲)

In MEKC, theobromine and theophylline follow a similar trend. In the range of 50-250 ppm, no significant reduction in the number of plates with an increase in concentration can be noticed. At 500 ppm, both compounds already reach their sample capacity. In the case of caffeine, the number of plates continuously decreases with an increase in concentration. For caffeine, at 100 ppm, sample

capacity is already at its maximum value. A representative separation is shown in Figure V.10.

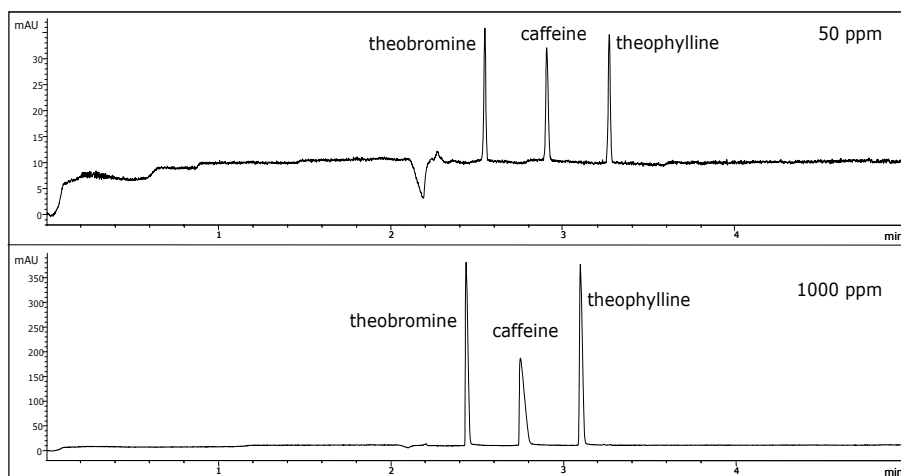


**Figure V.10** Influence of sample concentration in MEKC. Running buffer: 60 mM SDS in 50 mM borate pH 9

In MEEKC, although the number of plates for a 50 ppm caffeine sample is three times more than that measured for the other 50 ppm samples, it decreases rapidly, and at 500 ppm the peak is badly distorted. For theobromine and theophylline, the efficiency is similar for MEKC and MEEKC. For theophylline, sample capacity is reached at 500ppm, while for theobromine it is still not reached at 1000 ppm. An example of the separation with peak distortion for caffeine is shown in Figure V.11.

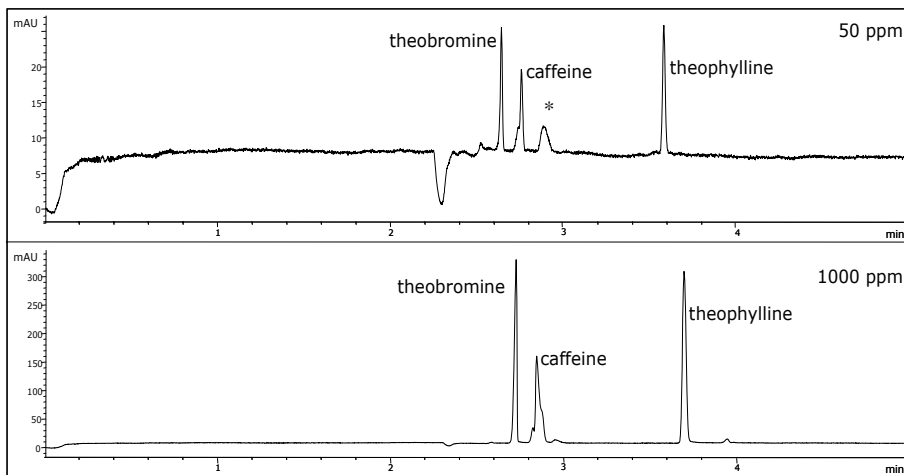


**Figure V.11** Influence of sample concentration in MEEKC. Running buffer: 60 mM SDS in 50 mM borate pH 9, containing 2% 1-butanol (w/v) and 0.41% n-heptane (w/v). \*: impurity

In CEC, although the efficiency is about three times lower than in the other two modes, Figure V.8 clearly shows that the number of plates is hardly affected by an increase in analyte concentration. This observation is also registered by a representative separation as shown in Figure V.12. Once more, the polar nature of the sample components affects the overall efficiency of the CEC separation.

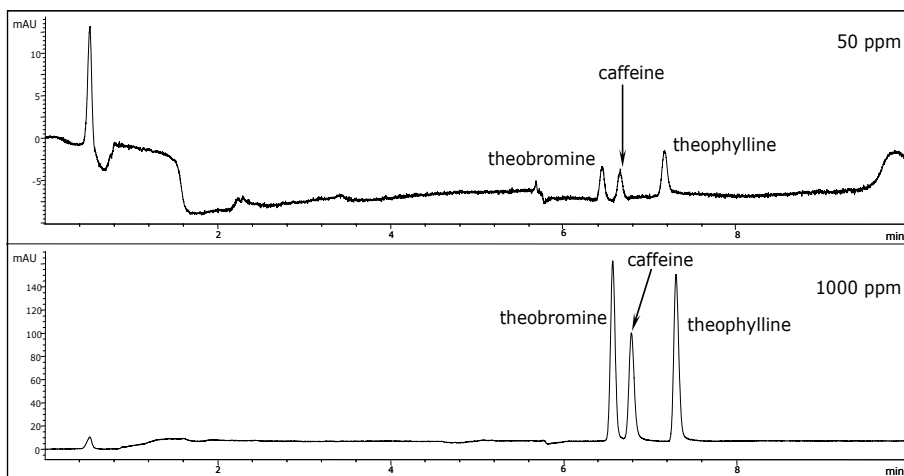


**Figure V.12** Influence of sample concentration in CEC. Mobile phase: 25 mM NH<sub>4</sub>OAc with unadjusted pH / CH<sub>3</sub>CN 25/75

### V.3.2.3 Evaluation of a 0.05% impurity level

The determination of a 0.05% impurity level in a prescribed drug is a standard measurement for any chromatographic technique used in the pharmaceutical industry. The technique should be capable to detect impurities next to the active pharmaceutical ingredient (API) at a concentration, which is 0.05% of the main peak. These experiments were only performed in the MEKC and MEEKC modes due to column failure in the CEC mode.

A solution containing 15 mg/mL caffeine and 0.0075 mg/mL theobromine and theophylline each was injected at 50 mbar for a time varying between 1 and 25 s in the MEKC and MEEKC modes.

In the MEKC mode, at 1s injection, the theobromine and theophylline peaks could already be detected at a signal-to-noise ratio of 5. This value is generally considered sufficient for a qualitative identification. In order to quantify these impurities, a signal-to-noise ratio of 10 is necessary. This level was reached for a 2 s injection, as shown in Figure V.13. At 25 s injection, the caffeine peak completely covers the theobromine peak, preventing quantitation.

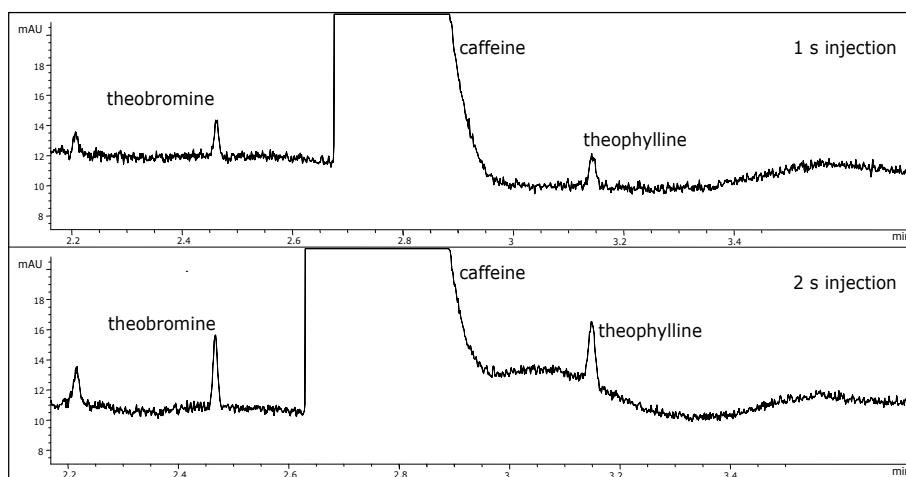


**Figure V.13** Illustration of 0.05% impurities separation in MEKC. Signal to noise ratio 5 for 1 s injection; signal to noise ratio 10 for 2 s injection

In the case of MEEKC, a signal-to-noise ratio of 5 was obtained for a 2 s injection and a signal-to-noise ratio of more than 10 for a 5 s injection (Figure V.14). That this injection time supersedes the time in MEKC can be explained by the higher noise level that is common in MEEKC. At 25 s injection time, the caffeine peak also covers the theobromine peak.

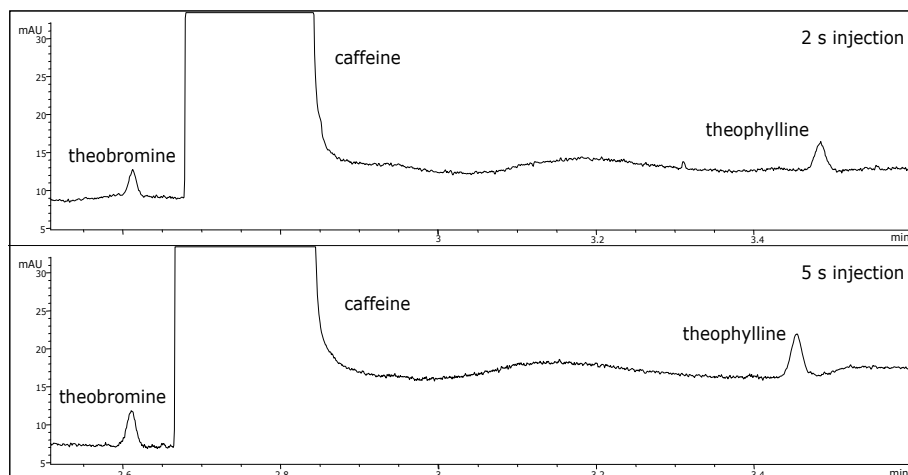


**Figure V.14** Illustration of 0.05% impurities separation in MEEKC. Signal to noise ratio 5 for 2 s injection; signal to noise ratio 10 for 5 s injection

### Conclusions

Of the three techniques, in terms of peak capacity, CEC has the advantage of a practically unlimited elution time, while MEKC and MEEKC suffer from the drawback of a restricted elution time window. In terms of peak capacity it can therefore be concluded that CEC outperforms MEKC and MEEKC.

In terms of sample capacity, CEC also performs better, as the reduction in efficiency with the amount of sample introduced into the column is small for the investigated sample range, while for MEKC and MEEKC the drop in efficiency is noticeable for the same range. The 0.05% impurity level test failed in this particular CEC analysis. This is mainly related to the fact that the best-known conditions for analysis of the xanthines is by CZE and MEKC. These compounds are actually too polar for suitable interactions with the C18-stationary phase in CEC. This type of column is clearly not appropriate for basic solutes, due to the silanol activity which, actually, is needed to provide EOF.

Overall, CEC appears to outperform the other electrodriven separation techniques. The main limitations of CEC are still practical. Matters such as column blockage or stationary phase degradation can occur after a few weeks' use. Also the interaction of basic compounds with the active silanol sites on the stationary phase is a major issue if this technique is to be considered for use in the pharmaceutical industry, knowing that the majority of active substances are

basic. Once these problems are solved, it can be expected that CEC will start competing with HPLC.

---

**References**

1. H-Y Huang, W-C Lien - *Electrophoresis* 2005, 26, 3134–3140
2. H-Y Huang, W-C Lien, C-W Chiu - *J. Sep. Sci.* 2005, 28, 973–981
3. JC Medina, N Wu, ML Lee – *Anal Chem* 73 (2001) 1301-1306
4. JC Giddings – *Anal Chem* 39 (1967) 1027-1029
5. E Grushka – *Anal Chem* 42 (1970) 1142-1147
6. Y Shen, ML Lee – *Anal Chem* 70 (1998) 3853-3856
7. JG Dorsey – *Microchem J* 61 (1999) 6-11

## Chapter VI

### P a c k e d   C o l u m n   C E C   \*

#### VI.1 Introduction

Several decades ago, electroosmosis was proposed as a means of driving a mobile phase through a packed bed as opposed to the pressure-driven flow used in liquid chromatography [1–3]. The full potential of electroosmosis became apparent when Jorgenson and Lukacs demonstrated the high efficiencies achievable in narrow capillaries, marking the start of the development of capillary electrodriven separation techniques [4]. The subsequent success of capillary electrophoresis (CE) raised expectations that capillary electrochromatography (CEC) would follow at the same pace. Although CEC has been practically introduced and was theoretically consolidated more than a decade ago, it is still not considered a viable alternative to HPLC or micellar electrokinetic chromatography (MEKC) [5–7]. The limited use of CEC so far can be attributed to several causes. The existing commercial CEC systems are CE systems with minor modifications allowing external pressurization of both the in- and outlet vial. Ideally commercial CEC systems should be available which offer the possibility of gradient analysis by gradually changing the composition of the mobile phase in the inlet vial. However, the main reason for the limited use of CEC so far seems to be related to limitations in column manufacturing.

Contrary to CE, for which capillaries are readily available and where column-to-column reproducibility is excellent, packed columns for CEC are expensive, fragile, short-lived, and often show reproducibility problems. A gradual improvement has been observed in the manufacturing of packed capillaries during the last decade. Several packing strategies, roughly comparable in terms

---

\* Published as "An efficient slurry packing procedure for the preparation of columns applicable in capillary electrochromatography and capillary electrochromatography-electrospray-mass spectrometry", authors F Lynen, A Buica, A de Villiers, A Crouch and P Sandra in *J Sep Sci* 28 (2005) 1539–1549

of column performance, have been described [8–10]. Gravity, centripetal, and electrokinetic forces have been used for column packing, but slurry packing involving conventional HPLC pumps has been favoured in most studies. Apart from common HPLC solvents, supercritical fluids have also been used for packing [10]. Initially large bore, heavy walled capillaries (1–2 mm ID) were slurry packed followed by drawing of these capillaries down to the required final diameter in a glass drawing machine at high temperature [7, 11]. However, this approach was not further pursued because of the many practical problems encountered.

After the early work of Pretorius, Jorgenson, and Tsuda that involved large bore columns or large particle sizes, thereby limiting the obtained plate numbers, Knox and Grant were the first to report high column efficiencies in CEC on quartz columns of 200  $\mu\text{m}$  ID [6, 7]. No outlet (retaining) frit was used while the inlet frit was made by sintering a paste of native silica gel with wetted sodium silicate. Yamamoto *et al.* obtained plate numbers >200,000 per meter for practically non-retained compounds (benzyl alcohol and benzaldehyde) on a packed bed containing 1.6  $\mu\text{m}$  solid octadecyl silica (ODS) particles with native silica frits to keep the packing material in place [12]. Smith and Evans obtained 387,000 plates per meter for a retained pharmaceutical compound ( $k = 4.3$ ) on 50  $\mu\text{m}$  capillaries packed with 3  $\mu\text{m}$  porous ODS-1 particles [13]. An inlet frit made from sodium silicate was used and they proposed the sintering of the packed bed itself for the production of the outlet (retaining) frit. Frits made from mixtures of native silica and/or wetted with sodium silicate are mechanically more stable and easier to make. Frits made directly from the packed bed lead to less band broadening and are less prone to bubble formation [7, 14, 15]. Under conditions of low ionic strength, this made it possible to perform CEC without pressurization at both column ends [16]. Additionally, it has been shown that sintering of frits is best done in water because the presence of organic solvents leads to formation of carbonaceous residues on the packing material, interacting with the analytes and lowering the column performance [17]. By using a combination of packing against gravity and ultrasonic agitation to maximize the time the slurry is kept in suspension, Boughtflower *et al.* were able to slow down the packing process, leading to very homogeneous packed beds [18]. Further improvement resulted on using frits made out of the packed bed and sintering in water, generating

efficiencies above 200,000 plates per meter. Lumley *et al.* combined the use of frits made out of the packed bed with a balanced density solvent [19, 20] to make capillaries in a reproducible way. Higher efficiencies have been reported on using a combination of smaller and/or non-porous particles [21, 22]. Over 700,000 plates per meter were obtained for the separation of 16 polyaromatic hydrocarbons [23–26]. This performance could be obtained by using a combination of an electrokinetic packing method, 1.5  $\mu\text{m}$  non-porous ODS particles, and a separation voltage up to 55 kV. The inlet frit could be made from native silica because no peak broadening interaction is occurring between polyaromatic hydrocarbons (PAHs) and native silica. The major problem of columns packed with solid particles, however, is that they suffer from a limited sample capacity, severely reducing the sensitivity of the method. Alternative approaches using columns packed with particles with larger pore sizes have also led to efficiencies up to 430,000 plates per meter [27]. However, a general problem with the above-mentioned approaches is the often complicated packing procedure. Some attempts were made to simplify the procedures but this often resulted in decreased peak efficiencies [28].

An additional problem with packed columns in CEC has been the coupling to mass spectrometry. This is mainly related to the formation of gas bubbles via the frits [6, 7, 29]. In CEC-UV, bubble formation can easily be suppressed by applying pressure on both sides of the capillary but in CEC-MS this problem proved much more difficult to solve. A solution was found in the use of monolithic stationary phases. No frits are thereby required, facilitating the coupling to the MS [8, 30]. Much progress has been made in terms of efficiencies for these polymeric beds but these efficiency values are generally lower compared to classical packed columns. Gas bubble formation is also claimed to be suppressed by applying pressure only at the inlet side of a packed capillary. This approach, called pressurized CEC (presCEC) offers additional advantages in terms of sample loading and the possibility of gradient analysis.

The efficiencies, which can be achieved in pCEC vary between microLC and CEC because of the peak broadening effect of the parabolic flow profile in pressure-driven systems [31, 32]. Notwithstanding the problems encountered in packed column CEC-MS, various combinations of packed column CEC and ESI/MS have been reported for the analysis of mixtures of peptides, corticosteroids,

benzodiazepines, DNA adducts, unsaturated fatty acid methyl esters, vitamin D2 and D3, and nucleosides [33–35]. Gas bubble formation could be circumvented through reducing the ionic strength of the buffer, the applied voltage and/or the EOF (e.g. by reducing the pH).

In recent years, an optimised procedure for the in-house manufacturing of slurry packed capillaries with conventional equipment was developed, combining the advantages of many of the above-described methods. Efficient capillaries can be packed with 3  $\mu\text{m}$  ODS particles in a reproducible manner without gas bubble formation. This is illustrated by the straightforward coupling to conventional ESI/MS.

## **VI.2 Experimental**

### **VI.2.1 Materials**

Fused silica capillaries of 50  $\mu\text{m}$  ID were purchased from Composite Metal Services Ltd (Worcester, UK). Trishydroxymethylaminomethane (TRIS), triethylamine, formic acid, the steroids, and the test compounds used for CEC-UV were provided by Sigma-Aldrich (Atlasville, South Africa). Hydrochloric acid was from Merck (Darmstadt, Germany). The carbamate test mixture was purchased from Supelco (Bornem, Belgium). All solvents ( $\text{CH}_3\text{CN}$ , methanol, benzyl alcohol, and toluene) were HPLC grade and were provided by Riedel-de Haen (Midrand, South Africa). Milli-Q water was obtained by purification and deionisation of tap water in a Milli-Q plus water system Millipore (Bedford, MA, USA). 3  $\mu\text{m}$  Spherisorb ODS-1 was kindly donated by Dr. P. Meyers (X-Tec, Leeds, UK). Nucleosil 300-5 pure silica particles used for the temporary frit production were purchased from Macherey-Nagel (Duren, Germany). The sodium silicate solution was made by dissolving 180 mg native Nucleosil silica in 500  $\mu\text{L}$  of a 19% (w/w) NaOH solution. After one hour in an ultrasonic bath heated at 50°C, a transparent solution was obtained.

### VI.2.2 Packing procedure

A schematic representation of the packing procedure is presented in Figure VI.1.

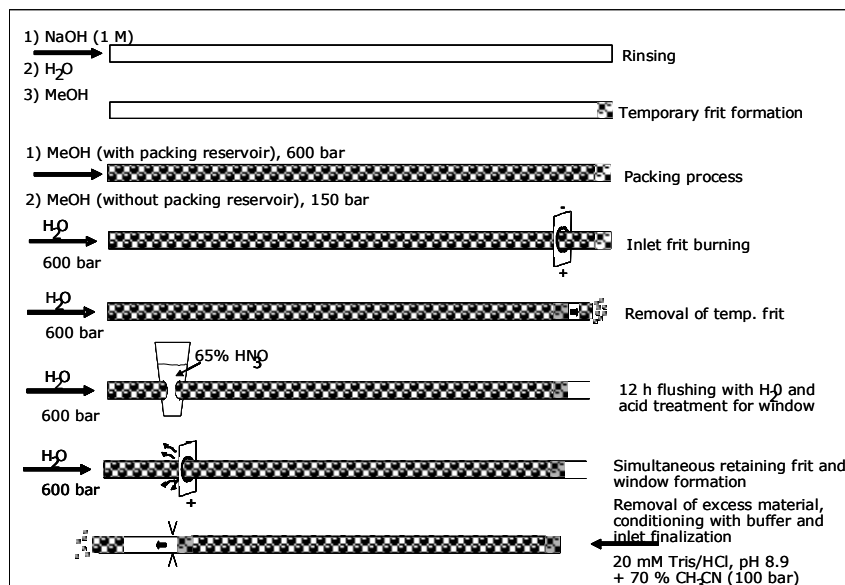


**Figure VI.1** Schematic representation of the column manufacturing process

Fused silica capillaries were rinsed for 15 min with 1 M NaOH, H<sub>2</sub>O, and methanol and dried for 10 min under N<sub>2</sub>. Temporary frit material is made by slightly wetting pure 5 μm Nucleosil silica particles with a 2/1 water/sodium silicate solution (v/v) such that the material is just sticking to the wall of a glass vial. The tip of the capillary with removed polyimide coating is dipped in the material such that a small amount is introduced into the column. The frit is subsequently sintered with a glowing heating filament, resulting in a permeable temporary frit able to withstand the 600 bar used during packing [36]. The permeability and mechanical strength of the temporary frit are evaluated by pumping methanol through the capillary until the pressure reaches 100 bar. After interruption of the flow, the speed at which the pressure decreases is used as an indication of the permeability of the frit. As a rule of thumb, a speed of pressure decrease of 0.5 bar/s from 100 to 90 bar was found to be indicative of good permeability on a 50 μm capillary. 100 mg of the packing material is suspended in 2 mL of the balanced density solvent consisting of methanol, benzyl alcohol, and toluene (33/27/40) [20]. The slurry is placed for 30 min in an ultrasonic bath and

introduced into the packing reservoir (Figure VI.2.A). The latter (an emptied HPLC column, 15 cm in length and 4.6 mm ID, with a hole of 1 mm through the outlet filter) is connected to the capillary as depicted in Figure VI.2.B. The inlet of the capillary is thereby positioned close to the bottom of the reservoir. The pressure (LC-307 pump, Gilson Medical, Villiers le Bel, France) is then quickly raised to 600 bar while the system is submitted to ultrasonic agitation for 1 h. The pressure is further maintained for 1 h before it is slowly released. The capillary is flushed for 3 h with methanol at 150 bar followed by conditioning with water for 2 h at maximum pressure (600 bar). The inlet frit is sintered for 5 s with a heating ribbon (Figure VI.2.C). The temporary frit is removed while the system is kept under pressure, immediately flushing out the extraneous particles. The system is further pressurized for at least 12 h to consolidate the packed bed. Simultaneously, a 65% HNO<sub>3</sub> solution is applied at the position intended for the UV detection window.

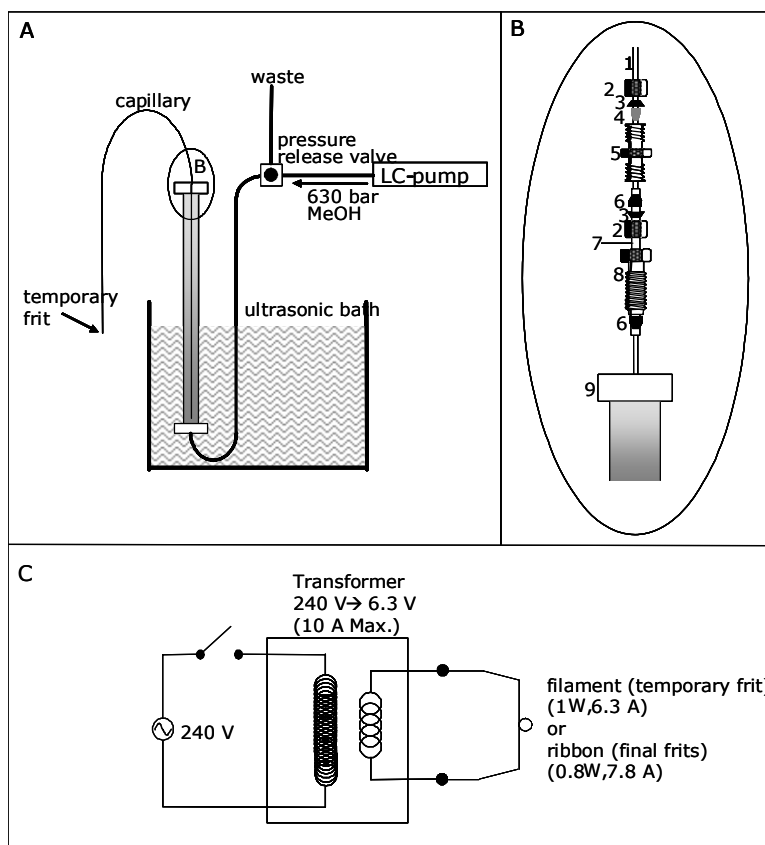


**Figure VI.2** Schematic drawing of the tools used in the column manufacturing. A: packing set-up, B: close-up of connection between capillary and packing reservoir (1: fused silica capillary, 2: 1/16" Swagelock nut, 3: 1/16" Swagelock back ferrule, 4: vespel ferrule (0.4 mm ID), 5: 1/16"x1/16" Swagelock union, 6: 1/16" Waters ferrule, 7: 1/16" stainless steel HPLC tubing, 8: 1/16" Waters nut, 9: packing reservoir inlet, C: schematic drawing of the frit burning device

The outlet (retaining) frit is formed in the same way as the inlet frit. The dissipating heat from the frit formation also crackles and removes the polyimide coating where the acid has been applied. The obtained window is 5 mm away from the retaining frit. Excess material at the window site is removed by flushing the column at 100 bar with a 70% CH<sub>3</sub>CN/20 mM Tris/HCl (pH 8.9) buffer solution, which is also used for the initial evaluation of the column [18]. Before placing the column in the CEC system, particular care is taken so that the free space between frit and column inlet is less than 0.5 mm.

### VI.2.3 Analytical conditions

CEC-UV and -MS analyses were performed on an HP<sup>3D</sup>CE system equipped with a diode array detector Agilent Technologies (Waldbronn, Germany). New columns were submitted to a voltage conditioning process by stepwise increase of the voltage up to 30 kV in 60 min. All injections were done electrokinetically. A voltage ramp of 3 min was used in the analyses. The buffer and sample compositions are detailed in the results and discussion part. A sheath flow interface was used for ESI/MS detection on an Agilent MSD Ion Trap XCT system Agilent Technologies (Waldbronn, Germany). Detection was performed in the positive ionisation mode and accordingly the MS capillary potential was set at – 3.5 kV while the interface was grounded. The sheath flow, consisting of a H<sub>2</sub>O/methanol (1/1) containing 0.1% formic acid was delivered by a 1/100 split of a 300 µL/min flow from an LC 1100 series binary pump Agilent Technologies (Waldbronn, Germany). The nebulizing gas (N<sub>2</sub>, 5 psi) and drying gas (N<sub>2</sub>, 8 L/min, 250°C) assisted ion formation and evaporation. No collision induced dissociation (CID) was used. All data were manipulated with the Chemstation software.

## VI.3 Results and discussion

### VI.3.1 Development of the packing procedure

The tools required for packing the capillaries are detailed in Figure VI.2. A standard LC pump equipped with an electronic pressure controller and able to go up to 600 bar is suitable. A pressure release valve should be included in the packing device because once the packing is completed the pressure drop through the capillary is exceedingly slow. A packing reservoir can easily be made from an empty LC column (150 mm x 4.6 mm ID) with a 1 mm hole drilled in the outlet filter. The most suitable way to connect the capillary to the packing reservoir proved to be GC-type connection parts as shown in Figure VI.2.B. Graphite ferrules or PEEK connections were not able to sustain the packing pressure while vespel ferrules were reliable and could be re-used. Initially, capillaries were packed in the downward direction [27, 28, 37] but it quickly became clear that this easily results in columns with poorly packed beds, leading to void volumes once they are submitted to an electric field. Much improved packed beds were

obtained by packing against gravity. Ultrasonic agitation was required to keep the particles in suspension for a sufficiently long time during the packing.

Before the packing is started a temporary frit is formed. The best results were obtained by using in-column silica based temporary frits [18]. The sodium silicate content is critical. Lower amounts increased the permeability but weakened the mechanical strength while higher amounts decreased the permeability to unacceptable levels. The influence of the particle size on the column performance is the same as in HPLC but some additional characteristics of the packing material play an important role in CEC. These include the sodium content, the carbon load, the degree of end-capping and the pore size of the particles. The latter three aspects affect the magnitude of the EOF.

A high EOF allows working closer to the optimal linear velocity in CEC, thereby increasing the separation efficiency. In HPLC a high carbon load and end-capping of the particles is advantageous by increasing the retention factor and by minimizing adsorption of basic compounds.

In CEC this is a drawback because, together with a small pore size, it reduces the EOF [7]. In most HPLC packings the metal content is deliberately kept low because of peak broadening effects associated with metal complexation and their indirect influence on silica acidity [38, 39]. In packed column CEC, however, the sodium content of the silica particles is important as it is known to influence the mechanical strength of the frits [40]. This was one of the reasons for selecting Spherisorb ODS-1 as packing material because the Na<sup>+</sup> content is ca. 1500 ppm [40].

The composition of the solvent used in the packing process also influences the packing speed. Most described procedures make a distinction between the slurry solvent and the packing solvent; the former generally being a small amount of solvent (0.5–2.5 mL) in which the packing material is “slurried” and that is able to keep it in suspension for a sufficiently long time to allow packing of the capillary to take place [18]. Methanol, acetone, and a “balanced density” solvent consisting of methanol, benzyl alcohol, and toluene (33/27/40) were investigated as slurry solvents. Although good columns were obtained when using methanol as slurry and packing solvent, the packed bed was often too short because of the quicker settling down of the slurry in the packing reservoir [18]. Dried acetone as packing and slurry solvent resulted in better columns compared to the “wet”

alternative but the column performance was generally lower than those obtained by combining a “balanced density” solvent, described by Zimina et al. as a slurry solvent, and methanol as packing solvent [20]. Under these conditions, the packing time was maximized, leading to a gradual build-up of a dense packed bed. A drawback is that the refractive index of the particles is very similar to that of the slurry solvent, resulting in difficult visual observation of the build-up of the packed bed.

A frit in CEC must show sufficient mechanical stability and good permeability. Moreover, the characteristics of the stationary phase should be maintained as much as possible, frits should not lead to any peak broadening, and they should minimally influence the EOF. It has been observed that frits, providing negative surfaces, increase the EOF over the whole capillary [41]. On the other hand, it has been shown that the EOF is reduced in packed columns to 40–60% of the value obtained in open tubes [7]. These opposing effects are two of the main reasons why column-to-column reproducibility in terms of EOF is hard to achieve. For the fritting of the 50  $\mu\text{m}$  capillaries packed with the 3  $\mu\text{m}$  ODS particles, the optimum time with the used heating ribbon was found to be 5 s. Shorter fritting resulted in frits which were not mechanically stable while longer heating resulted in frits with a blackened stationary phase due to pyrolysis of the C18 groups. As a consequence, the column activity increased as is illustrated in Figure VI.3 showing the analysis of some aromatics and parabens on a column whose frits were made by heating for 10 s. Severe tailing is noted for the polar parabens. It is clear from these observations that frits should be produced at as low a temperature as possible to minimize undesired interactions. Most studies use empirical approaches in terms of filament length, applied voltage, etc. to obtain good fritting conditions. In terms of absolute values, the ideal fritting temperature still seems unclear and values varying between 450 and 800°C with fritting times ranging from 1 to 60 s have been reported [16, 33, 36, 42, 43].

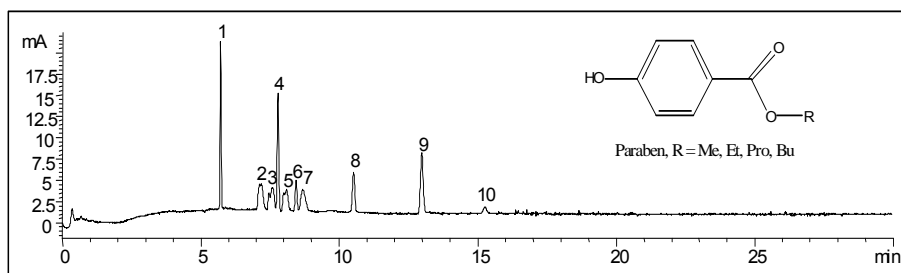


**Figure VI.3** Influence of the overheated frits on the peak shape of parabens. Column: 40 cm packed length. MP: 20 mM TRIS.HCl pH 8.9/CH<sub>3</sub>CN 30/70. Injection: 10 kV \* 1 s. Voltage: 30 kV. Peaks: 1: thiourea, 2: methylparaben, 3: ethylparaben, 4: acetophenone, 5: propylparaben, 6: benzene, 7: butylparaben, 8: naphthalene, 9: fluorene, 10: anthracene (800 µg/mL each). Insert: general structure of a paraben

Applying the conditions described, problems with bubble formation did not occur. Note that the fritting was performed with a heating ribbon providing frits of 1 mm length or less. The absence of gas bubble formation in all experiments can be related to the combined effect of sintering of the packed bed itself in water and the reduced size of the frit. An important observation was that the length of the empty capillary before the inlet frit strongly affected the magnitude of the EOF, as shown in Figure VI.4.

The best repeatability of the EOF and the highest column efficiencies were obtained in the case where nearly no void volume, i.e. empty capillary, was present before the inlet frit. This observation is highly reproducible and was made for all capillaries with different buffers. Some results are summarized in Table VI.1.

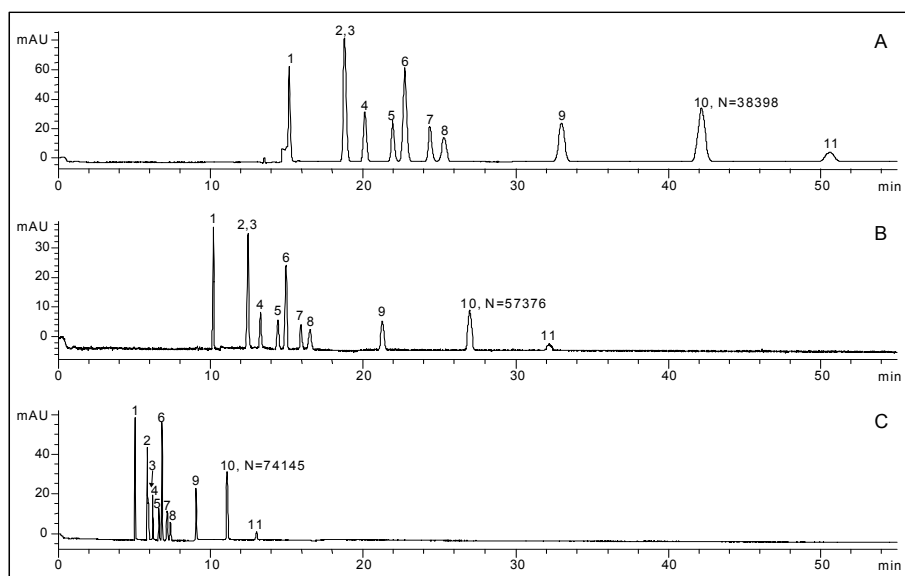


**Figure VI.4** Influence of the void volume between column outlet and inlet frit. Packed bed 35 cm. A: 4 mm void space before inlet frit, B: 2 mm void space before inlet frit, C: 0.5 mm void space before inlet frit. MP: 20 mM TRIS.HCl pH 8.9/CH<sub>3</sub>CN 30/70. Injection: 10 kV \* 1 s. Voltage: 30 kV. Peaks: 1: thiourea, 2: methylparaben, 3: phenol, 4: ethylparaben, 5: propylparaben, 6: butylparaben, 7: acetphenone, 8: benzene, 9: naphthalene, 10: fluorene, 11: anthracene (800 ppm each in CH<sub>3</sub>CN)

**Table VI.1** Influence of the length of empty capillary before the inlet frit on the obtained retention time of fluorene, plate number and current. Experiments performed on a capillary packed with 35 cm of 3  $\mu$ m ODS1. Conditions as in Figure VI.4.

MP	empty space before frit (mm)	RT (min)	plates	current ( $\mu$ A)
25mM TRIS/HCl, pH 8.0, 80% CH <sub>3</sub> CN	4	27.7	39,947	2.5
	2	15.9	68,508	3.2
	0.5	8.1	90,867	1.5
25mM TRIS/HCl, pH 8.0 + 70% CH <sub>3</sub> CN	4	ND	/	3.7
	2	24.9	65,938	5.5
	0.5	11.9	70,284	1.7
20mM TRIS/HCl, pH 8.9 + 70% CH <sub>3</sub> CN	4	42.1	38,398	4.5
	2	26.7	57,376	5.4
	0.5	11.1	74,145	1.1

The detection window is mostly made by locally heating the polyimide coating with a heated filament. It was observed that care must be taken to avoid side effects associated with these high temperatures. The rapid expansion of vapours

in the capillary causes a thermal shock effect that can create void spaces in the packed bed and even lead to collapse of the nearby retaining frit.

To avoid these problems the acid treatment approach was favoured [44]. 65% nitric acid solution is used during the consolidation step of the packed bed with water before formation of the retaining frit in the close vicinity. This allowed for simultaneous frit formation and cracking of the weakened coating by the residual heat on the side of the filament at the intended window spot. The coating could then very easily be removed at this location by slight scratching with a capillary cutter. It was found that the acid can easily be applied at a localized spot on the capillary by using a 1.5 mL Eppendorf vial punctured with two narrow holes to pass the capillary through (Figure VI.1). The highly viscous concentrated acid solution did not substantially leak out of such a vial. After removal of the Eppendorf vial, the capillary outer wall was extensively rinsed with water.

### **VI.3.2 Evaluation of the columns**

The good efficiencies of the prepared columns are clear from Figure VI.4.C, Figure VI.5, and Table I. The highest efficiencies were obtained with 25 mM Tris/HCl, pH 8.0 buffer containing 70% CH<sub>3</sub>CN. The run-to-run repeatability in terms of migration times and peak areas were below 1% and 9%, respectively, as illustrated in Table VI.2. These efficiencies are similar to or better than values reported in the literature for the same type of packing material [18, 42].

Some points should be taken into consideration when comparing column performances. A complicating factor is the uncommon compounds that are often used to calculate column efficiencies. With analytes carrying a (partial) charge, peak sharpening phenomena can take place due to various electrophoretic effects. Therefore standard polyaromatic hydrocarbons seem the obvious choice. Additionally, several reports describe impressive column efficiencies for common polyaromatic analytes but at field strengths not routinely achievable on most systems. In this study, the applied voltage was limited to 30 kV, the instrumental limit for most systems [4, 45]. Reproducibility in column making is also good, as illustrated in Figure VI.5 which compares two columns of the same length prepared with a time difference of four months.

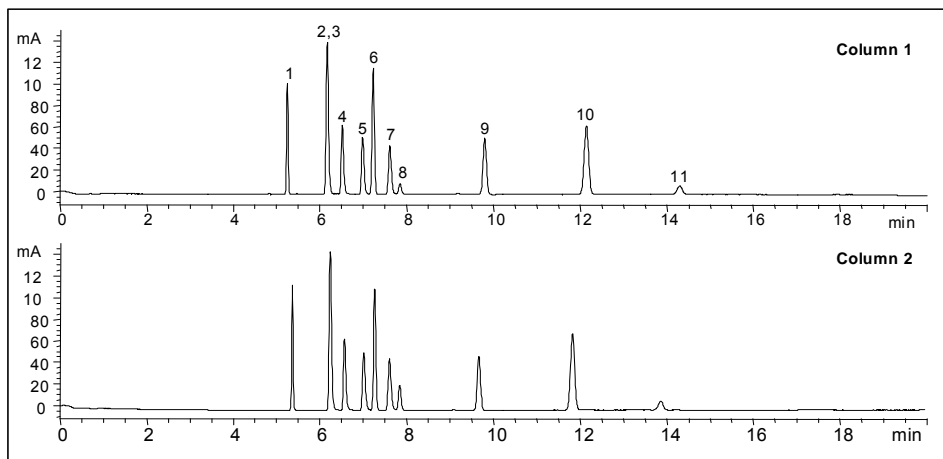


**Figure VI.5** Column repeatability. MP: 25 mM TRIS.HCl pH 8.0/CH<sub>3</sub>CN 30/70. Voltage: 30 kV. Injection: 10 kV \* 1 s. Detection: 200 nm. Peaks: 1: thiourea, 2: methylparaben, 3: phenol, 4: ethylparaben, 5: propylparaben, 6: butylparaben, 7: acetphenone, 8: benzene, 9: naphthalene, 10: fluorene, 11: anthracene

**Table VI.2** Run-to-run repeatability in terms of retention time and peak efficiency. n=5, column: 35 cm packed bed, total length: 44 cm. MP: 25 mM TRIS.HCl pH 8.0/CH<sub>3</sub>CN 30/70. Injection: 10kV\*1s. Voltage: 30 kV. Detection: 200 nm.

Compound	RT	RSD% k	area	RSD%	plates/ column	plates/m	RSD%	
thiourea	5.27	0.2	0.00	106	6.8	144,000	412,000	1.4
propylparaben	6.99	0.3	0.32	110	4.2	112,000	320,000	2.3
benzene	7.80	0.4	0.48	32	8.8	80,000	229,000	1.3
fluorene	12.10	0.6	1.30	287	3.9	91,000	260,000	1.0

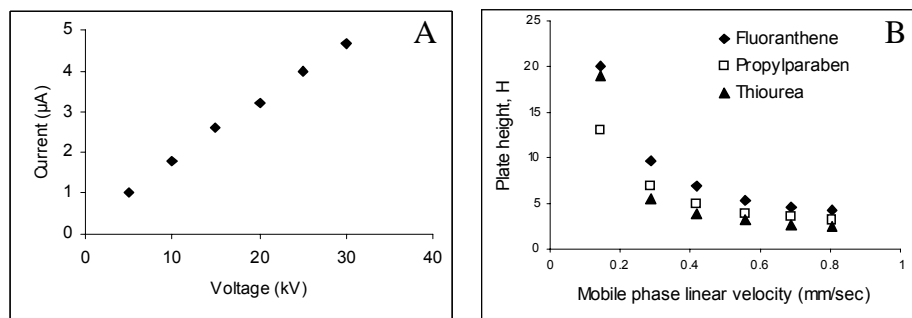


**Figure VI.6.A** Ohm's plot for the columns evaluated with 20mM TRIS.HCl buffer, pH 8.9, 70% CH<sub>3</sub>CN. **B.** Corresponding H-u plot for three increasingly retained compounds

In Figure VI.6.A the system current for a packed column is plotted versus the applied voltage. Because no deviation of linearity is observed, it can be concluded that Joule heating leading to peak broadening is not taking place. This is also clear from the H-u plot (Figure VI.6.B) showing that the minimum plate height is not yet reached at 30 kV. The obtained plate heights correspond to reduced plate heights ( $H/d_p$ ) varying from 0.8 for the unretained thiourea to 1.4 for the most retained compound (fluoranthene).

The columns were applied and compared to commercially available columns for several CEC applications described before, such as the analysis of triglycerides [46] and fatty acid derivatives [47]. Similar chromatographic patterns were obtained but an additional feature of the packing procedure presented is that no gas bubbles are formed, facilitating the coupling to MS.

### VI.3.3 Coupling to electrospray ionisation mass spectrometry

CEC-MS capillaries are typically 50 to 60 cm in length and were produced in the same way as described in the experimental part but without making a UV window. This simplified the procedure and gave the column greater mechanical strength. A commercially available sheath flow interface was used with a make-up flow of H<sub>2</sub>O/methanol (1/1) containing 0.1% formic acid to enhance the ionisation process [48]. Compared to CEC-UV, a reduction in efficiency with ca. 20% was observed. This is caused by two factors. First, an ESI interface originally designed for LC-MS inevitably leads to peak broadening. Secondly,

longer packed beds generally provide reduced efficiencies (expressed per meter) because of the difficulty of obtaining long and homogeneous packings. Ideally, shorter packed beds should be used but this must then be followed by a long empty part of capillary because of the long minimum capillary length required for CEC-MS (48 cm in this combination).

Two CEC-MS applications are presented, the analysis of some steroids and carbamates.

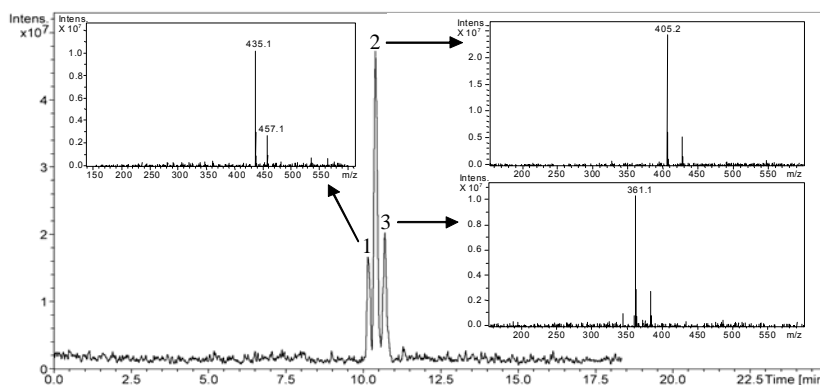


**Figure VI.7** CEC-MS base peak chromatogram of a mixture of 1: triamcinolone acetonide, 2: hydrocortisone acetate and 3: prednisolone

Figure VI.7 shows the CEC-MS base peak chromatogram of a mixture of triamcinolone acetonide (peak 1), hydrocortisone acetate (peak 2), and prednisolone (peak 3) on a capillary of 48 cm effective length, 50  $\mu\text{m}$  ID, and packed with 3  $\mu\text{m}$  ODS-1 (Spherisorb). The mobile phase was 0.1% TEA-HOAc, pH 8.9 –  $\text{CH}_3\text{CN}$  (1/9). A sample solution of 1000 mg/L in  $\text{CH}_3\text{CN}$  was injected electrokinetically (5 s at 10 kV), the voltage was 30 kV, the make-up flow was methanol/ $\text{H}_2\text{O}$  + 0.1%  $\text{HCOOH}$  at 3  $\mu\text{L}/\text{min}$ , and the MS scan range was 150–600 amu. The  $[\text{M}+\text{H}]^+$  ions are the most intense signals and the molecular ions are confirmed by the sodium adducts.

The base peak chromatogram of a carbamate mixture is shown in Figure VI.8.A. Conditions were similar to those in Figure VI.7 except that the capillary length was 60 cm, the mobile phase ratio was 25% 0.1% TEA-HOAc, pH 8.9 – 75%  $\text{CH}_3\text{CN}$  and injection 12 s at 10 kV of a sample solution of 100 mg/L in methanol.

The mass spectra of oxamyl and aldicarbsulfoxide are shown in the insert of Figure VI.8A. The sodium  $[M+Na]^+$  adducts are the most intense signals for carbamates. The overlapping peaks could be perfectly isolated by ion extraction ( $m/z$  210  $[M+H]^+/232$   $[M+Na]^+$  and  $m/z$  222  $[M+H]^+/244$   $[M+Na]^+$ ) as shown in Figure VI.8.B and Figure VI.8.C for propoxur and carbofuran, respectively.

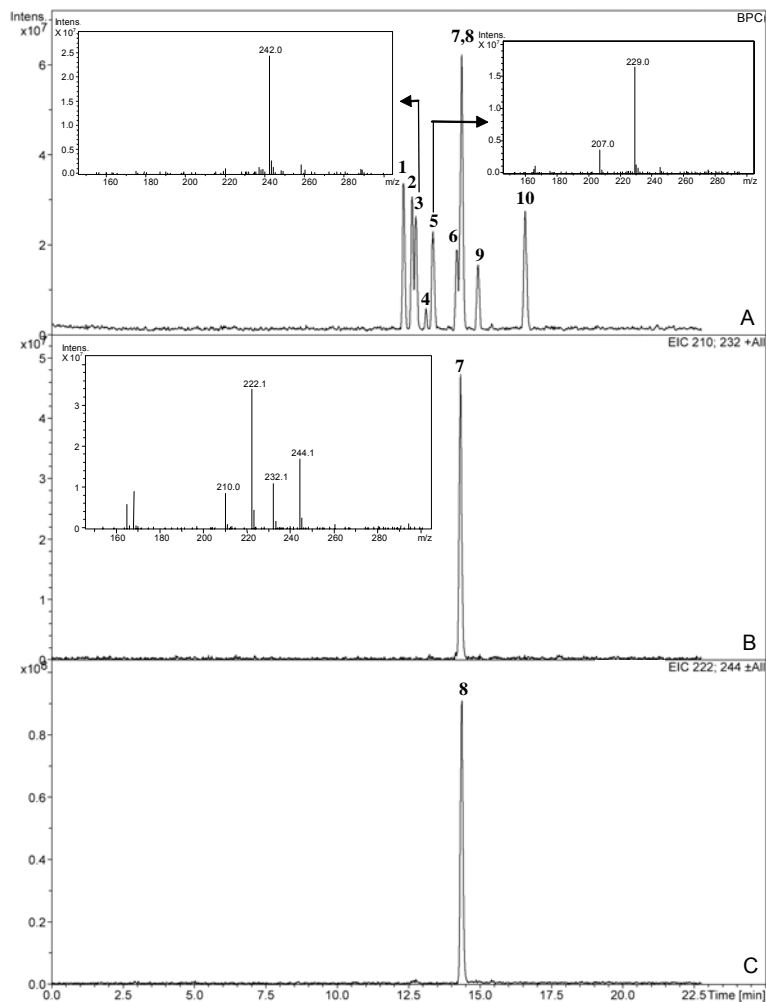


**Figure VI.8** Base peak chromatogram of an analysis of a mixture of 10 carbamates by CEC-MS. Signal identity (100 ppm each), 1: aldicarb sulfone, 2: 3-hydroxycarbofuran, 3: oxamyl, 4: methomyl, 5: aldicarbsulfoxide, 6: aldicarb, 7: propoxur, 8: carbofuran, 9: sevin (carbaryl), 10: methiocarb

### Conclusions

Air bubble formation in slurry packed CEC columns can be adequately suppressed by optimizing the column packing procedure. Of particular importance are a slow and controlled packing process and the frit manufacturing procedure. The latter must be short, sintered in water at high pressures and be made from the packed bed itself. Columns prepared in this way are highly efficient and coupling to ESI/MS does not pose any problem.

---

### References

1. DL Mould, RLM Syngé – *Analyst* (London) 77 (1952) 964–970
2. DL Mould, RLM Syngé – *Biochem J* 58 (1954) 571–585
3. V Pretorius, BJ Hopkins, JD Schieke – *J Chromatogr* 99 (1974) 23–30
4. JW Jorgenson, KD Lukacs – *J Chromatogr* 218 (1981) 209–216
5. T Tsuda – *Anal Chem* 59 (1987) 521–523
6. JH Knox, IH Grant – *Chromatographia* 24 (1987) 135–143
7. JH Knox, IH Grant – *Chromatographia* 32 (1991) 317–328
8. Q Tang, ML Lee – *TrAC* 19 (2000) 648–663
9. TD Maloney, LA Colon – *J Sep Sci* 25 (2002) 1215–1225
10. S Roulin, R Dmoch, R Carney, KD Bartle, P Meyers, MR Euerby, C Johnson – *J Chromatogr A* 887 (2000) 307–312
11. T Tsuda, I Tanaka, G Nakagawa – *Anal Chem* 56 (1984) 1249–1252
12. H Yamamoto, J Bauman, F Erni – *J Chromatogr A* 593 (1992) 313–319
13. NW Smith, MB Evans – *Chromatographia* 38 (1994) 649–657
14. H Rebscher, U Pyell – *Chromatographia* 38 (1994) 737–743
15. RT Kennedy, JW Jorgenson – *Anal Chem* 61 (1989) 1128–1135
16. SE Van den Bosch, S Heemstra, JC Kraak, H Poppe – *J Chromatogr A* 755 (1996) 165–177
17. H Rebscher, U Pyell – *J Chromatogr A* 737 (1996) 171–180
18. RJ Boughtflower, T Underwood, CJ Paterson – *Chromatographia* 40 (1995) 329–335
19. B Lumey, TM Khong, D Perret – *Chromatographia* 54 (2001) 625–628
20. TM Zimina, RM Smith, P Myers – *J Chromatogr A* 758 (1997) 191–197
21. S Ludke, T Adam, KK Unger – *J Chromatogr A* 786 (1997) 229–235

22. RM Seifar, S Heemstra, WT Kok, JC Kraak, H Poppe - *Biomed Chromatogr* 12 (1998) 140–140
23. C Yan, Electrokinetic Packing of Capillary Columns *US Patent* 1995, 5, 453, 163
24. CG Bailey, C Yan - *Anal Chem* 70 (1998) 3275–3279
25. R Dadoo, RN Zare, C Yan, DS Anex - *Anal Chem* 70 (1998) 4787
26. C Yan, R Dadoo, H Zhao, RN Zare - *Anal Chem* 67 (1995) 2026–2029
27. R Stol, H Poppe, WT Kok - *Anal Chem* 75 (2003) 5246–5263
28. J Saevels, M Wuyts, A Van Schepdael, E Roets, J Hoogmartens - *J Pharm Biomed Anal* 20 (1999) 513–520
29. RA Carney, MM Robson, KD Bartle, P Meyers - *J High Res Chromatogr* 22 (1999) 29–32
30. IM Lazar, LJ Li, Y Yang, BL Karger - *Electrophoresis* 24 (2003) 3655–3662
31. M Stahl, A Jakob, A Von Brocke, G Nicholson, R Bayer - *Electrophoresis* 23 (2002) 2949–2962
32. AR Ivanov, C Horvath, BL Karger - *Electrophoresis* 24 (2003) 3663–3673
33. C Desiderio, S Fanali - *J Chromatogr A* 895 (2000) 123–132
34. E Barcelo-Barrachina, E Moyano, MT Galceran - *Electrophoresis* 25 (2004) 1927–1948
35. CW Klampfl - *J Chromatogr A* 1044 (2004) 131–144
36. MM Dittmann, GP Rozing, G Ross, T Adam, KK Unger - *J Cap Elec* 5 (1997) 201–212
37. SA Haq, RE Beevers, MR Cottrell, IA Whitcombe - *Int Scientif Com* 2001, 20–24 ([www.iscpubs.com](http://www.iscpubs.com))
38. CF Poole, SK Poole - *Chromatography Today* Elsevier, Amsterdam 1991
39. KD Bartle, P Myers - *Capillary electrochromatography* Royal Society of Chemistry, Cambridge 2001
40. MM Robson, MG Cikalo, P Myers, MR Euerby, KD Bartle - *J Microcol Sep* 1997, 357–372
41. EM Hilder, CW Klampfl, M Makca, PR Haddad, P Myers - *Analyst* 125 (2000) 1–4
42. TD Maloney, LA Colon - *J Sep Sci* 25 (2002) 1215–1225
43. DB Strickmann, BC Chankvetadze, G Blaschke, C Desiderio, S Fanali - *J Chromatogr A* 887 (2000) 393–407

44. LA Colon, TD Maloney, AM Fermier – *J Chromatogr A* 887 (2000) 43–53
45. SS Lane, R Boughtflower, C Paterson, M Morris – *Rapid Comm in Mass Spectrom* 10 (1996) 733-736
46. P Sandra, A Dermaux, V Ferraz – *J Microcolumn Sep* 9 (1997) 409–419
47. A Dermaux, P Sandra, V Ferraz – *Electrophoresis* 20 (1999) 74–79
48. F Lynen, Y Zhao, C Becu, F Borremans, P Sandra – *Electrophoresis* 20 (1999) 2462–2474

## **Chapter VII**

### **O p e n T u b u l a r C E C**

Open tubular capillary electrochromatography (OT-CEC) offers several advantages over packed column CEC and monoliths. The column manufacturing is simpler compared to the latter, the wall thickness can be controlled such as to optimize the retention and the kinetics of interaction and the permeability is much higher. It is important that after wall modification the EOF is still present to sustain the flow in the column. This can be achieved by either coating thin layers still allowing the residual silanol groups to affect the EOF or by coating with a layer which is charged, creating a new EOF in this way. The various types of gels investigated in this thesis are described below together with their evaluation in open tubular CEC.

#### **VII.1 Sol-gel procedures**

All sol-gel reactions were performed with mixtures containing the precursor(s), solvent, catalyst and water. Equimolar amounts of water were used relative to the precursor(s) to ensure complete hydrolysis. The details of the optimized procedures are presented.

##### **VII.1.1 C8 gel**

The C8 gel was prepared by mixing tetraethoxysilane (TEOS, 500  $\mu\text{L}$ , 2.3 mmol), octyltriethoxysilane (C8-TEOS, 362  $\mu\text{L}$ , 1.15 mmol), ethanol (213  $\mu\text{L}$ , 20% v/v), water (92  $\mu\text{L}$ , 6.3 mmol) and 0.1 M HCl (22  $\mu\text{L}$ ). The molar ratio tetraethoxysilane/octyltriethoxysilane was 2/1. Ethanol was 20% (v/v) of the final mixture. The clear sol-gel solution was stirred at room temperature for 4 h in a closed vial. The reaction was completed by heating at 120°C for 15 h under

a gentle helium flow. The sol-gel material required for TGA and DSC analysis was left in a vial for this purpose. The capillaries were filled with the gel prior to the thermal treatment.

#### **VII.1.2 C18 gel**

The C18 gel was prepared by mixing tetraethoxysilane (250  $\mu\text{L}$ , 1.12 mmol) and octadecyltrimethoxysilane (263  $\mu\text{L}$ , 0.61 mmol) in ethanol (1.538 mL, 75% v/v) at 60°C in a closed vial. After 2 h acidulated water (12 mM HCl, 61  $\mu\text{L}$ , 3.4 mmol  $\text{H}_2\text{O}$ ) was added and the reaction was allowed to proceed for another 2 h at 60°C. Thermal treatment was performed in the same way as for the C8 gel.

#### **VII.1.3 Aminopropyl gel**

To obtain the amino gel, aminopropyltriethoxysilane (APTS, 250  $\mu\text{L}$ , 1.1 mmol) was mixed with ethanol (188  $\mu\text{L}$ , 40% v/v) for a couple of minutes before acidulated water (12 mM HCl, 154  $\mu\text{L}$ , 8.5 mmol  $\text{H}_2\text{O}$ ) were added. The reaction mixture was stirred at room temperature overnight in a closed vial. The product was a clear gel with low viscosity; the gel was thermally treated at 90°C overnight under gas flow.

#### **VII.1.4 Cyanopropyl gels**

Two types of cyano gel were produced. Cyano gels were obtained either by using 3-cyanopropyltriethoxysilane (3CPTS) as sole precursor or 3-cyanopropyltriethoxysilane/tetraethoxysilane as co-precursors for this type of gel. For the *pure cyano* gel, 3-cyanopropyltriethoxysilane (300  $\mu\text{L}$ , 1.25 mmol) were mixed with 75  $\mu\text{L}$  ethanol for a couple of minutes before 34  $\mu\text{L}$  acidulated water (12 mM HCl, 34  $\mu\text{L}$ , 1.88 mmol  $\text{H}_2\text{O}$ ) were added. The reaction mixture was stirred at room temperature for 4 h in a closed vial. The product was a clear gel with low viscosity; the gel was thermally treated at 80°C overnight under gas flow.

For the mixed cyano gel (3CPTS/TEOS 1/1), 3-cyanopropyltriethoxysilane (205  $\mu\text{L}$ , 0.7 mmol) was mixed first with tetraethoxysilane (149  $\mu\text{L}$ , 0.7 mmol) TEOS

and then 100  $\mu\text{L}$  ethanol were added; the clear solution was stirred for a couple of minutes before adding acidulated water (12 mM HCl, 62  $\mu\text{L}$ , 3.4 mmol). The reaction mixture was stirred at room temperature for 4 h in a close vial. The product was a clear gel with low viscosity; the gel was thermally treated at 80°C overnight under gas flow.

### VII.1.5 Cyclodextrin-bound gels

A 200 mg sample of  $\alpha$ -,  $\beta$ -, or  $\gamma$ -cyclodextrin (CD), dried *in vacuo* at 100°C for 24 h, was added with stirring in anhydrous dimethylformamide (DMF) to complete dissolution. After the mixture becomes clear, isocyanatopropyltriethoxysilane (ICPTS) is added in stoichiometric (1:1) quantity. The reaction mixture is stirred at 70°C for 48 h. The resulting light yellow solution is placed under vacuum at 70°C in order to remove the solvent and the non-reacted isocyanate. The cyclodextrin-derivative is then used for the sol-gel reaction. The reaction scheme is shown in Figure VII.1.

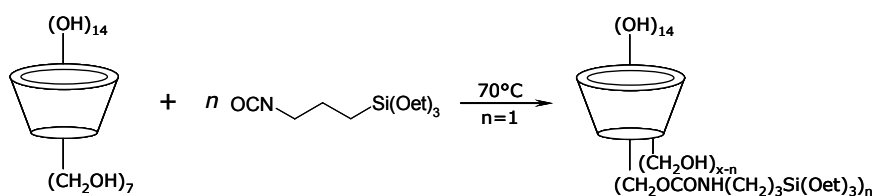


**Figure VII.1** Reaction scheme for the derivatization of cyclodextrins with isocyanatopropyltriethoxysilane

The cyclodextrin-derivatives were dissolved in anhydrous DMF and TEOS was added with stirring (derivative approximately 13% molar). Water was added in stoichiometric quantity to ensure the complete hydrolysis of all silanol groups. In contrast to the previous procedures, it was found that this time a basic pH favoured the formation of a clear gel (NaOH 0.3 M). The clear light yellow reaction mixture was stirred for 2.5 h at room temperature. The thermal treatment was carried out at 80°C under gas flow.

## VII.2 Evaluation of the gels

### VII.2.1 C8 gel

The apparent pH for C8 wet gel was found to be 5-5.5 as measured with a short-range colour-fixed indicator stick. The results from thermogravimetric analysis (TGA) and differential scanning coulometry (DSC) are shown in Figure VII.2. It can be seen that the C8 gel is slowly losing weight as a function of temperature (approximately 2% in the interval 50-250°C). At 250°C, an endothermic effect is visible from the DSC, suggesting accelerated decomposition.

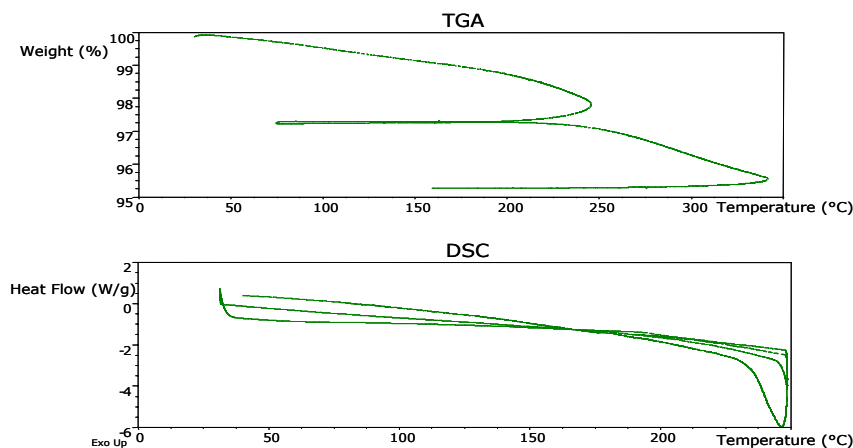


Figure VII.2 TGA and DSC of a C8 gel

### VII.2.2 C18 gel

Fast solidification was observed during the polymerization of octadecyltrimethoxysilane for gels using as precursor only C18-TMOS. It is mentioned in the literature [1] that no covalent chemical network is built, but the result is a thermoreversible physical network due to crystallization of long alkyl chains. Therefore, no real gel is formed if the only precursor used is C18-TMOS. Addition of TEOS was essential to the formation of a network by covalent bonding. Even in this case, if the same sol-gel procedure was followed, C18-TMOS/TEOS gel transformed quickly into a dense suspension of white, fine particles. Thermoreversible solidification was observed in the case of the C18/TEOS gels; the transition point was at about 30°C.

The apparent pH for C18 wet gel was found to be 5-5.5 as measured with a short-range colour-fixed indicator stick.

The C18 gel gave the same thermal response as in the case of the C8 gel, namely a 2% mass loss in the interval 50-250°C and a rapid decomposition starting at 250°C (Figure VII.3).

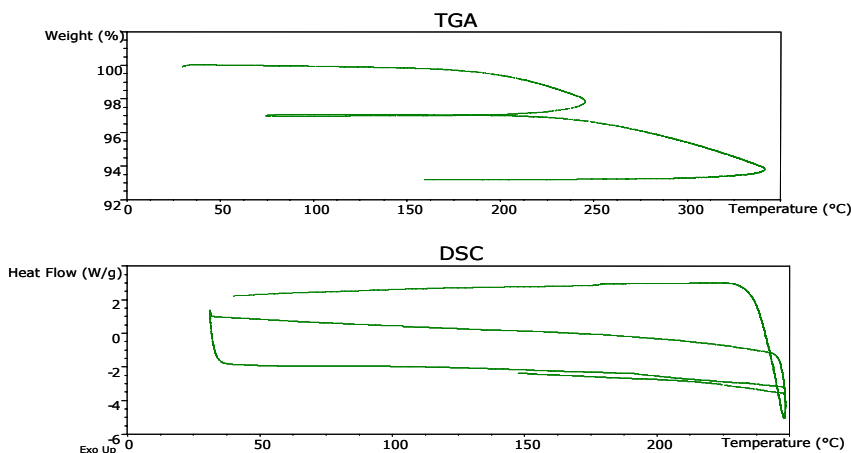


Figure VII.3 TGA and DSC for a C18 gel

### VII.2.3 Aminopropyl gel

Aminopropyltriethoxysilane was used as sole precursor for the amino gel. Combination in any ratio and even at higher temperature with a co-precursor, *i.e.* tetraethoxysilane, led to the production of a white, wax-like product, not suitable for capillary coating.

Thermal analyses revealed lower thermal stability compared to C8 and C18 gels (Figure VII.4), mass loss starting at about 45°C.

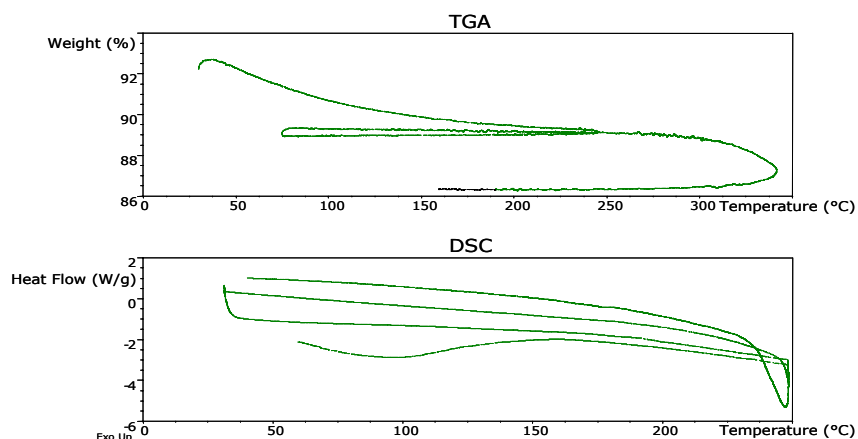


Figure VII.4 TGA and DSC for amino gel

### VII.2.4 Cyanopropyl gels

Both types of cyano gel are thermally stable up to temperatures around 100°C (Figure VII.5). The materials are suitable for coating the walls of the capillary columns.

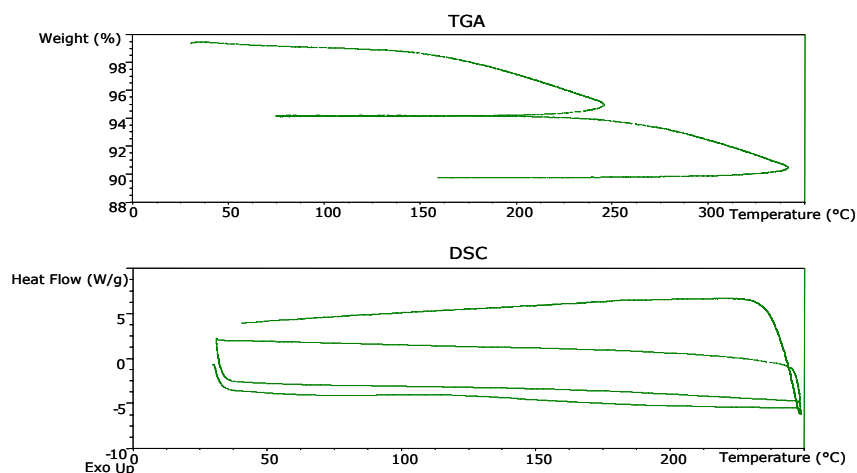


Figure VII.5 TGA and DSC for the cyanopropyl/tetraethoxysilane

### VII.2.5 Cyclodextrin gels

The cyclodextrin gels showed thermal stability up to about 180°C, at which temperature carbonization of the organic moiety starts. The mass loss exhibited at about 100°C can be due to the evaporation of water and DMF.

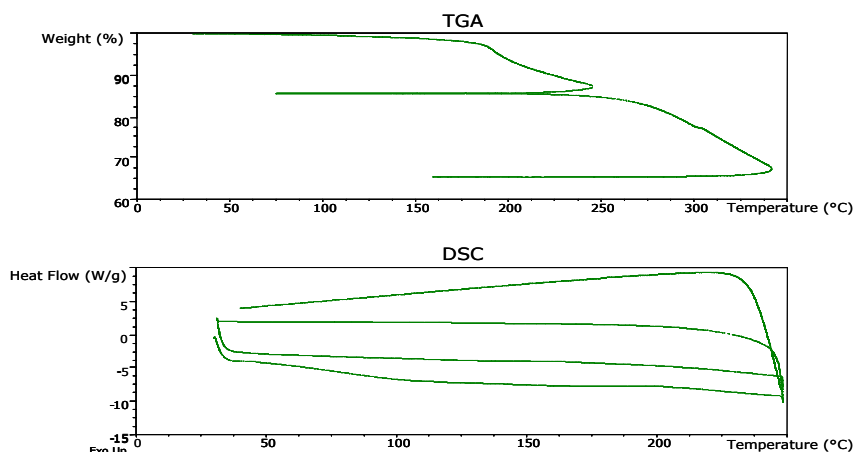


Figure VII.6 TGA and DSC for  $\beta$ CD gel

### VII.3 Column coating procedure

Fused silica capillaries (50  $\mu$ m ID) were flushed with 1 M NaOH, water and methanol for 1 h each, then dried at 180°C for 2 h while purging with He. Before coating, the detection window was burned at the desired distance from the outlet end of the capillary. The capillary was installed in a CE cassette; the coating took place inside the CEC system. Pressure was applied (4 bar for 5 min, inlet to outlet) and the filled capillary was allowed to rest for 10 min for C8 and C18 gels and 30 min for the other gels. The gel was then forced out of the capillary by pressure (4 bar for 5 min). As the gels had a low viscosity, coating took place at 25°C, except in the case of the C18 gel, where 40°C was necessary to maintain low viscosity.

The coated capillary was then installed in a GC system, where thermal treatment took place overnight while purging with He. Thermal treatment was performed at 120°C for the C8 and C18 coated capillaries, at 90°C for the cyanopropyl and at 80°C for the cyclodextrin based columns, respectively. Before the first run, the columns were rinsed with methanol, water and mobile phase and a step-wise voltage gradient was applied in order to ensure current stabilization.

The capillary coating was investigated by scanning electron microscopy (SEM). It can be seen that coating with an inhomogeneous gel (Figure VII.7A) produced growths that ultimately led to column blockage. On the other hand, when a

homogeneous gel was used, the surface was smooth (Figure VII.7B). In the case of the C8 coating (Figure VII.7C), the rugged surface is probably due to the higher growing rate of the 3D network, but column blockage only seldom occurred.

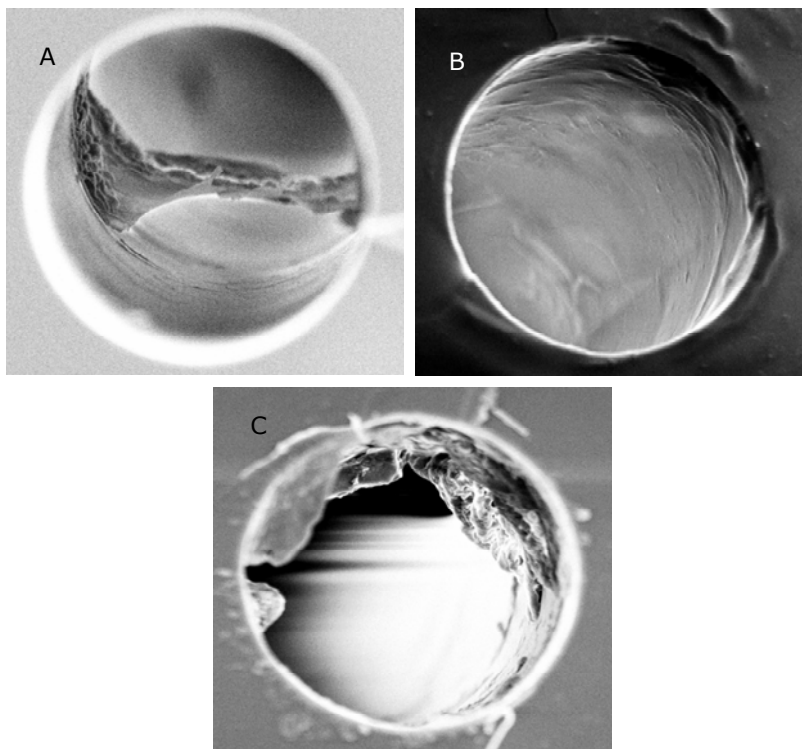


**Figure VII.7** SEM images of 50 μm capillaries coated with an inhomogeneous C18 gel (A), with a homogeneous C18 gel (B) and with C8 gel (C)

The CEC instrument was used for the coating, in order to obtain an improved reproducibility by controlling the temperature and the pressure under which the gel was introduced into the capillary.

Applying 4 bar pressure at the inlet for 5 min at 25°C was sufficient for the coating of the capillary. The gel was expelled from the capillary under the same conditions.

Thermoreversible solidification was observed in the case of the C18 gels; the transition point was at about 30°C; therefore maintaining the capillary at 40°C prevented the solidification before and during the coating procedure.

The time the gel stays inside the column ("*in-situ*") affects the thickness of the layer that will become the stationary phase. This time was varied between 5 min and 1 h. 10 min was found to be optimal for the C8 and C18 gels. The coating time for the other gels was 30 min.

The detection window was burned before coating the capillary. Burning the window after the coating procedure leads to the blackening of the coating due to pyrolysis of the organic moieties resulting in changed column selectivity and a loss of detection sensitivity by light scattering.

## **VII.4 Evaluation of the columns**

### **VII.4.1 Experimental**

#### **VII.4.1.1 Method**

C8 and C18 columns were flushed with ethanol, water and mobile phase before the first run. Cyano and amino columns were flushed with acetone, water and mobile phase before the first run. A change in pH was preceded by a flush of at least 1 h with the new mobile phase. C18 columns needed longer flushing times in order to achieve a stable EOF. Before the first run, voltage conditioning was done by increasing the voltage stepwise from 0 to 25 kV over 60 min. On column UV-Vis detection was performed at 254 nm. Mobile phases were degassed before runs in an ultrasonic bath. Runs were performed at 20°C unless stated otherwise. Capillary dimensions were 40 cm (31.5 cm  $L_{\text{eff}}$ ) x 50µm ID, unless stated otherwise.

#### **VII.4.1.2 Test mixtures**

Three test mixtures were used for the evaluation of the open tubular columns. The polycyclic aromatic hydrocarbons mixture (PAHs) contained thiourea, naphthalene, anthracene, fluorene and fluoranthene, with a concentration of about 200 ppm each in acetonitrile. The phenone mixture contained thiourea, aceto-, propio-, butyro-, hexano-, heptano- and octano-phenone, approximately 200 ppm each in acetonitrile. The paraben mixture contained thiourea, methyl-,

ethyl-, propyl- and butylparaben at 200 ppm each in acetonitrile/water 50/50. All products were purchased from Sigma-Aldrich (Bornem, Belgium).

#### **VII.4.2 Results and discussion**

A fundamental evaluation of the column performance was done with the C8 and C18 columns. The conditions derived from this thesis were extrapolated for the amino, cyano and cyclodextrin columns.

##### **VII.4.2.1 Efficiency and retention**

High efficiencies were observed on the C8 and C18 columns, with values exceeding 500,000 plates/m for the least retained compounds. However, a rapid decrease in efficiency is observed with increasing retention of the compounds. The effect has been described before and it is due to the low phase ratio of open tubular columns [2]. The effect is more pronounced for columns with an ID larger than 10  $\mu\text{m}$ . Capillaries with an ID of 50  $\mu\text{m}$  were selected in this thesis because the columns with smaller internal diameters showed irreproducible characteristics. Additionally, detection problems occurred when using these capillaries.

The C18 columns displayed higher efficiencies compared to the C8 columns for all analyzed test mixtures (Figure VII.8-10). The presence of longer chains, combined with the possible more efficient sol-gel process, thicker wall coating and therefore higher phase ratio could explain this fact.

Another drawback of the deleterious phase ratio is the relatively small difference in elution time between the unretained and the most retained compounds (*i.e.* thiourea and fluoranthene for the PAHs, thiourea and octylphenone for the phenones, respectively).

The small "elution window" will complicate the practical use of the columns. Thicker phases (with a higher phase ratio) will therefore be required for these applications.

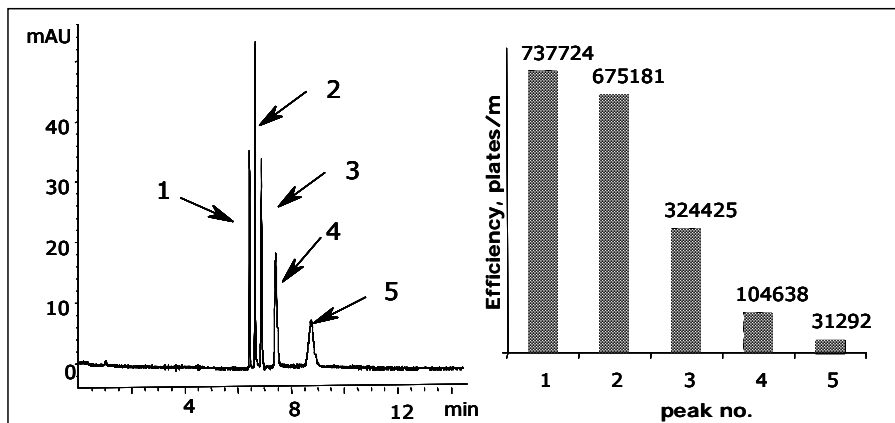


**Figure VII.8** Parabens separation on a C8 column. Mobile phase: 50 mM MES pH 6/CH<sub>3</sub>CN 75/25. Injection: 30 mbar 3 s. Voltage: 25 kV. Peaks: 1. thiourea, 2. methyl-; 3. ethyl-; 4. propyl-; 5. butyl-paraben. The graph indicates the efficiencies for the corresponding peaks

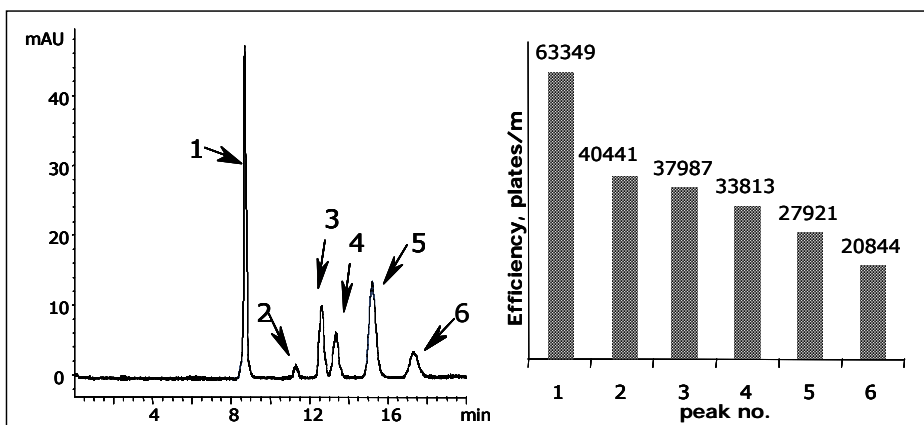


**Figure VII.9A** PAHs separation on a C8 column. Mobile phase: 50 mM MES pH 6/CH<sub>3</sub>CN 55/45. Injection: 50 mbar 3 s. Voltage: 25 kV. Peaks: 1. thiourea, 2. naphthalene; 3. bi-phenyl; 4. fluorene; 5. anthracene; 6. fluoranthene. The graph indicates the efficiencies for the corresponding peaks

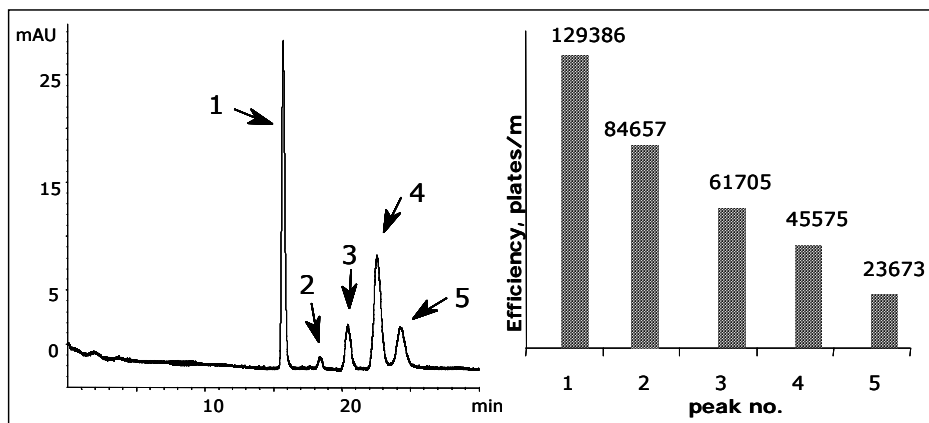


**Figure VII.9B** PAHs separation on a C18 column. Mobile phase: 50 mM MES pH 6/CH<sub>3</sub>CN 40/60. Injection: 3 kV 3 s. Voltage: 25 kV. Peaks: 1. thiourea, 2. naphthalene; 3. fluorene; 4. anthracene; 5. fluoranthene. The graph indicates the efficiencies for the corresponding peaks

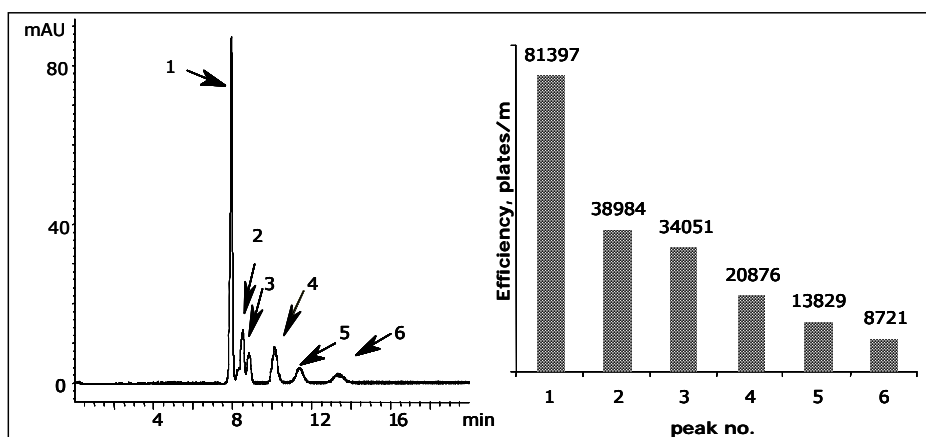


**Figure VII.10A** Phenones separation on a C8 column. Mobile phase: 50 mM MES pH 6/CH<sub>3</sub>CN 50/50. Injection: 40 mbar 2 s. Voltage: 25 kV. Peaks: 1. thiourea, 2. C3-phenone; 3. C4-phenone; 4. C6-phenone; 5. C7-phenone; 6. C8-phenone. The graph indicates the efficiencies for the corresponding peaks

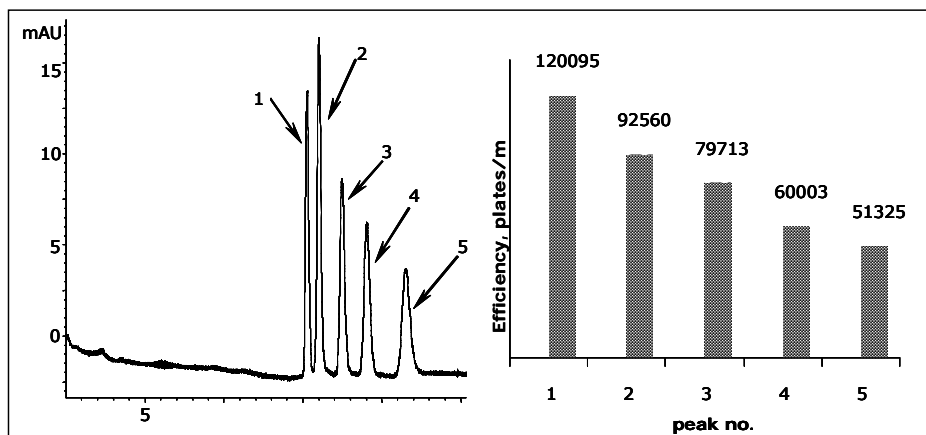


**Figure VII.10B** Phenones separation on a C18 column. Mobile phase: 50 mM MES pH 6/CH<sub>3</sub>CN 40/60. Injection: 3 kV 3 s. Voltage: 25 kV. Peaks: 1. C3-phenone; 2. C4-phenone; 3. C6-phenone; 4. C7-phenone; 5. C8-phenone. The graph indicates the efficiencies for the corresponding peaks

#### VII.4.2.2 Influence of organic modifier

Organic solvents are used in the electrodriven separations due to their capacity of extending the applications to more hydrophobic species. This type of non-aqueous solvents reduce significantly the Joule heating effect, which translates in the possibility of using higher separation voltages and, therefore, decreasing analysis time. Even though it has been established that organic solvents can produce EOF even without electrolyte [3], the practice makes use of mobile phases up to 80% organic modifier. The literature reports the use of acetonitrile, methanol and tetrahydrofuran as modifiers of choice.

In this thesis, acetonitrile was used for the evaluation of the open tubular CEC columns due to its higher eluotropic force (same as for RP-LC) and because it generates a higher EOF than methanol.

The EOF velocity has been calculated from the elution time of thiourea, which is assumed to be unretained at all compositions tested. The influence of the *percentage of organic modifier* on the EOF velocity and current is illustrated in Figure VII.11 for C8 and C18 columns.

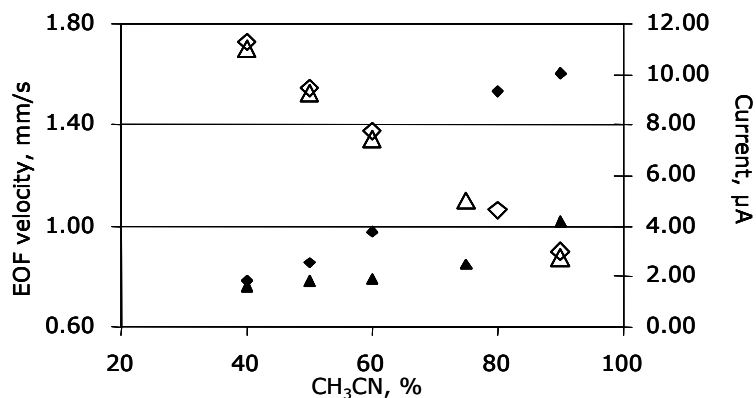


**Figure VII.11** Effect of acetonitrile percentage variation on the current (◇C8 column, △C18 column) and on the EOF velocity (◆C8 column, ▲C18 column). Average of 3 determinations

The EOF shows a steady increase with the increase in acetonitrile percentage. Even if the increase in EOF is non-linear for the acetonitrile 40-90% interval, the current showed a linear dependence for the same interval, with an  $R^2$  of 0.9986 and 0.9993 for the C8 and C18 column, respectively. A higher content in organic modifier translates into lower current, thus reducing self-heating during a run.

In reverse phase LC a linear relationship exists between capacity factor ( $\ln k$ ) and the percentage of organic modifier in the mobile phase. The same behaviour can be observed in the open tubular CEC columns evaluated in this thesis as is demonstrated in Figure VII.12 for a series of parabens.

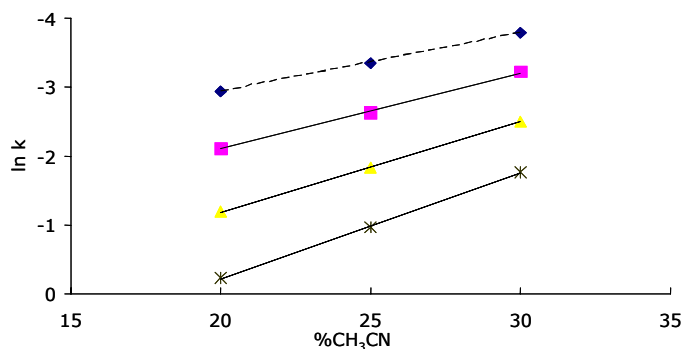


**Figure VII.12**  $\ln k$  vs percentage of acetonitrile for parabens (◆ methyl-, ■ ethyl-, ▲ propyl-, ✱ butyl-paraben) on a C8 column. Average of 3 determinations

### VII.4.2.3 Influence of buffer composition on the EOF, current and retention

Electrodriven capillary experiments are usually performed at a *pH* of 7 or higher to ensure a substantial EOF, which is generally reducing the analysis time. As described above, in CEC the amount of organic modifier in the mobile phase is also influencing the EOF.

In Figure VII.13 the magnitude of the EOF is plotted against the *pH* of the running buffer for a fixed acetonitrile percentage. It can be seen that the EOF (as measured by the migration time of thiourea) is increasing with *pH* and that the EOF is larger for the C8 column. This can be related to the higher shielding effect that the bulkier C18 groups have on the free silanol groups compared to the C8 groups. However, an increased retention was previously also shown in Figures VII.8 and VII.9 for the C18 columns compared to the C8 ones. This observation can then be explained by the combined effect of a higher total carbon load and higher effective shielding of silanol groups on the C18 columns.

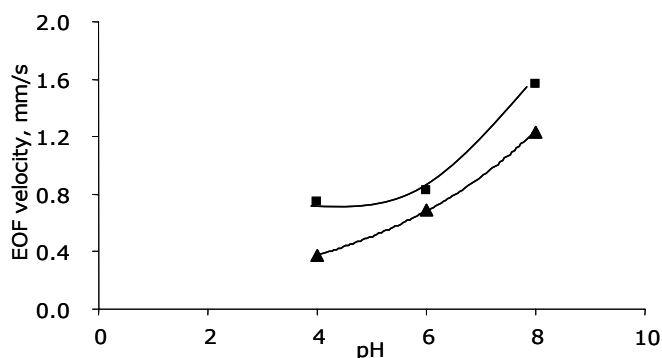


**Figure VII.13** Influence of *pH* on the EOF velocity for ■ C8 and ▲C18 stationary phase. Mobile phase: 20 mM phosphate/ CH<sub>3</sub>CN 50/50. Voltage: 25 kV. Average of 3 determinations

PAHs, parabens and phenones are neutral in the working *pH* range (4-8), therefore an increase in *pH* should not affect the selectivity, but only speed up the analysis. For the PAH mixture on a C8 column, for example, when the *pH* increases from 4 to 8 (for the same organic modifier content, *i.e.* 45% acetonitrile), analysis time decreased 2.8 times, but the selectivity for the pairs

naphthalene – bi-phenyl and fluorene – anthracene remained basically the same (1.59 – 1.65 and 1.54 – 1.56, respectively).

The aminopropyl columns showed a similar behaviour to that described by Colon et al. [4] with regard to the dependence of the magnitude and direction of the EOF on the pH. In these columns there are two functional groups present (-OH and -NH<sub>2</sub>) carrying opposite charges in the used pH range. The EOF direction can therefore reverse depending on the pH. At low pH, the direction of the EOF is from cathode to anode due to a positive total wall charge. At high pH, due to a negative total wall charge, the EOF direction is like in uncoated capillaries. There is a certain narrow pH interval where the EOF velocity is practically zero. In the case of tested capillaries, the value was found to be at pH 4.6 (Figure VII.14).

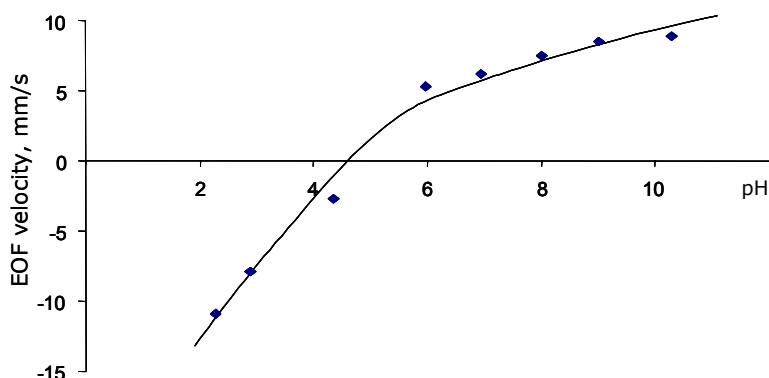


**Figure VII.14** EOF velocity vs pH for aminopropyl columns. Buffer: 20 mM phosphate. Voltage:  $\pm 25$  kV. Average of 3 determinations

The pH value for this "switch" in direction for the EOF depends on the sign *and* number of the net charges on the capillary surface. Hence, manufacturing conditions play an important role.

*Ionic strength* is another important variable affecting electrodriven separations. The EOF velocity decreases with an increase in buffer concentration, which is related to a reduction in the double layer thickness and therefore in the double layer potential,  $\zeta$ .

Low ionic strengths lead to a thicker double layer, by which the transport at interface level is diminished, and a loss in efficiency is noticed (Figure VII.15). On the other hand, high buffer concentrations may result in excessive current

generation and in the case of mobile phases with organic modifiers, even salt precipitation might result.

Interesting to notice is the slight increase in number of plates/m for the early eluting peaks in the case where buffer concentration is 0 mM. A suitable explanation is not available at the moment.

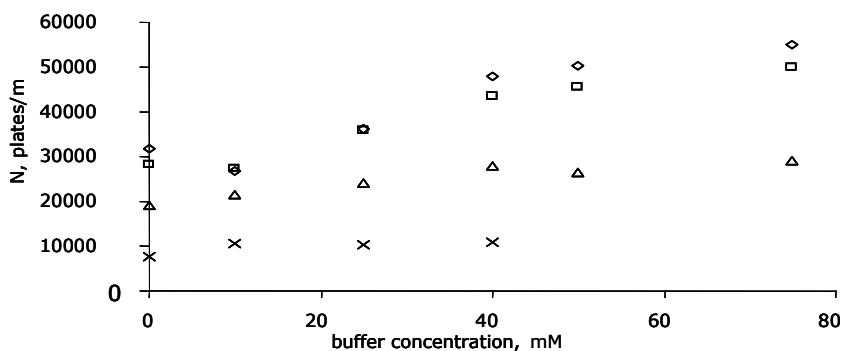


**Figure VII.15** Efficiency versus buffer concentration for the methyl- (◇), ethyl- (△), propyl- (□) and butyl- (×) paraben on a C8 column. Average of 3 determinations. Mobile phase: MES pH 6/ CH<sub>3</sub>CN 45/55. Voltage: 25kV

The effect of buffer concentration on efficiency is less expressed for the late eluting peaks.

#### VII.4.2.4 Influence of the applied electric field

As a rule of thumb, electrodriven separation techniques should be run at the highest possible voltage where the Joule heating effect is not yet taking place. The Joule heating can be visualized in a plot representing the measured current vs the applied voltage. The voltage at which deviation from linearity occurs is where Joule heating starts.

Another way to determine if Joule heating is taking place is by plotting the magnitude of the EOF vs the applied voltage [5]. A linear behaviour demonstrates the absence of Joule heating. This approach has been used in this study (Figure VII.16).

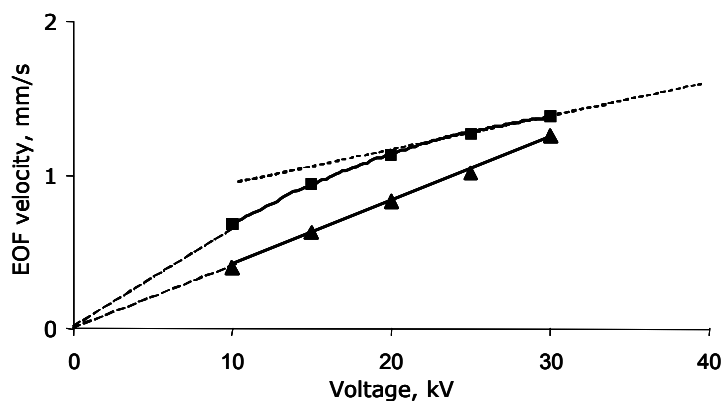


**Figure VII.16** EOF velocity vs applied voltage for C8 (■) and C18 (▲) columns. Mobile phase: 50 mM MES/ CH<sub>3</sub>CN 50/50. Average of 3 determinations

The C18 columns show a larger linear behaviour compared to the C8 columns studied here, indicating some degree of Joule heating for the latter. This can be related to the fact that the C8 columns show a higher generated current due to the higher number of non-shielded silanol groups present at the capillary wall compared to C18 columns.

#### VII.4.2.5 Influence of the temperature

Temperature has several effects in CEC, such as a reduction in mobile phase viscosity resulting in an EOF increase, an increase in the analyte solubility in the mobile phase and a facilitation of mass transfer of the solute. The higher the temperature, the faster the separation; whereby the deleterious effect of Joule heating has to be taken in consideration. Figure VII.17 illustrates the  $h-u$  plots, at different temperatures, for thiourea and anthracene on a C8 column. For the retained compound (anthracene) it can be seen that the analyses were performed in the  $C$ -term region of the  $h-u$  curve. This suggests a slower diffusion in and out of the stationary phase at a lower temperature. These results differ from the ones obtained for the packed columns (described in Chapter VI) where a minimum of the  $h-u$  curve could not be reached. For the unretained thiourea, the  $h-u$  profile is virtually flat as it does not interact with the stationary phase; therefore not much loss in efficiency is noticed for the temperature and voltage range used in these experiments (15-30°C and 5-25 kV respectively).

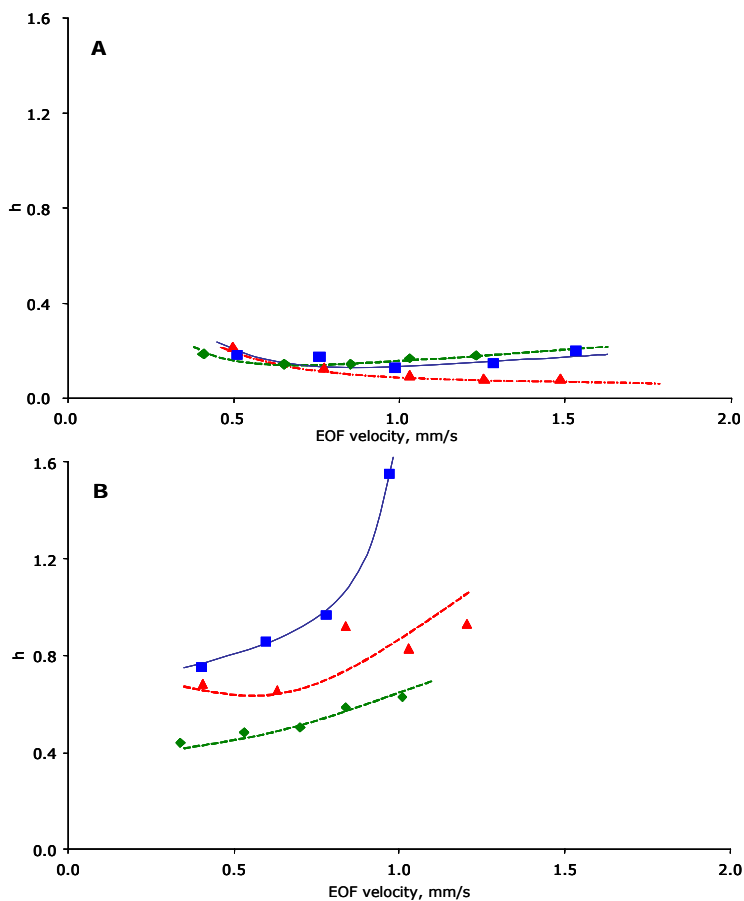


**Figure VII.17**  $h$ - $u$  plot for thiourea (A) and anthracene (B) at 15°C (■), 20°C (◆) and 25°C (▲). Average of 3 determinations. Mobile phase: 50mM TRIS pH 8/ CH<sub>3</sub>CN 50/50

#### VII.4.2.6 Evaluation of the repeatability

Tests to evaluate the run-to-run (on one column,  $n=6$ , PAHs test mix) and column-to-column ( $n=5$ ) repeatability in terms of migration time were performed on C8 columns. The former was satisfactory, with variation (expressed in %RSD) not exceeding 1.23%. The column-to-column reproducibility did not exceed 8.62%, which is comparable to the results previously reported in the literature (Table VII.1) [6-9].

**Table VII.1** Repeatability for one column run-to-run (A) and column-to-column reproducibility (B).

(C)MP: 50/50 50 mM TRIS pH 8/CH<sub>3</sub>CN; injection: electrokinetic, 5 kV 3 s; voltage 25 kV. Average of 6 determinations, RT in min.

(D) MP: 55/45 50 mM TRIS pH 8/CH<sub>3</sub>CN; injection: electrokinetic, 5 kV 3 s; voltage 25 kV. Average of 5 determinations, RT in min.

Compound	A		B	
	RT	%RSD	RT	%RSD
thiourea	3.653	1.23	4.248	5.46
naphthalene	4.791	1.21	5.628	6.84
flourene	5.785	0.78	6.798	7.20
anthracene	6.665	0.50	7.861	7.74
fluoranthene	7.535	0.41	8.945	8.62

### VII.5 Application: Open Tubular Capillary Electrochromatography of Carbohydrates

Formatted: English (U.K.)

Formatted: English (U.K.)

The interest in carbohydrates ranges from structural elucidation of simple carbohydrates to fundamental biochemical processes such as photosynthesis or glycolysis. For a complete structural elucidation, highly selective and efficient separations have to be coupled with a structural analysis method that can provide the information. Spectroscopic methods such as NMR and MS are used for this purpose. There are reports on carbohydrate separations in packed CEC and monolithic CEC columns [10, 11]. While in packed CEC the separations generally take place on C18 stationary phases, in the case of monolithic columns, cyano or amino groups appear to offer a different selectivity for the separation [12, 13].

For UV spectrometric or laser induced fluorescence (LIF) detection, the most frequently used method is pre-column derivatization of the carbohydrates through reductive amination (Figure VII.18). The carbonyl group can react with the amino group of a label forming a Schiff base. In a second step, the Schiff base is reduced with sodium cyanoborohydride to form a stable secondary amine. To shift the initial equilibrium towards the product and to prevent a further reaction of the final secondary amine with the carbonyl compounds, an at least five fold excess of amine is used [14].

In this thesis 9-aminopyrene-1,4,6-trisulfonic acid (APTS) was used to derivatize the sugars originating from glycoproteins (Figure VII.19). The effectiveness of

the various open tubular columns was evaluated under CEC conditions for these carbohydrates.

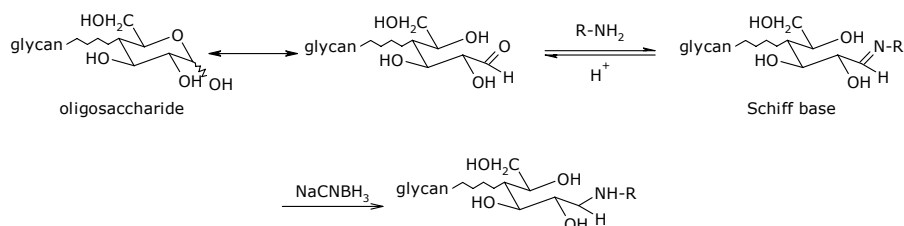


**Figure VII.18** Reductive amination reaction

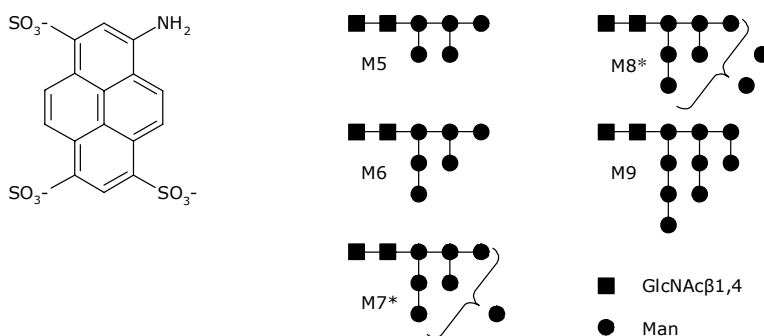


**Figure VII.19** Derivatization reagent (fluorescent label) 9-aminopyrene-1,4,6-trisulfonic acid (APTS) and oligosaccharides used for the test mixture (M=mannose, Mx\*= x mannose units in a molecule, \* indicates the presence of isomers)

APTS-labeled compounds are detected by fluorescence ( $\lambda_{\text{ex}}$  488 nm,  $\lambda_{\text{em}}$  512 nm), but they also provide a good signal for UV detection (200 nm and 350 nm). The sulfonate groups on the structure also induce negative charges on the molecules, increasing their electrophoretic mobilities.

## VII.5.1 Experimental

### VII.5.1.1 Columns

C8 and C18 capillaries were flushed with acetonitrile, water and mobile phase before the first run. Cyano and amino columns were flushed with acetone, water and mobile phase before the first run. Any change in pH was preceded by a flush of at least 1 h with the new mobile phase.

### VII.5.1.2 Sample preparation

Glycans were released from the glycoproteins (1 mg) by enzymatic deglycosylation with peptide-N-glycosidase F as described previously [15]. The liberated N-glycans were purified from the reaction medium by SPE on a Carbohydrate column [16]. The glycans were eluted with 2 mL of 25% CH<sub>3</sub>CN containing 0.05% TFA. After lyophilisation, the residue was redissolved in 100 µL Milli-Q water.

Maltopentaose, -hexaose and -heptaose (3 nmol each), dextrin15 (15 µg) and the N-glycans (20 µL of the stock solution) were derivatized by reductive amination [17]. After drying, 2 µL of 100 mM APTS in 0.9 M citric acid and 1 µL of 1 M NaCNBH<sub>3</sub> in THF were added. After incubation at 55°C for 2 h, 10 µL of Milli-Q water and 80 µL ice-cold acetone were added and the mixture was kept at -20°C for 10 min. The reaction tube was centrifuged at 12,500 rpm for 15 min. The supernatant was removed and the precipitated sugars were redissolved in 25 and 100 µL of Milli-Q water for the N-glycans and the maltooligomers, respectively [18].

### VII.5.1.3 Analytical conditions

CEC-LIFD analyses were performed on a Beckman P/ACE 2100 capillary electrophoresis system equipped with a laser-induced fluorescence detector (3 mW, 488 nm Ar ion laser).

Samples were introduced by hydrodynamic injection at 35 mbar during 5 s. Temperature was maintained at 20°C. Other experimental conditions were as described in the results and discussion section.

### VII.5.2 Results and discussion

A mixture containing linear glucose chains of 5, 6 and 7 glucose units derivatized with APTS (G5-7) was used for the initial testing and for the optimization of the method. The optimized separation conditions were then used for the separation of the derivatized RNaseB sample. Separation of APTS-derivatized sugars by using CEC showed a different profile than the same separation performed by CZE

[15]. The most important differences that could be noticed were a higher selectivity on the C8 stationary phase and that the separation was best performed with reversed EOF. On the cyano columns the test mixture could be separated with both direct and reversed voltage.

For all evaluated columns, a group of extra peaks appears at the beginning of the separation when using a reversed voltage for the analysis. This is due to smaller molecules that reacted with APTS, which migrate faster than the compounds of interest. In the case of direct voltage, this group will not reach the detection window; therefore they do not appear in the chromatograms.

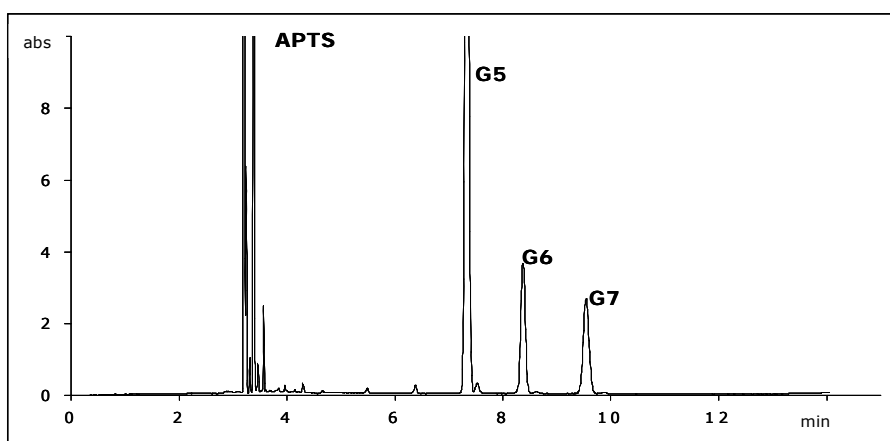


**Figure VII.20** Separation of G5-G7-APTS derivatives on C8 column. Mobile phase: 25 mM NH<sub>4</sub>OAc/CH<sub>3</sub>CN 80/20. Voltage: -25 kV

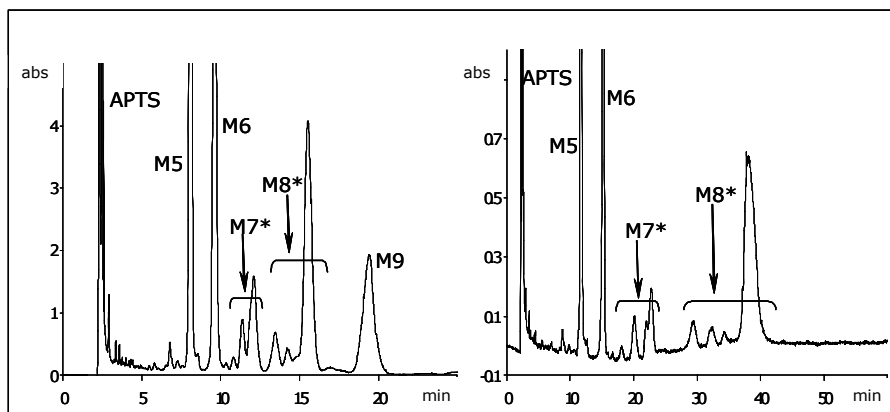


**Figure VII.21** Separation of APTS-derivatized RNaseB sugars on a C8 column. Buffer: 25 mM  $\text{NH}_4\text{OAc}/\text{CH}_3\text{CN}$  A. 70/30, B. 80/20. Voltage: -25 kV

Upon the analysis of the RNaseB sugars (Figure VII.21), it can be seen that longer analysis times are requested to elute the compounds. In the case of lower organic content, M9 elutes too late and it is not included in the chromatogram. C8 columns showed more selectivity for these compounds when compared to CZE experiments in bare silica tubes [15]. Even though it is considered that the interaction of solute-stationary phase lies mainly with the hydrophobic part of the analyte (in this case, the label), the fact that some of the isomers of M7 and M8 show some degree of separation in the case of the C8 stationary phase, but not in bare silica, proves that the separation mechanism is more complex than that. A loss in efficiency can be observed from the early eluting peaks to the late eluting ones (Fig VII.22). This phenomenon has been noticed before, during column evaluation experiments.

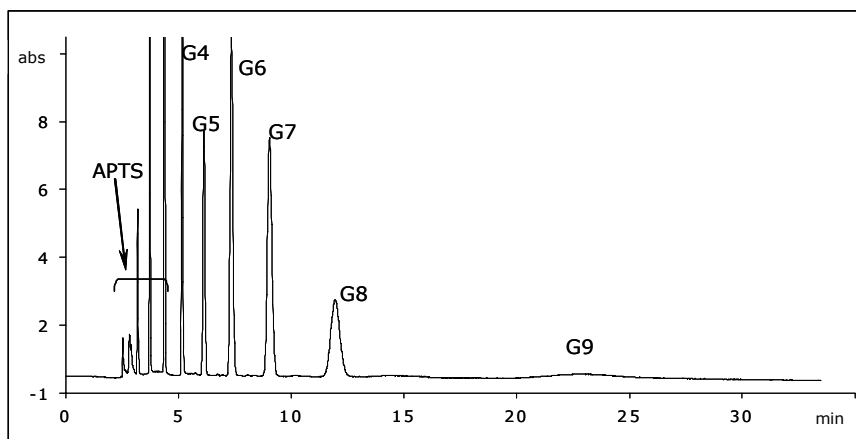


**Figure VII.22** Maltooligosaccharide ladder. APTS-derivatives separated on aminopropyl column. Buffer: 25 mM  $\text{NH}_4\text{OAc}$ . Voltage: -25 kV

In practice, sugars are separated in LC using amino columns. Even in the case of open tubular CEC this stationary phase proved suitable. However, a problem was the reproducibility of the separations. The stability of the aminopolysiloxanes in water has been previously studied [18]. It has been stated that the practical application of aminopropyl-modified silica gels is rather limited by their relatively high solubility in water. The removal of the aminopropyl from the matrix is due to the hydrolysis of the siloxane bonds. Additionally, it appeared that the organic modifier used in this study (*i.e.* acetonitrile) speeded up the stationary phase deterioration. However, compared to the separations obtained on C8 columns, the efficiency is higher on the amino columns resulting in an improved separation of some of the isomers (Figure VII.23).

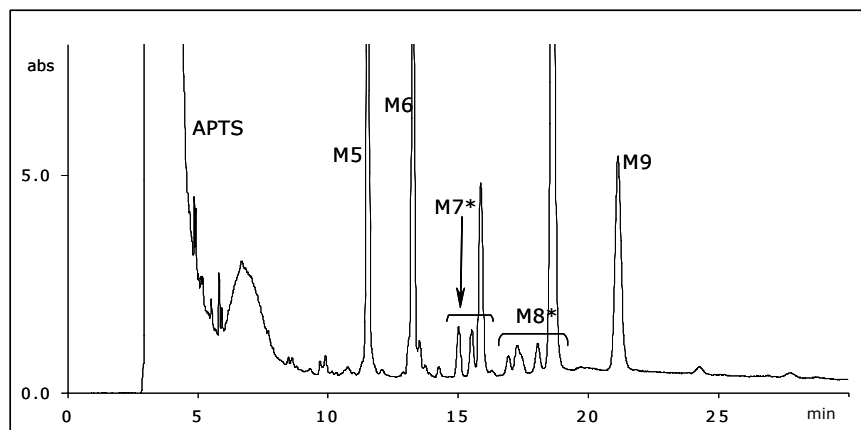


**Figure VII.23** Separation of APTS-derivatized RNaseB sugars on aminopropyl column. Buffer: 25 mM NH<sub>4</sub>OAc. Voltage: -25 kV

The column stability of cyano columns was noticeably better than in the case of amino columns. Working at different values of the pH (3, 6.5 and 8.5) with cyano columns led to different separation profiles for the G5-G7 test mixture. Both direct and reverse voltage could be used and as already noticed for C8, the reverse voltage mode gave better efficiencies. Therefore, reverse voltage was preferred for the separation of the RNaseB sugars (Figure VII.24).

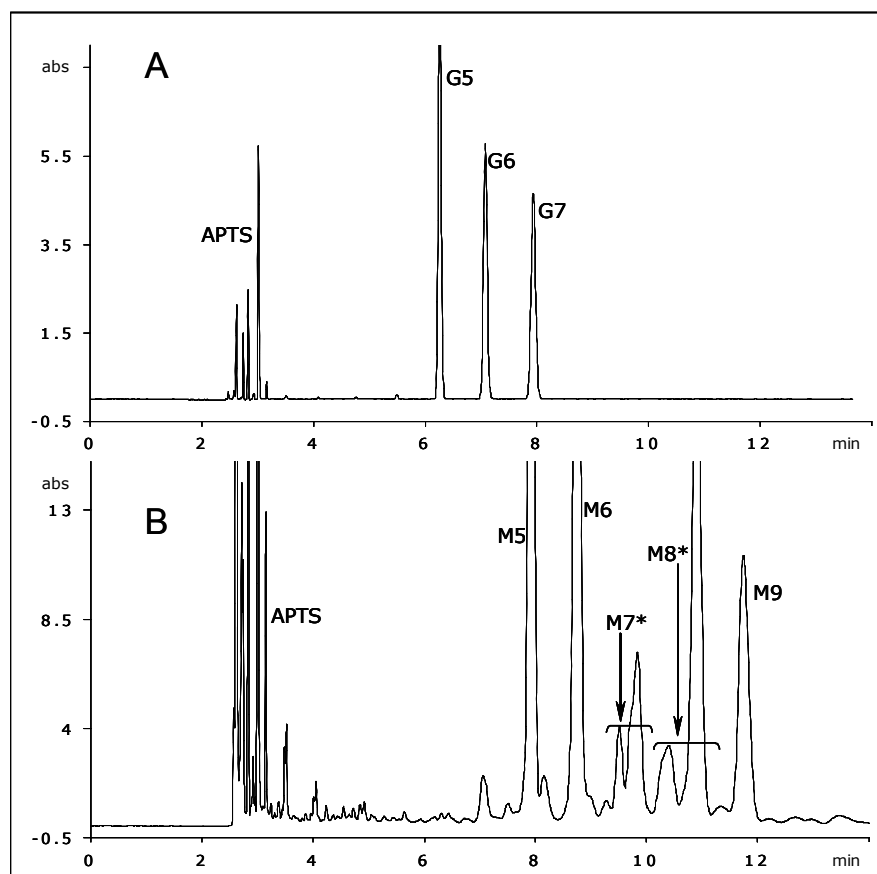


**Figure VII.24** Separation of A. APTS-derivatized G5-G7 test mix and B. APTS-derivatized RNaseB sugars on cyanopropyl column. Buffer: 25 mM  $\text{NH}_4\text{OAc}$ . Voltage: -25 kV

While studying the influence of the organic modifier content on the carbohydrate separations, it was noticed that the retention times increased with the increase in the percentage of acetonitrile on the cyano phase (Figure VII.25). This can be due to a normal phase-like behaviour, but as well to a variation in EOF velocity for this type of columns.

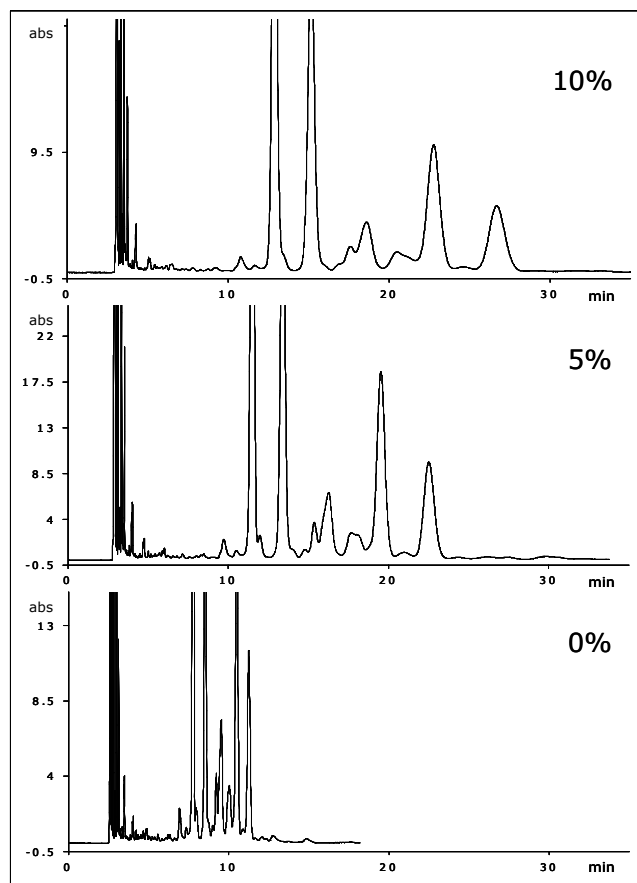


**Figure VII.25** Influence of organic modifier content on the separation of APTS-derivatized RNaseB sugars on cyanopropyl column. Buffer: 25 mM  $\text{NH}_4\text{OAc}$  containing 0, 5 and 10%  $\text{CH}_3\text{CN}$ . Voltage: -25 kV

### VII.5.3 Conclusions

To the best of our knowledge, there are no reports of carbohydrate separations on sol-gel open tubular CEC columns. Separation of APTS-derivatized sugars by using open tubular CEC showed a different profile compared to the same separation performed by CZE. The most important differences that could be noticed were a higher selectivity (on the C8 stationary phase) and a reversed EOF (for the aminopropyl stationary phase). On some columns (*e.g.* cyanopropyl) the test mixture could be separated with both direct and reversed voltage, exhibiting different resolutions.

## VII.6 Application: Open Tubular Capillary Electrochromatography of Central Nervous System Stimulants

Xanthines are a group of alkaloids that are commonly used for their effects as mild stimulants. Caffeine is a central nervous system stimulant, having the effect of warding off drowsiness and restoring alertness. Beverages containing caffeine such as coffee, tea, coke and energy drinks enjoy such a great popularity that they make caffeine the world's most popular and legal psychoactive drug. Other stimulant xanthines are theobromine and theophylline. With all effects combined, caffeine, theobromine and theophylline are ergogenic drugs: they increase the capacity for mental or physical labour [20].

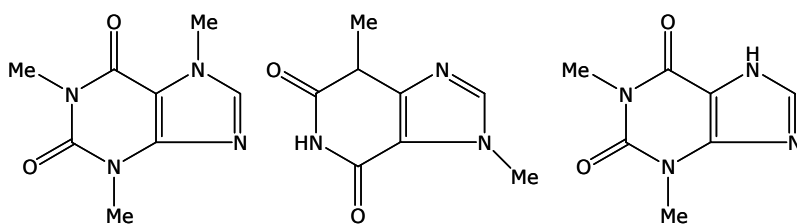


**Figure VII.26** Molecular structures of caffeine, theobromine and theophylline

In this study the use of open tubular CEC was investigated in combination with micelle formation for the analysis of xanthines.

### VII.6.1 Experimental

#### VII.6.1.1 Columns

Coated capillaries (C8 and C18, 60 cm  $L_{\text{tot}}$  x 50  $\mu\text{m}$  ID) were flushed with methanol, water and mobile phase before the first run. Any change in pH was preceded by a flush of at least 1 h with the new mobile phase.

#### VII.6.1.2 Sample preparation

Approximately 15 g of powder from three commercially available cocoa-based products were extracted under reflux with water (95-105°C) for 3 h. Prior to injection, the sample was filtered again through a 0.45  $\mu\text{m}$  syringe filter.

Caffeine, theobromine and theophylline standards were dissolved in water, ultrasonicated and filtered prior to injection.

### **VII.6.1.3 Analytical conditions**

Samples were introduced by hydrodynamic injection at 50 mbar during 6 s. Temperature was maintained at 20°C if not otherwise stated. Detection was at 200 and 276 nm. Other experimental conditions are described in the results and discussion section.

## **VII.6.2 Results and discussion**

### **VII.6.2.1 Separation on C8 stationary phase**

CEC combines two separation mechanisms, an interaction with the stationary phase and/or different migration in an electrical field. In HPLC, analytes to be separated in the reversed phase mode should be ion-suppressed. This can be achieved by modifying the pH of the mobile phase or by using an ion-pairing agent. Ion-pairing can counteract the presence of the charge and increase the hydrophobicity of the analytes. Surfactants can also act as ion-pairing agents. The use of surfactants in CEC was reported. Polymeric surfactants are used to coat the capillary wall and, if the concentration of the surfactant is above the critical micellar concentration, a combination of both open tubular CEC and MEKC can be obtained [21-23]. In packed CEC, the addition of surfactants can be used to increase the speed of analysis [24, 25] and enhance separation [26, 27]. The addition of a surfactant (such as SDS) can influence separation in CEC in different ways, especially when used at a concentration close to its critical micellar concentration<sup>1</sup>. One phenomenon that can occur is the adsorbance of the surfactant on the stationary phase by hydrophobic interactions and/or electrostatic interactions with the silanol groups, depending on the charge of the surfactant. This will affect EOF. If the analytes are charged, ion-pairing will occur and the separation mechanism can be changed. If the concentration of the surfactant is high enough, micelles will form.

---

<sup>1</sup> Critical micellar concentration in water for SDS is 8mM, dependant on the pH and the organic modifiers used in solution.

The need for SDS as mobile phase additive was evaluated in a series of experiments in which the mobile phases contained various concentrations of borate and SDS.

For the C8 column it appeared that the best separation was obtained with the addition of 10 mM SDS in 10 mM borate buffer. Note that under these conditions SDS is forming very few micelles and that mostly wall modifications occur. The analysis time when using SDS (Figure VII.27A) was half the analysis time when not using SDS in the running buffer (Figure VII.27B).

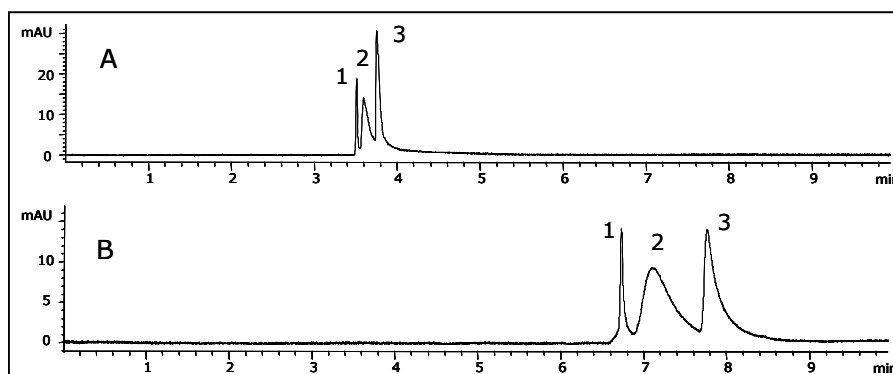


**Figure VII.27** Influence of SDS concentration on the separation of theobromine (1), caffeine (2) and theophylline (3) on a C8 stationary phase. Buffer: 10 mM borate pH 8.6 containing A. 10 mM SDS, B. 0 mM SDS. Voltage: 20 kV

#### VII.6.2.2 Analysis on C18 columns

The need for SDS as a mobile phase additive was evaluated in a series of experiments in which mobile phases consisted of 5 to 25 mM borate (pH 8.5) without SDS. Because none of these mobile phases led to the separation of the analytes of interest, all runs on C18 columns were done using mobile phases that contained 10 mM SDS.

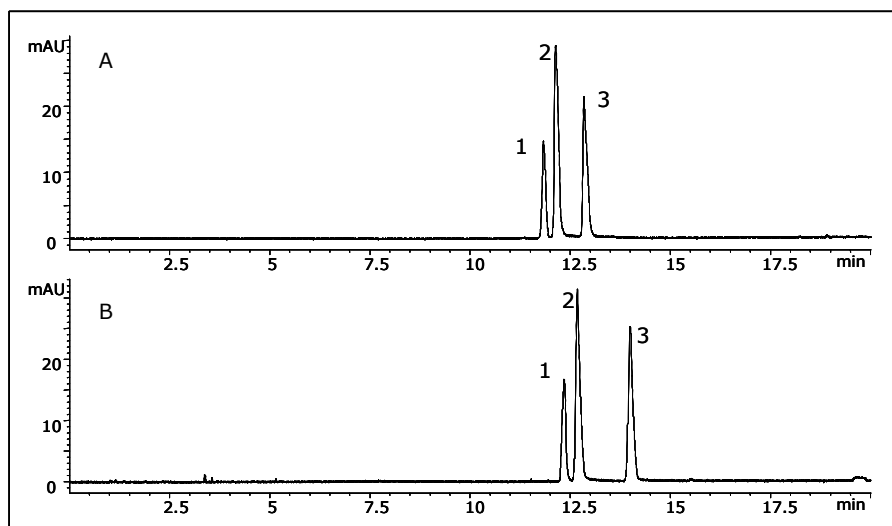


**Figure VII.28** Influence of buffer concentration on the separation of theobromine (1), caffeine (2) and theophylline (3) on a C18 stationary phase. Buffer: A. 10 mM borate pH 8.5 containing 10 mM SDS, B. 25 mM borate pH 8.5 containing 10 mM SDS. Voltage: 10 kV

Better results were obtained for the separations performed on the C18 phase. Efficient separations are observed in Figures VII.28 and VII.29 for different ionic strengths of the borate buffers. pH 8.5 provided better resolution compared to pH 9.0. Therefore the conditions used for the analysis of the real sample extracts were: 25 mM borate pH 8.5 containing 10 mM SDS, voltage: +10 kV, injection: 50 mbar \* 6 s, temperature: 20°C. Wavelengths monitored: 200 nm and 276 nm.

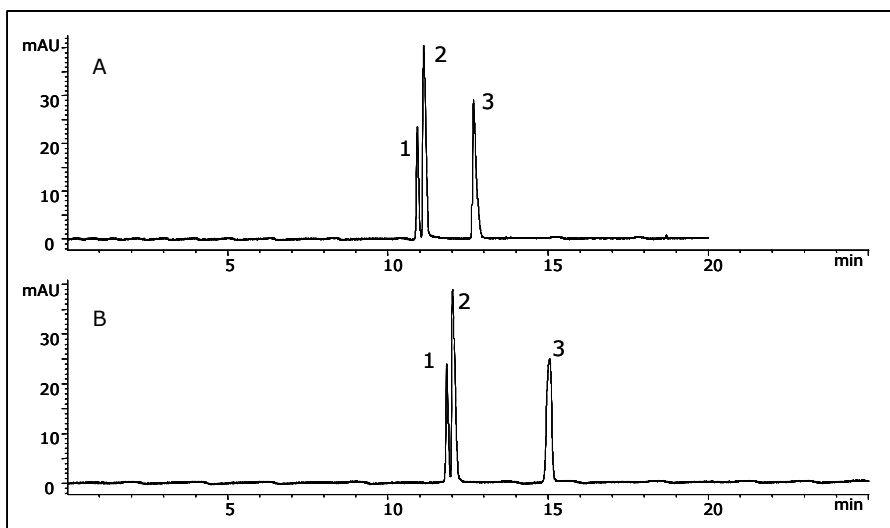


**Figure VII.29** Influence of buffer concentration on the separation of theobromine (1), caffeine (2) and theophylline (3) on a C18 stationary phase. Buffer: A. 10 mM borate pH 9.0 containing 10 mM SDS, B. 25 mM borate pH 9.0 containing 10 mM SDS. Voltage: 10 kV

### VII.6.2.3 Real sample analysis

As all three analytes of interest have very similar UV spectra, their identification was done according to their retention times and by spiking.

Theobromine was present in all three tested beverages. Caffeine was also present in the instant cocoa and instant cocoa and malt beverage, but due to the high quantity of theobromine and the matrix, it shows as a shoulder on the theobromine peak (Figures VII.30 and VII.31).

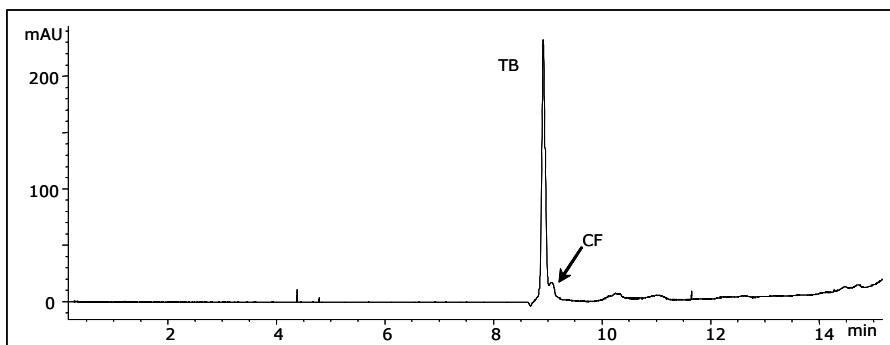


**Figure VII.30** Analysis of instant cocoa beverage. Separation conditions 25 mM borate pH 8.5 containing 10 mM SDS, voltage: +10 kV, injection: 50 mbar \* 6 s, temperature: 20°C

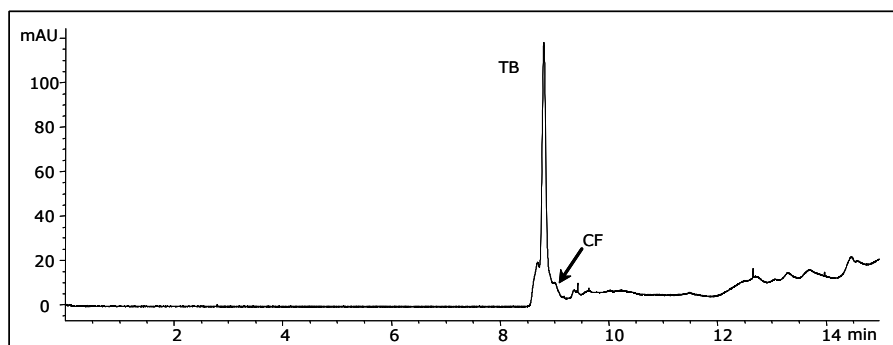


**Figure VII.31** Analysis of instant cocoa and malt beverage. Separation conditions 25 mM borate pH 8.5 containing 10 mM SDS, voltage: +10 kV, injection: 50 mbar \* 6 s, temperature: 20°C

In the cocoa powder, the theobromine quantity was so high that its peak completely overlapped the (possible) caffeine peak, even in the caffeine-spiked sample (results not shown).

Theophylline was not found in the samples.

### VII.6.3 Conclusions

For the separation of central nervous system stimulants (*i.e.* caffeine, theophylline and theobromine), the C18 phase showed the highest resolution and addition of SDS improved the separation.

On average it has, however, to be concluded that poor separation and peak shapes were obtained and that MEKC would largely outperform open tubular CEC for this application (see Chapter V).

### VII.7 Application: Separation of positional isomers by Open Tubular Capillary Electrochromatography

Isomer separations are based on the differences in affinity for selectors. Therefore, an extensive effort was made into the development of new stationary phases [28]. The separation of enantiomers by CE has proven to be most successful. Chiral separations can be performed by HPLC, but CE can offer advantages in terms of speed for method development, but suffers from the drawback that the selector is flushed out after the analysis. CEC is a technique

that offers the advantage of LC (fixed stationary phase that includes the selector) and of CE, through the high separation efficiencies that are achievable.

Cyclodextrins, and in particular  $\beta$ -cyclodextrin, are the most widely used selectors for positional isomer and enantiomer separations.

The general interaction mechanism is designated as an *inclusion complexation* (Figure VII.32). This mechanism represents the attraction of the apolar molecule or a segment thereof to the apolar cavity. When an aromatic group is present, the orientation in the cavity is selective due to the electron sharing of the aromatic CH groups with those of the glucoside oxygens. Linear acyclic hydrocarbons occupy more random positions in the cavity.

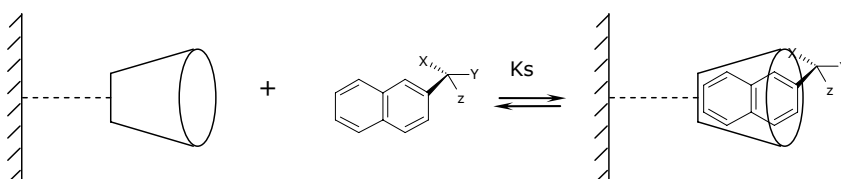


**Figure VII.32** Inclusion complexation scheme

The first important consideration for proper retention and chiral isomer recognition is a proper fit of the molecules into the cyclodextrin cavity. This fit is a function of both size and shape of the analyte relative to the cyclodextrin cavity. Next, the high density of secondary hydroxyl groups at the larger opening of the toroid acts as an energy barrier for polar molecules attempting to complex, and preferential hydrogen bonding occurs. Amines and carboxyl groups interact strongly with these hydroxyl groups as a function of the pK of the analyte and pH of the aqueous system.

In this thesis the cyclodextrins were incorporated into the silica polymer network coating the open tubular columns and the columns were evaluated for their potential for positional isomer and enantiomer separation.

## VII.7.1 Experimental

### VII.7.1.1 Columns

$\alpha$ -,  $\beta$ - and  $\gamma$ -cyclodextrin-based columns were manufactured according to the procedure described earlier in this chapter. New columns were submitted to a

voltage conditioning process by stepwise increase of the voltage from 0 to 25 kV in 60 min.

#### **VII.7.1.2 Test mixtures**

Positional isomers (i.e. dihydroxybenzenes and nitrophenols) were used in order to evaluate column selectivity through inclusion mechanism.  $\pm$ Mandelic acid was also used in evaluation tests. All samples were at an approximate concentration of 200 ppm for each compound in water/acetonitrile 50/50.

#### **VII.7.1.3 Analytical conditions**

Samples were injected by pressure (50 mbar \* 4 s). Detection was at 210, 230 and 254 nm. Runs were performed at 20°C. Other conditions are described in the legends of the results and discussion section.

### **VII.7.2 Results and discussion**

#### **VII.7.2.1 Dihydroxybenzene positional isomers**

The  $pK_a$  values for dihydroxybenzenes are  $\sim 10$ , and in order to separate them in the ion-suppressed mode the pH was kept 2 pH units below their  $pK_a$  values.

Figure VII.33 shows the separations for the dihydroxybenzene test mixture. The tailing can be attributed to the interactions of the compounds with the cyclodextrin cavity. By progressively increasing the organic modifier, peak shapes improved.

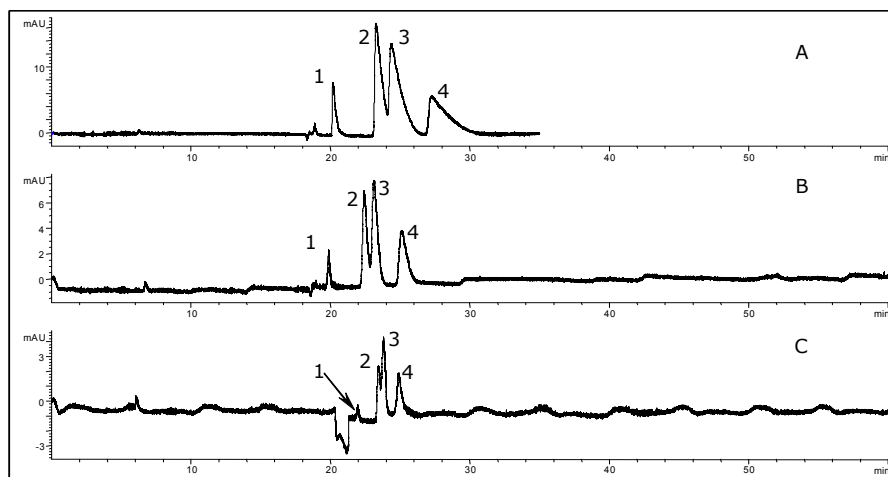


**Figure VII.33** Influence of organic modifier content on the separation of dihydroxybenzenes on  $\beta$ -cyclodextrin stationary phase. Mobile phase: 50 mM phosphate pH 7.3/ CH<sub>3</sub>CN A. 100/0, B. 95/5, C. 90/10. Voltage: 25 kV. Peaks: 1. EOF marker, 2. *m*-, 3. *o*-, 4. *p*- dihydroxybenzene

The elution order of the positional isomers (*i.e.* *m*, *o*, *p*) can be explained by the geometry and stability of their inclusion complexes (Figure VII.34). The *ortho* and *meta* isomers give similar complexes, and the difference in elution can be attributed to a difference in the stability of the complex. When the percentage of organic modifier in the mobile phase increases, the two isomers start co-eluting. The geometry of the *para* isomer seems to help the stability of its complex within the cyclodextrin cavity, which could explain this isomer's increased retention in comparison with the other two.

Dihydroxybenzenes were (partially) separated only on  $\beta$ -cyclodextrin-based stationary phase. The other two types ( $\alpha$ -,  $\gamma$ -) of cyclodextrin-based stationary phases showed no selectivity towards this specific sample. This is related to the size of the cyclodextrin cavity. If it is too small, the interaction is minimal; if it is too large, the dissociation of the complex is facilitated and the interaction is not selective.

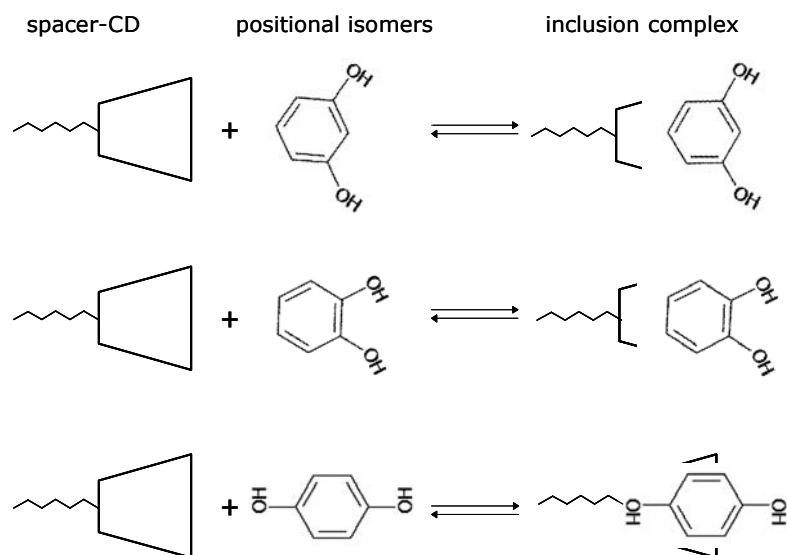
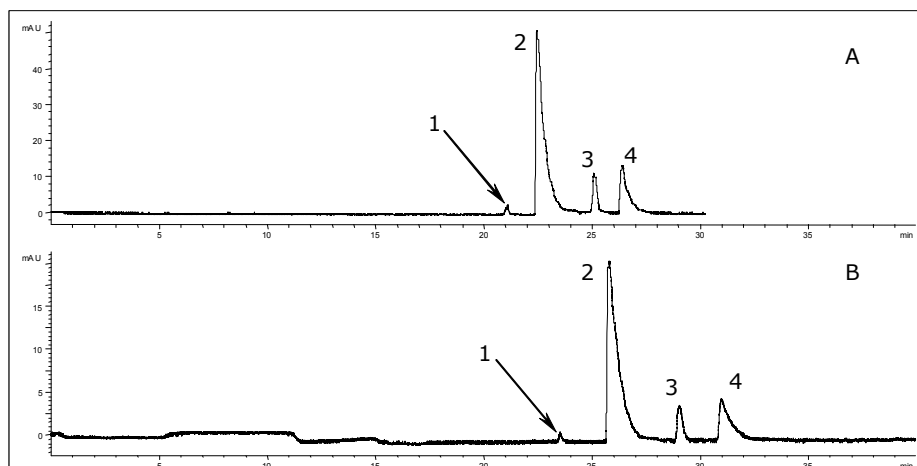


Figure VII.34 Inclusion complexes for positional isomers

#### VII.7.2.2 Nitrophenol positional isomers

The  $pK_a$  of nitrophenols is in the range of 7.17-8.28, therefore at the operating pH (pH 6) they are in the ion-suppressed mode. The elution order is the same as in the case of dihydroxybenzenes – *i.e.* m, o, p. The separation mechanism is probably also the same, but in the case of nitrophenols the isomers were separated on all three types of stationary phases ( $\alpha$ -,  $\beta$ -,  $\gamma$ -cyclodextrin).

In principle, solvent strength is independent of isomer recognition as it affects only the displacement of the analyte from the cavity. Comparison of methanol and acetonitrile is illustrated in Fig VII.35. Using acetonitrile in reversed phase HPLC generally gives the most efficient separation, but exhibits a stronger displacement effect. A similar behaviour has been noticed in the case of CEC (Figure VII.35).



**Figure VII.35** Influence of the nature of the organic modifier on the separation of nitrophenols on  $\beta$ -cyclodextrin stationary phase. Mobile phase: 50 mM MES pH 6.1/organic modifier 95/5. Organic modifier: A.  $\text{CH}_3\text{CN}$ , B: methanol. Peaks: 1. EOF marker, 2. m-, 3. o-, 4. p- nitrophenol

### VII.7.2.3 Mandelic acid enantiomers

The possibility of a chiral separation of these enantiomers on the cyclodextrin-derived stationary phase was investigated for open tubular CEC columns. The results, however, were inconclusive.

### VII.7.3 Conclusions

Sol-gel cyclodextrin-based stationary phases showed different selectivities towards positional isomers. This phenomenon is due to the differences in the stability constants of the inclusion complexes formed during separation. It was found that a screening process is needed in order to evaluate the suitability of a stationary phase for a specific isomer mix. The stationary phases obtained by covalently attaching cyclodextrins to precursors further used in sol-gel reaction were found to be stable under CEC running conditions.

---

### References

1. L Matejka, O Dukh, D Hlavata, B Meissner, J Brus – *Macromolecules* 34 (2001) 6904-6914

2. W Li, DP Fries, A Malik – *J Chromatogr A* 1044 (2004) 23-52
3. MM Dittmann, GP Rozing in "*Capillary Electrochromatography*", ed. by KD Bartle and P Myers, the Royal Society of Chemistry, London, 2001, 64-84
4. Y Guo, GA Imahori, LA Colon – *J Chromatogr A* 744 (1996) 17-29
5. A Dermaux – *PhD Dissertation*, University of Gent, Belgium, 1999
6. JJ Pesek, MT Matyska, S Cho – *J Chromatogr A* 845 (1999) 237-246,
7. Q Tang, ML Lee – *J Chromatogr A* 887 (2000) 265-275,
8. Y-C Wang, Z-R Zeng, C-H Xie, N Guan, E-Q Fu, J-K Cheng – *Chromatographia* 54 (2001) 475-479,
9. JJ Pesek, MT Matyska, V Krishnamoorti – *J Chromatogr A* 1044 (2004) 317-322
10. S Suzuki, Y Kuwahara, K Makiura, S Honda – *Chromatography* 19 (1998) 242-243,
11. RR Zhao, BP Johnson – *J Liq Chromatogr Related Techn* 23 (2000) 1851-1857
12. AH Que, MV Novotny – *Anal Chem* 74 (2002) 5184
13. D Allen, Z El Rassi - *J Chromatogr A* 1029 (2004) 239-247
14. A Paulus and A Klockow-Beck in "*Analysis of Carbohydrates by Capillary Electrophoresis*", ed KD Altria, Glaxo Wellcome R&D, UK, 1999
15. K Sandra, B Devreese, I Stals, M Claeysens, J Van Beeumen – *J Am Soc Mass Spectrom* 15 (2004) 413-423
16. NH Packer, MA Lawson, DR Jardine, JW Redmond – *Glycoconjugate J* 15 (1998) 737-747
17. RA Evangelista, MS Liu, FTA Chen – *Anal Chem* 67 (1995) 2239-2245
18. K Sandra, J Van Beeumen, I Stals, P Sandra, M Claeysens, B Devreese – *Anal Chem* 76 (2004) 5878-5886
19. BV Zhmud, J Sonnefeld – *J of Non-Crystalline Solids* 195 (1996) 16-27
20. PB Dews – *Caffeine: Perspectives. Recent Res.*, Newtonville, MA, USA. Editor(s): Dews, Peter B. (1984) 86-103
21. MW Kamande, SM Mwongela, LS Wabuyele, IM Warner – *Abstracts of Papers, 229th ACS National Meeting, San Diego, CA, United States, March 13-17, 2005* (2005) ANYL-151

22. AM Powe, LE Luna, A Demir, IM Warner – *Abstracts of Papers, 229th ACS National Meeting, San Diego, CA, United States, March 13-17, 2005* (2005) ANYL-147
23. X Zhu, MW Kamande, S Thiam, CP Kapnissi, SM Mwangela, IM Warner – *Electrophoresis* 25 (2004) 562-568
24. S Liu, Z Xie, X Wu, X Lin, L Guo, G Chen, Guonan – *J Chromatogr A* 1092 (2005) 258-262
25. S Liu, X Wu, Z Xie, X Lin, L Guo, C Yan, G Chen – *Electrophoresis* 26 (2005) 2342-2350
26. T Yokoyama, M Zenki, M Macka, PR Haddad, Paul – *Bunseki Kagaku* 54 (2005) 107-120
27. JC Valette, AC Bizet, C Demesmay, JL Rocca, E Verdon – *J Chromatogr A* 1049 (2004) 171-181
28. S Eeltink, GP Rozing, WTh Kok – *Electrophoresis* 24 (2003) 3935-3961

## *G e n e r a l   C o n c l u s i o n s*

---

In this thesis the main capillary electrodriven chromatographic techniques were compared in terms of column manufacturing and fundamental chromatographic performance.

The first stage of this thesis aimed at developing improved packed and open tubular CEC columns. For packed CEC columns, the manufacturing of the frits proved of critical importance, together with the slow build-up of the packed bed. The making of open tubular columns is a relatively simple, "one pot" sol-gel reaction taking place in mild conditions. The nature of the gel and the resulting selectivity of the column could easily be changed by changing the precursors. The gels were also easy to introduce in the capillary. Detection could be made through the coating, facilitating the manufacturing but reducing sensitivity. The biggest concern regarding the manufacturing of open tubular CEC columns lay in the control of the thickness of the coating.

In a second stage of this thesis the packed and open tubular CEC columns were evaluated chromatographically and compared with the results obtained by MEKC and MEEKC. The parameters taken into consideration were thereby retention, efficiency, selectivity, resolution, peak tailing, repeatability, sample and peak capacity and column lifetime, which are briefly outlined below.

The retention of the analytes was excellent on the packed columns. By comparison, open tubular columns showed low retention, due to low phase ratios. For both MEKC and MEEKC, the retention depends on the nature of the micelles and of the analytes, but both techniques suffer from a limited elution window.

All electrodriven separation techniques showed high efficiencies. For open tubular CEC columns the number of plates, however, decreased rapidly with retention. This is due to the poor phase ratio and limited sample capacity.

Resolution is acceptable for packed CEC, MEKC and MEEKC. In the case of open tubular CEC it can be concluded that the low retention is the main problem affecting resolution.

For apolar analytes, the peak shape in general was good for packed and open tubular CEC. Some tailing was observed in MEKC and MEEKC experiments, dependent on the composition of the micelles. Severe peak distortion was observed in the separation of basic compounds on packed CEC due to the interaction of these analytes with the silanol groups present in the stationary phase.

Run-to-run repeatability was not a problem for any of the techniques. In day-to-day and column-to-column experiments, packed and open tubular CEC columns showed an expected much lower repeatability in terms of retention and selectivity than MEKC and MEEKC.

The sample capacity was good for packed CEC. Column overload occurred only at high quantities of sample. It was observed that even if the sample capacity was not reached, the efficiency was strongly dependent on the polarity of the sample. In the case of MEKC and MEEKC, sample capacity is lower compared to CEC.

For peak capacity, CEC has the advantage of a practically non-limited elution window, while MEKC and MEEKC suffer of the drawback of the existence of an elution window which is limited in time by the elution of the micelles.

All columns have a limited life time, but most problems were observed with open tubular columns due to a loss of selectivity caused by column bleeding. The lifetime of packed columns is limited because of their frailty and of the frits blocking.

Based on the results obtained in this thesis, packed CEC, MEKC and MEEKC outperform open tubular CEC. Nevertheless, open tubular techniques remain theoretically better providing that the capillary diameter is further reduced. The

combination of thicker films and narrower capillaries could pave the way for successful open tubular CEC in the future. Highly sensitive detectors have to be developed to cope with such columns.

Considering the progress in the last couple of years towards miniaturisation in the separation sciences (notably in micro- and nanoLC), the present state of the electrodriven chromatographic separation methods allows room for much improvement. They all suffer from shortcomings. The (mostly) in-house manufacturing of packed columns, the lack of detectors sensitive enough to cope with very narrow bores that are required by the theory, the impossibility of coupling micellar techniques to MS are just a couple of the pitfalls. There is a gap between the theoretical predictions and the practical implementation capability of these methods. Without much more improvement in electrodriven chromatographic techniques they will still be considered just orthogonal tools in separation sciences and not key techniques, restricted to research laboratories and not widely and routinely used by the industry.

## Summary

---

The work is divided into two parts that deal with the theoretical (**Part A: Electrodriven Separation Methods, Chapters I-IV**) and the practical (**Part B: Experimental Electrochromatography, Chapters V-VII**) aspects of CEC.

Theoretical aspects of CEC are discussed in **Chapter I: Capillary Electrochromatography**. The importance of electrophoresis and electroosmosis is highlighted, as well as practical parameters influencing these phenomena. A short discussion about the limitations that CEC is confronted with, follows.

**Chapter II: Instrumental Aspects** deals with the set-ups currently used for running CEC experiments. The different parts of a CEC system are discussed, *i.e.* injection, separation and detection.

Fundamental aspects of sol-gel technology are discussed in **Chapter III: Sol-Gel Technology**. The reactions involved in a sol-gel process, as well as the means for gel characterization are presented. Applications with relevance to the present work are listed.

Column technology is discussed in **Chapter IV: Column Manufacturing Techniques in CEC**, for both packed and open tubular column formats. The packing materials, column designs, packing techniques and reproducibility issues are presented. For open tubular columns, stationary phase requirements and column formats are discussed.

**Chapter V: Peak and Sample Capacity in CEC, MEKC and MEEKC** presents a comparison between the three electrochromatographic separation techniques in terms of separation power and sample capacity. Two equations are proposed for

calculating peak capacity. The sample capacity is measured through plots representing the efficiency versus analyte quantity and by investigating a 0.05% impurity level relative to the main compound.

**Chapter VI: Packed column CEC** deals with the evaluation of packed columns and the possibility of their coupling to MS. The columns are evaluated in terms of efficiency and repeatability; both parameters are good. The details of the coupling to MS are discussed. Two examples for successful separation and detection are given, namely steroids and carbamates. It was shown that bubble formation could be avoided by a proper column manufacturing process.

The manufacturing and evaluation of open tubular columns is presented in **Chapter VII: Open Tubular CEC**. The gels used for coating the capillaries are characterized by TGA and DSC. The capillary coating procedure is described. The open tubular columns are evaluated in terms of selectivity and efficiency, and the influence of the operational parameters described. Three applications are presented, namely the separation of carbohydrate derivatives by OTCEC-LIF, the separation of central nervous stimulants from cocoa beverages and the separation of positional isomers on cyclodextrin-based stationary phases.